Reactive oxygen species play a dual role in the resistance and susceptibility of *Camellia* to flower blight disease

A thesis presented in partial fulfilment of the requirements

for the degree of

Master of Science

in

Plant Biology

at Massey University, Manawatū

New Zealand

Cade Fulton

2020

Abstract

Reactive oxygen species (ROS), a group of highly reactive biomolecules, are known to rapidly accumulate in plant tissue as an early defence response to pathogen invasion. However, ROS can also contribute to pathogen virulence. Currently, little is known about the activity of these compounds during the interaction between *Camellia* and the *Camellia* flower blight (CFB) necrotrophic fungal pathogen, *Ciborinia camelliae* L. M. Kohn (Sclerotiniaceae). It has been shown that there is a spectrum of resistance and susceptibility to the disease within the *Camellia* genus. This study aimed to elucidate the role that ROS play during *C. camelliae* interactions with *Camellia* on this spectrum of resistance. To achieve this, hydrogen peroxide accumulation was first visualised and compared between the CFB resistant *Camellia lutchuensis* and the susceptible *Camellia* 'Nicky Crisp' in response to *C. camelliae*. Following the inoculation of flower petals with *C. camelliae* ascospores, widespread apoplastic hydrogen peroxide accumulation and upregulation of genes encoding NADPH oxidase and cell wall peroxidase began 12 hours earlier in the resistant *C. lutchuensis* species than the susceptible *C.* 'Nicky Crisp', which showed very little observable accumulation. In addition, the quantity of hydrogen peroxide significantly increased in the resistant *C. lutchuensis* petals, but no change was observed in the susceptible *C.* 'Nicky Crisp' within the same timeframe. The application of exogenous antioxidants to scavenge the hydrogen peroxide accumulation resulted in disease development in the normally resistant *C. lutchuensis*, while the incidence of disease was significantly reduced in the susceptible *C.* 'Nicky Crisp'. Therefore, it was hypothesised that early ROS accumulation contributes to CFB resistance and that late ROS accumulation contributes to CFB susceptibility. This work further expands knowledge of plant interactions with necrotrophic fungal pathogens from the Sclerotiniaceae family by demonstrating that ROS both positively and negatively regulates CFB development based on temporal accumulation, thereby discovering a dual role for ROS accumulation during this interaction.

Acknowledgements

First and foremost, I would like to thank my supervisor, Associate Professor Paul Dijkwel, who gave me his unending support and guidance throughout both my research work and the entire degree programme. His knowledge and passion for plants served as a role model for me and I greatly appreciate the opportunity he gave me to undertake this project. I would also like to thank Dr Matthew Denton-Giles for his co-supervision. He offered valuable advice to improve my experiments and generously shared his expertise and research into *Camellia*, both of which further enabled me to complete this project.

I am very grateful to the New Zealand Camellia Society and Memorial Trust Scholarship for their support in this project and for their passion for this beautiful flower, both of which were drivers to find successful outcomes for them. I would like to especially thank Emeritus Professor Vince Neall, who took time to meet and teach me about *Camellia* in the local gardens, as well as to give me useful tips in the care of the plants. I also greatly appreciate the support of the following organisations for additional scholarships awarded to me: the Graduate Women New Zealand Manawatū Postgraduate Scholarship, the Don Scott Agricultural Education Trust Scholarship, the Johannes August Anderson Postgraduate Scholarship, the Joan Dingley Memorial Scholarship in Mycology, and the John P Skipworth Scholarship. I would like to acknowledge Associate Professor, Pieter Pelser, University of Canterbury, and Professor Matthew Dickenson, University of Nottingham, both of whom, through their lectures during my undergraduate degree, helped me to realise my deep interest in the diversity of plants and plant pathology.

The team at the Manawatū Microscopy & Imaging Centre were extremely helpful and informative while assisting me in capturing the images I needed to demonstrate my work. Lesley Taylor at the Massey University Plant Growth Unit also provided support in caring for our plants which were stored in their green houses.

A special thanks to Dr Nikolai Kondratev, whose instruction and assistance during my first ventures into laboratory research work were invaluable. I will always be very grateful for his patience and encouragement in learning new techniques. Dr Tina Sehrish was also extremely helpful with my lab work. To my fellow lab colleagues, Hannah, Tina, Asmat, and Trevorne: thank you for making our time in and out of the lab so enjoyable and adding to my whole experience in obtaining this degree.

To my husband, Chris, I will be eternally grateful for his love and support, and for encouraging me through my studies during the birth and tending of our two children, Audrey and Claire. Finally, I would like to thank my parents, Lily and Bill Fulton. They helped me to find the courage to take the necessary steps to change my career.

Table of Contents

List of Figures and Tables

Abbreviations

°C	degrees Celsius
µg	microgram
µL	microlitre
µm	micrometre
µM	micromolar
$^1O_2$	singlet oxygen
AtMPK3	*Arabidopsis* mitogen-activated protein kinase 3
AtMPK6	*Arabidopsis* mitogen-activated protein kinase 6
BAK1	Brassinosteroid insensitive 1-associated receptor kinase
BHA	butylated hydroxyanisole
bp	base pair
ANOVA	analysis of variance
Avr	avirulence
Ca^{2+}	calcium
CAT	catalase
CDPK	calcium dependent protein kinase
CFB	*Camellia* flower blight
cm	centimetre
Cq	quantitation cycle
cv.	cultivar
DAB	3,3’ diaminobenzidine
DAMP	damage-associated molecular pattern
DEG	differentially expressed genes
DNA	deoxyribonucleic acid
EDTA	ethylenediaminetetraacetic acid
EF-1α	eukaryotic elongation factor-1 alpha
ELI3-2	elicitor-activated gene 3

ETI	effector-triggered immunity
ETS	effector-triggered susceptibility
F5H	ferulate 5-hydroxylase
g	gram
GOI	gene of interest
H_2O_2	hydrogen peroxide
H_2DCFDA	2',7' -dichlorodihydrofluorescein diacetate
h	hour
hpi	hours post-inoculation
HR	hypersensitive response
ICMP	International Collection of Microorganisms from Plants
IPR	invasion pattern receptors
JA	jasmonic acid
kb	kilobase pairs
MAMP	microbial-associated molecular pattern
MAPK	mitogen-activated protein kinase
min	minute
mL	millilitre
mm	millimetre
mM	millimolar
NADPH	nicotinamide adenine dinucleotide phosphate
NBS-LRR	nucleotide-binding sites and leucine-rich repeat domains
NCBI	National Center for Biotechnology Information
NLP	Nep1-like protein
NOX	nicotinamide adenine dinucleotide phosphate oxidase
NPR1	nonexpressor of pathogenesis-related genes 1
O_2	molecular oxygen
O_2^-	superoxide radical

OH•	hydroxyl radical
OA	oxalic acid
P	p-value
PAMP	pathogen-associated molecular pattern
PCD	programmed cell death
PCR	polymerase chain reaction
PDA	potato dextrose agar
PER	peroxidase
Pmol	picomole
PRR	pathogen recognition receptor
PTB1	polypyrimidine tract-binding protein 1
PTI	pathogen-associated molecular pattern triggered immunity
PVDF	polyvinylidene fluoride
qRT-PCR	quantitative real-time polymerase chain reaction
R proteins	resistance receptor protein
RBOH	respiratory burst oxidase homolog
RLP23	*Arabidopsis thaliana* leucine-rich repeat R protein 23
RNA	ribonucleic acid
ROS	reactive oxygen species
s	second
SA	salicylic acid
SOBIR1	Suppressor of brassinosteroid insensitive 1-associated receptor kinase interacting receptor-like kinase 1
SOD	superoxide dismutase
StAR	wheat kinase steroidogenic acute regulatory protein
START1	steroidogenic acute regulatory protein related lipid transfer protein
TAE	tris-ascetate-EDTA
TGA	*Arabidopsis* basic leucine zipper type transcription factor
Tub α-3	tubulin alpha-3

VvC3H	*p*-coumarate 3-hydroxylase
VvCCR	cinnamoyl CoA reductase
WKS1	wheat kinase steroidogenic acute regulatory protein related lipid transfer

1 Introduction

1.1 *Camellia* flower blight

The *Camellia* genus, taxonomically located in the Theaceae family, includes agriculturally important species such as *Camellia sinensis*, the tea plant, and ornamental species such as *Camellia japonica* 'Kate Shepard' (Vijayan, 2009). *Camellia* species are largely distributed throughout China and southeastern and eastern Asia, where cultivation of the genus originated in China and Japan before spreading to Europe and the Americas (Taylor & Long, 2000). Today, this genus holds cultural and ornamental value to growers and enthusiasts around the globe. Also, as a genus that blooms in the autumn and winter months, nectar rich species can provide a much-needed source of energy to some birds, bees and butterflies when other food sources are scarce (Kunitake, Hasegawa, Miyashita, & Higuchi, 2004; Sun, Huang, Chen, & Huang, 2017). However, *Camellia* flower blight (CFB) disease is a significant problem in the genus, causing brown petal lesions and premature flower fall (Fig. 1.1) (Kohn & Nagasawa, 1984). The causal agent of CFB is the fungal pathogen, *Ciborinia camelliae*, which was first identified in Japan in 1919 (Hara, 1919) before becoming widespread in other parts of the globe such as in the United States by the 1970's, in New Zealand where the first case was identified in 1993, and in Europe a few years later (Stewart & Neilson, 1993; Taylor & Long, 2000). *C. camelliae* is a necrotrophic fungal pathogen of the Sclerotiniaceae family that includes several well-studied and economically important broad host-range pathogens. Close relatives of *C. camelliae* include *Botrytis cinerea* (grey mould fungus) and *Sclerotinia sclerotiorum* (white mould fungus) (Dean et al., 2012; Palomares-Rius et al., 2014). Many plant species that are susceptible to pathogens from this family include commercially important species such as grapes, strawberries and peaches, as well as solanaceous vegetables like potatoes and tomatoes (Dean et al., 2012).

Figure 1.1 *Camellia* 'Nicky Crisp' bloom *in situ* with typical *Camellia* flower blight (CFB) petal lesions.

The disease cycle of CFB begins when ascospores are released from the reproductive fruiting bodies of *C. camelliae*, apothecia (Fig. 1.2) (Taylor, 2004). When ascospores land on *Camellia* petals and the conditions are suitable, the ascospores will germinate and hyphae will lengthen and then penetrate the

Figure 1.2 An immature *Ciborinia camelliae* apothecium.

petal cuticle (Denton-Giles, Bradshaw, & Dijkwel, 2013; Vingnanasingam, 2002). A short asymptomatic phase of intercellular hyphal growth occurs in the tissue which is then followed by a symptomatic phase of hyphal growth into the subepidermal and mesophyll layers of tissue. Finally, necrotic lesions form in the petals and the fungus spreads throughout the flower quickly killing the bloom within a few days. The bloom falls to the ground and the fungal hyphae harden and envelop the flower, forming sclerotia (Vingnanasingam, 2002). The fungus lies dormant in this form until the next flowering season when apothecia develop from the sclerotia and the cycle repeats.

Contemporary CFB disease control methods such as fungicide application and biological control methods have been unsuccessful thus far in eradicating the disease once it is established in an area, because the ascospores are windblown and can travel great distances (Van Toor, Jaspers, & Stewart, 2005; Van Toor, Jaspers, & Stewart, 2001). Consequently, *Camellia* researchers are investigating new and more innovative management strategies for petal blight. Several recent studies have shown that there is a spectrum of resistance and susceptibility to CFB within the *Camellia* genus, which provides a new avenue of research for blight management (Couselo, Vela, Salinero, & Mansilla, 2014; Denton-Giles et al., 2013; Kondratev, Denton-Giles, Bradshaw, Cox, & Dijkwel, 2020). Gaining a better understanding of the inherent defence responses that make some closely related species more resistant to a pathogen invasion than others and of how these responses operate specifically in *Camellia* may provide new ways to combat CFB.

There are many cases of closely related plant species within the same genus showing variation in resistance and susceptibility to disease-causing phytopathogens. For example, many popular ornamental plants such as those found within the rose (*Rosa*) and geranium genera (*Pelargonium*) contain species and cultivars with a range of resistance and susceptibility to infection by the broad-host necrotrophic pathogen, *B. cinerea* (Hammer & Evensen, 1994; Uchneat, Spicer, & Craig, 1999). Research within the *Camellia* genus shows varying levels of resistance to anthracnose caused by *Colletotrichum fructicola* in tea plant cultivars within the *Camellia sinensis* (L.) O. Kuntze species (Wang et al., 2018). Similarly, a spectrum of resistance and susceptibility to CFB has been discovered within popular ornamental *Camellia* species (Couselo et al., 2014; Denton-Giles et al., 2013; Taylor, 2004; Vingnanasingam, 2002). In studying 40 *Camellia* species and hybrids, Denton-Giles et al.

(2013) concluded that genotype influences CFB disease development on *Camellia* as measured by several parameters, such as the comparative area size of petal lesion formation. For example, lesions develop earlier and more severely on petals of susceptible species such as *C. japonica* and *C. granthamiana,* while lesions fail to develop or develop later and less severely on CFB resistant species such as *C. lutchuensis* and *C. transkonoensis* (Denton-Giles et al. (2013).

1.2 The classic plant immunity model

Biotic stresses on a plant can arise from a microbial environment that contains many plant disease-causing viruses, bacteria, fungi and oomycetes. As plants are unable to move quickly to evade danger, they have evolved many internal tactics to protect and defend themselves. Constitutive structural defences like plant cuticles and plant cell walls can be successful in protecting a plant. Phytoanticipins, which are chemicals that are constitutively present in plant tissue such as the toxic compound, α-Tomatine, can help to deter fungal invasion (Sandrock & VanEtten, 1998). If constitutive layers of defence fail to prevent an invasion, many plants have evolved the ability to recognise a pathogenic invader and activate an effective defensive response to resist an internal infection (Jones & Dangl, 2006). However, if a plant is not able to recognise an attack by a specific pathogen or mount an appropriate response to overcome the infection, it will remain susceptible to the invasion and progression of disease symptoms. Therefore, the classic plant pathology theory sets out the 'zigzag' model of plant resistance to pathogens (Jones & Dangl, 2006). The resistance pathway model describes a staged defence response during incompatible plant-pathogen interactions (Fig. 1.3a).

The first mechanism of resistance is known as the innate defence response or the PAMP-triggered immunity (PTI) response. In the innate defence response, a plant perceives the presence of a foreign organism when its pathogen recognition receptor (PRR) proteins recognise non-specific pathogen-associated molecular patterns (PAMPs) or microbe-associated molecular patterns (MAMPs). PRRs are situated across plant cell plasma membranes and detect the presence of pathogens by recognising specific molecules such as chitin from fungal cell walls and flagellin from bacterial flagella (Chinchilla, Bauer, Regenass, Boller, & Felix, 2006; Kaku et al., 2006). A well-understood model of PAMP recognition in plants describes how plasma membrane bound PRRs in *Arabidopsis* recognise bacterial flagellin fragments (Chinchilla et al., 2006). Recent updates to the classic plant resistance model include other signals that plants can recognise during an invasion, such as damage-associated molecular patterns (DAMPs) (Boller & Felix, 2009; Cook, Mesarich, & Thomma, 2015; Nothnagel, McNeil, Albersheim, & Dell, 1983; Ranf, Es9chen-Lippold, Pecher, Lee, & Scheel, 2011). DAMPs are described as the compounds that are released from damaged plant cells into the apoplastic space as result of a pathogen entering the host tissue, often by secreting cell wall degrading enzymes (Gibson, King, Hayes, & Bergstrom, 2011; Wanjiru, Zhensheng, & Buchenauer, 2002). When the recognition

of a PAMP/MAMP or DAMP by a plant receptor protein is successful, the plant activates PTI in an attempt to inhibit the pathogen invasion before it can establish itself within the plant tissue. PTI includes a range of responses such as cell wall strengthening, phytoalexin biosynthesis, and the oxidative burst, which is the rapid and localised accumulation of volatile molecules known as reactive oxygen species (ROS).

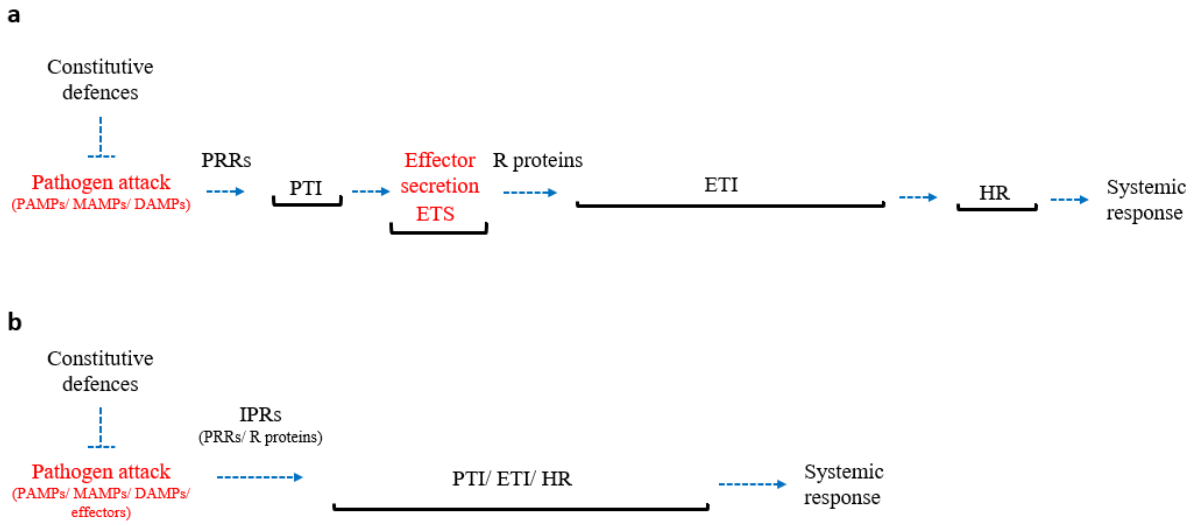

Figure 1.3. Classic plant immunity models are being revised.
(a) The classic plant immunity model follows a pathway with events taking place in consecutive order. The process begins when a pathogen overcomes its host plants' constitutive defences. The host plants' pathogen receptor proteins (PRRs) may recognise pathogen-associated molecular patterns (PAMPs), microbe-associated molecular patterns (MAMPs), and/ or damage-associated molecular patterns (DAMPs). Upon successfully recognising the presence of the pathogen with pathogen recognition receptors (PRRs), plant triggered immunity (PTI) is activated by the plant. In response, the pathogen secretes effector proteins to overcome the plant's defences, causing effector-triggered susceptibility (ETS) in the plant. If the plants' resistance receptor (R) proteins can recognise the effectors the plant then activates the effector triggered immunity (ETI) response. ETI culminates in the hypersensitive response (HR) in which the plant activates localised cell death to prevent the pathogen from further ingress into its tissue. Finally, a systemic response can be triggered in the plant, with signalling cascades that upregulate defence responses in distal tissue. **(b)** The more recently proposed 'Invasion Model' includes effectors in the group of compounds that can be initially recognised by the plant. Invasion pattern receptors (IPRs) include both PRRs and R proteins, and there is not a strong sequential delineation between PTI, ETI or the HR. Some, but not all, of these events may occur during a plant response to pathogen attack, and similar defence responses can occur during both PTI and ETI. The events in black above are plant-activated and the events in red are pathogen-activated. Arrow and T-bars represent positive and negative regulation, respectively.

In response to PTI, pathogens have evolved the ability to secrete effector proteins that can inhibit or circumvent the plant's innate defence response. In this case, the plant's effector-triggered susceptibility (ETS) may result in a compatible interaction between the plant and the pathogen, leading to disease development. However, another class of plant receptor may recognise the pathogen's effectors. These are called resistance receptor proteins (R proteins), and the most common type of these receptors are proteins containing nucleotide-binding sites and leucine-rich repeat domains (NBS-LRR). They make up almost half (approximately 150) of the R gene candidates in the *Arabidopsis* model plant system (Meyers, Kozik, Griego, Kuang, & Michelmore, 2003). If the plant

receptor proteins recognise the pathogens' secreted effectors, the effector is known as an avirulence factor (Avr) which is consistent with the 'gene-for-gene' model put forth in Flor's landmark paper in 1971 (Flor, 1971). The plant's recognition of effectors gives rise to the second stage of resistance set out in the classic plant immunity model that is termed effector triggered immunity (ETI) (Lo Presti et al., 2015). ETI includes many of the same activities as the innate response; however, this second stage is characterised as occurring more intensely and persists for a longer period of time. Sustained ETI can result in the hypersensitive response (HR), which is a type of localised programmed cell death in the plant tissue that can prevent microbes from spreading further into the plant from the initial site of infection (Bestwick, Brown, Bennett, & Mansfield, 1997). Finally, localised defence responses in a plant can trigger systemic responses in distal tissues with the involvement of plant stress hormones such as salicylic acid (SA), jasmonic acid (JA) and ethylene (Gaffney et al., 1993; Kazan & Lyons, 2014).

1.3 Expanding plant immunity models

As the field of plant pathology research has advanced, plant-pathogen interactions that fall outside the classic model of plant disease resistance are increasingly becoming apparent. Cook et al. (2015) reviewed several of these interactions and proposed a departure from the strict staged model (Fig. 1.3b). For a variety of reasons the authors suggest that a 'surveillance system' model would be more inclusive of the growing body of knowledge of disease resistance in plants, and their proposal is gaining traction in the field of plant pathology (Boutrot & Zipfel, 2017; Schellenberger et al., 2019). First, the 'surveillance system' or Invasion Model allows that in some cases there is not a clear delineation between PAMPs/ MAMPs/ DAMPs and effectors. Some effector proteins contain patterns that can be recognised by a plant and so this alternate model would also define them as a MAMP. For example, Nep1-like proteins (NLPs), effectors originally identified in *Fusarium oxysporum*, are recognised by the leucine-rich repeat R protein, RLP23, in *Arabidopsis thaliana* (Albert et al., 2015; Bailey, 1995). Second, there is evidence demonstrating commonality between the previously separated plant receptor groupings of PRR proteins active in PTI and the R proteins active in ETI. Consequently, the model suggests that receptor proteins should instead be grouped together into a general category of plant receptor proteins or invasion pattern receptors (IPRs). Additionally, Cook et al. (2015) posited that disease resistance does not strictly occur as a two-stage response with ETI following PTI, but rather that no absolute divide exists between the two stages. This is because many similar mechanisms of resistance are shared between PTI and ETI, such as ROS accumulation and downstream mitogen-activated protein kinase (MAPK) and calcium-dependent protein kinase (CDPK) signalling cascades, blurring any delineation between these two stages. Finally, the classic 'zig-zag' model that culminates in the HR and localised cell death to stop an invasion is typically best applied to biotrophic pathogens. This is because biotrophic pathogens benefit most from host plant

cells staying alive during the interaction in order to continuously extract nutrients from the plant. For example, the *Ustilago maydis* fungus is the causal agent of corn smut and it is used a model biotrophic fungus (Matei & Doehlemann, 2016). The fungus penetrates its host tissue, growing into the intercellular space while secreting effectors to supress the host plant's immune response (Skibbe, Doehlemann, Fernandes, & Walbot, 2010). So, an HR does not occur in the plant, which benefits the fungus, because the living plant cells are required to complete its sexual cycle and to extract nutrients for its own benefit (Bauer, Oberwinkler, & Vánky, 1997; Brefort et al., 2009). The localised cell death that would successfully inhibit a biotrophic fungal invasion may instead provide a necrotrophic fungus with an energy source. Necrotrophic fungi like *B. cinerea* and *S. sclerotiorum* have been shown to benefit from the HR and have even evolved other strategies to kill host cells by the secretion of toxins, cell wall degrading enzymes, and other necrosis inducing proteins (Bashi, Hegedus, Buchwaldt, Rimmer, & Borhan, 2010; Govrin & Levine, 2000; Kim, Min, & Dickman, 2008). Therefore, as knowledge of plant interactions with necrotrophic fungi have expanded, revisions to the classic plant immunity model have been required to better understand the dual roles that plant defence responses can have in either inhibiting or promoting disease in concert with the behaviour of the pathogen.

1.4 Reactive oxygen species (ROS) and homeostasis

ROS are highly reactive and volatile molecules playing complex roles throughout plant biological processes. The most abundant forms of ROS produced in plant cells are: singlet oxygen ($^1O_2$), the superoxide radical (O_2^-), hydrogen peroxide (H_2O_2), and the hydroxyl radical (OH•) (Fig. 1.4) (Camejo, Guzman-Cedeno, & Moreno, 2016). These molecules are also produced as by-products of normal respiratory processes in aerobic organisms, although at much lower levels in periods of non-stress. In times of normal plant function, when not under pathogenic invasion, ROS are mostly produced in cellular compartments like mitochondria, chloroplasts, and peroxisomes as by-products of the usual functions of these organelles (Apel & Hirt, 2004; Corpas, Gupta, & Palma, 2015).

As the production of ROS can damage a plant's own tissue and nucleic acids, plants produce enzymatic and non-enzymatic compounds in concert to prevent cellular levels of ROS from reaching damaging levels during periods of non-stress (Gechev, Van Breusegem, Stone, Denev, & Laloi, 2006). These ROS scavengers include enzymes such as superoxide dismutase (SOD) and catalase (CAT). Non-enzymatic ROS scavengers include antioxidant compounds like glutathione and ascorbic acid that naturally occur in plant tissue and play a role in the ascorbate-glutathione cycle (Foyer & Noctor, 2011). ROS production and scavenging in times of non-stress keep the cellular redox environment in a delicate equilibrium (Foyer & Noctor, 2005). However, within minutes of recognising a pathogen attack, ROS begin to accumulate in the plant tissue and quickly overcome the

on-going scavenging activity (Torres, 2010). At these elevated levels, ROS begin to take on numerous roles that illustrate the significance of these compounds in plant defence responses.

1.5 The roles of ROS in response to a pathogen invasion

1.5.1 The oxidative burst

One of the earliest activities to occur in the plant after recognition of a pathogen is the oxidative burst (Fig. 1.4) (Doke, 1983; Lamb & Dixon, 1997). Initially, localised ROS accumulation occurs in the cellular apoplast near pathogen material (Camejo et al., 2016; Heller & Tudzynski, 2011; Mellersh, Foulds, Higgins, & Heath, 2002). The respiratory burst oxidase homolog (RBOH) family of nicotinamide adenine dinucleotide phosphate (NADPH) oxidases (NOX) are a major source of ROS that are produced during the oxidative burst (Torres, Dangl, & Jones, 2002). The proteins are situated in plant cell plasma membranes and oxidises NADPH, which reduces molecular oxygen into $O_2{\cdot}^-$ (Keller et al., 1998). Apoplastic peroxidases (PER) also play a role in the apoplastic oxidative burst and have been shown to be required in the oxidative burst in *A. thaliana* in response to *F. oxysporum* elicitors (Bindschedler et al., 2006).

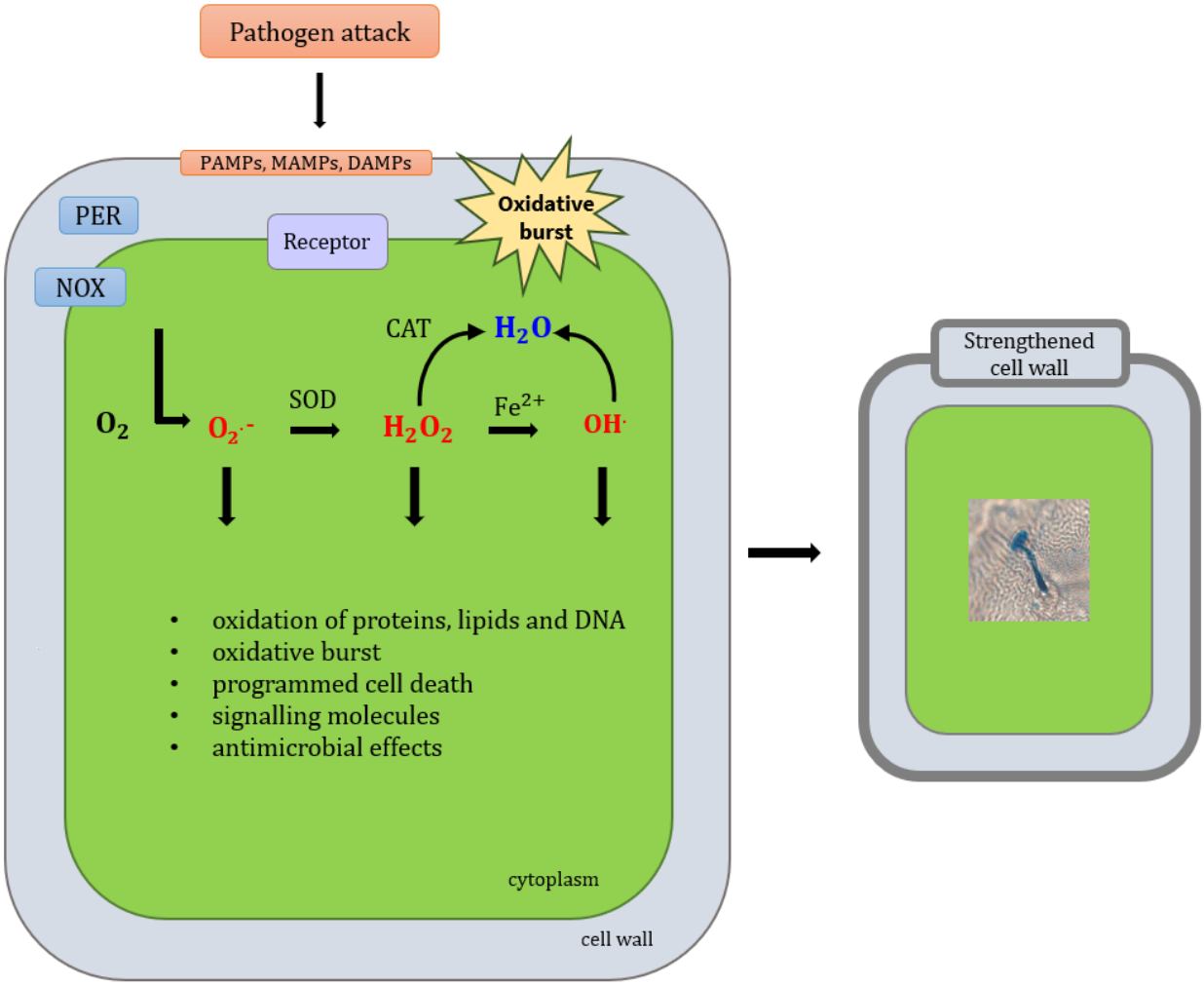

Figure 1.4 Model of the sequential reduction of molecular oxygen in plant cells to create reactive oxygen species when activated by pathogen attack.
When pathogen PAMPS, MAMPs or DAMPS are recognised by receptors in the plant cell plasma membrane, an oxidative response is activated by the plant. NADPH oxidase (NOX) and apoplastic peroxidase (PER) generate superoxide anions (O_2^-) from molecular oxygen (O_2). Superoxide dismutase (SOD) converts O_2^- into hydrogen peroxide (H_2O_2). Catalase converts H_2O_2 into water (H_2O) and oxygen. The hydroxyl radical $OH\cdot$ is a product from the Fenton reaction. ROS produced in plant cells as a defence response plays many roles such as: activating the oxidative burst, strengthening cell walls, inhibiting pathogen ingress with programme cell death, and acting as signalling and antimicrobial molecules.

Bindschedler et al. (2006) showed in *Arabidopsis* that both NOX mutants and cell wall PER antisense lines reduced normal ROS production when challenged by an avirulent bacterial pathogen that would normally induce high levels of ROS production in the wild-type plants. As a result, the mutant plants were much more susceptible to infection without functioning NOX and PER proteins in comparison to the control plants. Many studies and reviews demonstrate how gene expression of *NOX* and *PER* are a critical part of plant resistance to pathogenic invasion. Expression of these genes has been shown to operate in defence related pathways like mediating defence related-hormone signalling and CDPK signalling cascades (Ardila, Torres, Martinez, & Higuera, 2014; Drerup et al., 2013; Mammarella et al., 2015; Mitchell, Brown, Knox, & Mansfield, 2015; Survila et al., 2016).

1.5.2 Mediators of plant cell wall structural changes

At the site of the plant-pathogen interaction, the HR begins in the form of ROS-dependent structural changes in the plant cell wall (Mellersh et al., 2002; Thordal-Christensen, Zhang, Wei, & Collinge, 1997). This ROS-mediated cell wall fortification with lignin, suberin, and glycoproteins has been shown to inhibit pathogen ingress to the cell (Almagro et al., 2009; Bhuiyan, Selvaraj, Wei, & King, 2009; Passardi, Penel, & Dunand, 2004). Indeed, Kelloniemi et al. (2015) found that ROS and lignin biosynthesis were involved in cell wall strengthening in resistant immature grapes, while susceptible mature grapes lacked the same activities in response to infection by *B. cinerea.* In the absence of apoplastic H_2O_2 accumulation, the researchers observed a more developed, multicellular phenotype of a specialised cell called an appressorium in the grey mould-susceptible mature berries that penetrates the host tissue. At the same time, colocalization of H_2O_2 accumulation and regular appressoria formation were observed in the more resistant and immature veraison berries. In addition, the oxidative burst in the veraison berries was shown to precede upregulation of the *p*-coumarate 3-hydroxylase (VvC3H) and the cinnamoyl CoA reductase (VvCCR) enzymes that are involved in the monolignol pathway and produce the precursors of suberin and lignin (Umezawa, 2010). The researchers concluded that these activities together led to cell wall strengthening at the sites of appressorial penetration by *B. cinerea* in the resistant berries, confirmed by the lack of these activities in the susceptible berries. Numerous studies and reviews explore the involvement of ROS in pathogen induced cell-wall strengthening, and it is generally accepted to be a major factor in early plant defences against penetration (Liu et al., 2010; Mehari et al., 2017; Mellersh et al., 2002; Olson & Varner, 1993; Schulze-Lefert, 2004).

1.5.3 Regulators of programmed cell death (PCD)

After the crosslinking and thickening of the cell wall in response to a pathogen invasion, the HR causes localised programmed cell death (PCD) around points of fungal invasion. Programmed cell death is a highly regulated process that leads to the degradation of important cellular components such as lipids, proteins, and DNA, causing an irreversible breakdown of a cell (Dickman & de Figueiredo, 2013). Using observations and parallels originally drawn from animal cell apoptosis, the process of PCD in plants has been shown to result in organelle distention and disarray, plasma membrane lysis, and leakage of cellular contents (Dickman & Fluhr, 2013; Ellis, Yuan, & Horvitz, 1991; van Doorn et al., 2011). Programmed cell death is a well-studied and reviewed activity in plant defence systems where the volatile nature and signalling qualities of ROS function to kill host cells and inhibit pathogen infection (Coll, Epple, & Dangl, 2011; Dickman & Fluhr, 2013; Gechev et al., 2006; Lehmann, Serrano, L'Haridon, Tjamos, & Metraux, 2015; J. Wang et al., 2017).

In a study of cell death observed in wheat leaves around sites infected with the fungal pathogen *Puccinia striiformis* f. sp. t*ritici (Pst),* the causative agent of stripe rust disease in wheat, researchers

investigated a potential correlation between ROS accumulation and the gene encoding the Wheat kinase steroidogenic acute regulatory (StAR) protein related lipid transfer (START1) (WKS1) protein (*Yr36*), which is required for disease resistance in wheat (Li, Ren, Kang, & Huang, 2016). Researchers compared two near-isogenic wheat lines, one line with functioning *Yr36* (UC1041+*Yr36*) and another line without (UC1041), in their response to *Pst* inoculation. In the wheat line expressing *Yr36*, an oxidative burst was triggered when the *Pst* hyphae growth structures started differentiating and extending. Subsequently, the incidences of cell death occurring around the sites of penetration were significantly higher in the functioning *Yr36* lines than in the non-functioning lines. The researchers concluded that, based on the known roles of ROS and PCD in plant-pathogen interactions, it was likely that the ROS accumulation and localised cell death at infection sites contributed to the reduction of secondary hyphae growth from infection sites, thereby reducing the pathogen's virulence.

Localised PCD is generally a successful strategy against biotrophic pathogens because these microbes exist as parasites drawing in nutrients from functioning plant cells by using specialised structures such as fungal haustoria (Fatima & Senthil-Kumar, 2015). Necrotrophic pathogens, however, rely on consuming nutrients from dead host cells employing mechanisms such as the secretion of cell wall degrading enzymes and toxins for this purpose (Fatima & Senthil-Kumar, 2015). As such, evidence indicates that localised cell death may actually be beneficial to the necrotrophic pathogen lifestyle (Barna, Fodor, Harrach, Pogány, & Király, 2012; Glazebrook, 2005; Govrin & Levine, 2000). Other pathogens live as hemibiotrophs, switching from an initial biotrophic stage to a necrotrophic stage, possibly due to a quorum sensing mechanism that can detect limited nutrients (Fatima & Senthil-Kumar, 2015; Glazebrook, 2005). This may lead to a different situation, where localised cell death is at first harmful to the pathogen in its biotrophic phase but then benefits the pathogen in its necrotrophic phase (Fatima & Senthil-Kumar, 2015).

1.5.4 Inducers and regulators of signal transduction pathways

ROS have several qualities that intrinsically make them ideal signalling molecules. These qualities include instantaneous production in stressed plants and subsequent rapid removal when no longer required, a chemical reactiveness with many cellular components, an ability to permeate cell membranes, and mechanisms to induce distinct effects (Sewelam, Kazan, & Schenk, 2016). Consequently, ROS have been shown to play important roles as inducers and regulators in many of the signal transduction pathways that are activated in response to plant-pathogen interactions. In a thorough review of what is currently understood about the various signalling roles of ROS, Sewelam et al. (2016) proposed that ROS are positioned at the crossroads of a global, stress-induced, signalling defence system in plants.

Indeed, ROS have been shown to induce powerful MAPK signalling cascades that are involved in many plant processes. MAPK cascades work by translocating a signal from the initial site of

recognition by receptor molecules to regulate downstream target proteins. These cascades can lead to a wide range of outcomes such as the biosynthesis of pathogen-induced stress hormones like ethylene and salicylic acid, changes in downstream defence gene expression, and secondary metabolite synthesis (Asai, Ohta, & Yoshioka, 2008; Meng & Zhang, 2013). In *Arabidopsis* leaf cell protoplasts, Kovtun, Chiu, Tena, and Sheen (2000) demonstrated that H_2O_2 treatment activated an MAPK signalling cascade ending with the phosphorylation of *Arabidopsis* MAPK3 (AtMPK3) and *Arabidopsis* MAPK6 (AtMPK6). These two MAPKs both have well-established roles in pathogen defence responses (Galletti, Ferrari, & De Lorenzo, 2011; Nie & Xu, 2016). In more recent studies, however, some MAPK signalling cascades that occur during the PTI response were originally thought to be induced downstream of oxidative bursts but have now been placed upstream. This new view is based on results from observing normal MAPK signalling in response to flagellin or chitin in *Arabidopsis rbohD* (*NOX*) mutants where the oxidative burst is completely inhibited (Torres et al., 2002). Clearly, further studies are needed to elucidate the relationships between oxidative bursts and the many MAPK pathways in various levels of pathogen-induced defence responses.

Pathogen-induced changes in the cellular redox environment have also been shown to indirectly activate transcription factors such as in the well-understood stress hormone signalling pathway in *Arabidopsis* involving salicylic acid (SA). This pathway also involves a catalase ROS scavenger and two important proteins: nonexpressor of pathogenesis-related genes1 (NPR1), an SA receptor; and *Arabidopsis* basic leucine zipper type transcription factors (TGAs) (Despres et al., 2003). In normal conditions, NPR1 is localised to the cytoplasm of the cell. After SA biosynthesis is induced by pathogen invasion as part of a systemic defence response, ROS accumulation causes a change in the cellular redox environment (Ward et al., 1991). As a result, the disulfide bonds in NPR1 are reduced. The change in the redox environment also has an oxidative effect on TGA by increasing its affinity for NPR1. Both proteins undergo conformational changes and translocate to the nucleus and interact with each other. Their interaction regulates transcription of downstream defence-related genes such as *PR-1*, *PR-2* and *PR-5*, pathogenesis-related genes that are important in the systemic defence response pathway (Ward et al., 1991).

1.5.5 Antimicrobial compounds

Several studies and reviews include theories about the antimicrobial properties of ROS and their direct effect on pathogens, and how H_2O_2 is produced in plant cells at levels that are directly toxic to microbes (Fang, 2004; Shetty, Jorgensen, Jensen, Collinge, & Shetty, 2008; Thordal-Christensen et al., 1997; Vatansever et al., 2013). Shetty et al. (2007) concluded that the inhibition of *Septoria tritici* during its initial stage of wheat leaf invasion was due to the direct antimicrobial properties of H_2O_2 Molina and Kahmann (2007) showed that the *U. maydis* uses the YAP1 transcription factor to regulate genes that enable the fungal pathogen to scavenge ROS after an oxidative burst. After the

ROS are scavenged and stabilised, the *U. maydis* subsequently regains its virulence in maize tissue. However, it is still somewhat controversial as to whether H_2O_2 produced in an oxidative burst has a direct antimicrobial effect on plant invading pathogens. Lehman et al., (2015) suggested that rather than having antimicrobial effects, ROS are most likely to be cofactors in redox reactions that lead to expression of other defence related genes. Sewelam et al. (2016) agreed with this changing attitude and stated that research emphasis should be placed more towards the role of ROS acting as signalling molecules in larger and more complex pathways. These suggestions have also been somewhat supported by the fact that, unlike the antimicrobial phagocytosis performed by neutrophils that use ROS in mammalian systems, plant cells are not able to engulf pathogenic molecules and use the oxidative compounds to digest foreign microbes (Dickman & Fluhr, 2013; Flannagan, Cosio, & Grinstein, 2009). In summary, while some studies do show evidence of reductions in pathogenicity and virulence in pathogens after ROS treatments, and attribute such reductions to the antimicrobial properties of ROS, more recent literature generally accepts the idea that these types of results are more likely due to the compounds' involvement in complex pathways as signalling molecules.

1.6 The dual role of ROS in plant interactions with necrotrophic fungi

Increasingly, it is becoming apparent that the timing and intensity of ROS accumulation in plant tissue is a major factor in the ability of necrotrophic pathogens to infect a plant. In the early stages of plant interactions with close relatives of *C. camelliae*, *B. cinerea* and *S. sclerotiorum* from the Sclerotiniaceae family of necrotrophic fungal pathogens, these fungi can be susceptible to their host plants' ROS-mediated defences (Asselbergh et al., 2007; Mellersh et al., 2002; Williams, Kabbage, Kim, Britt, & Dickman, 2011). However, as these necrotrophic infections progress the plant-derived ROS accumulation becomes associated with susceptibility to the pathogen. For example, in their work into the interaction between tomato (*Solanum lycopersicum*) and *B. cinerea*, Asselbergh et al. (2007) showed that H_2O_2 accumulation and ROS-associated cell wall modification, together with its associated cell wall peroxidase gene upregulation, occurred earlier (4 hpi) in the abscisic acid-deficient tomato mutant than the wild-type (24 hpi). The authors also showed that the late H_2O_2 accumulation in the wild type plant was associated with cell death and susceptibility. In another example, this same study also showed that *S. sclerotiorum* initially suppresses ROS accumulation in its compatible host by secreting oxalic acid (OA), but then induces ROS accumulation and the HR to facilitate its invasion (Kim et al., 2008). Using the oxidant reactive 3,3'-diaminobenzidine (DAB) stain to visualise H_2O_2 accumulation in plant tissue, Williams et al. (2011) showed that inoculation with an OA-deficient A2 *S. sclerotiorum* strain resulted in strong DAB staining in tomato leaves surrounding infection points, as compared to the virtual absence of staining in leaves inoculated with a wild-type *Sclerotinia.* The plants infected with the OA-deficient *Sclerotinia* also had ROS-

associated callose deposition. This, combined with localised cell death from the HR, resulted in restricted growth of the fungus in the plant tissue.

The study of plant-derived ROS accumulation during the *Camellia – C. camelliae* and its relationship to other plant–pathogen interactions with the Sclerotiniaceae family of necrotrophic pathogens is still in its infancy. Prior work conducted at Massey University by Denton-Giles et al. (2013) investigated natural resistance levels of a range of *Camellia* species in response to infection by *C. camelliae*. A correlation was observed between ROS accumulation and resistance to infection. ROS accumulation was observed in *C. lutchuensis*, a highly resistant species to CFB, and little to no ROS accumulation was observed in *C.* 'Nicky Crisp', a highly susceptible species. In addition, markers of other ROS-related plant defence responses such as papillae formation and collapsed epidermal cells were singularly observed in infected petal tissue of *C. lutchuensis* but very rarely observed in *C.* Nicky Crisp' petals. Major differences were also found in the timing of ROS-associated gene upregulation in a comparison between the transcriptomes of the resistant *C. lutchuensis* and the susceptible *C.* 'Nicky Crisp' petals, with upregulation occurring earlier in *C. lutchuensis* (Kondratev et al., 2020).

1.7 Research objectives

Following previous studies into the *Camellia – C. camelliae* interaction, the focus of my study was to further elucidate the role of plant-derived ROS accumulation in the resistance and susceptibility of *Camellia* to *C. camelliae* infection. Based on prior research into plant interactions with several necrotrophic fungi from the Sclerotiniaceae family, it was hypothesised that (1) ROS accumulation plays a role in the *Camellia* defence response to *C. camelliae* infection and (2) plant-derived ROS accumulation both positively and negatively regulates CFB development.

The following objectives were put forth to test these hypotheses:

1. To identify a resistant and a susceptible species of *Camellia* suitable for experimentation. This was achieved by inoculating putatively resistant and susceptible *Camellia* species with an ascospore solution and comparing CFB lesion progression on the petals.
2. To visualise and quantify ROS accumulation in the tissue of ascospore inoculated and mock treated petals from CFB resistant and susceptible *Camellia* flowers. This was performed by applying an oxidant reactive stain to petals to microscopically observe the temporal trends of H_2O_2 accumulation in petals in response to *C. camelliae*. An oxidant reactive probe was also used to quantify the temporal changes of H_2O_2 in petal tissue after ascospore inoculation, compared with mock treated petals.
3. To quantify and compare changes in ROS-related gene expression in ascospore inoculated and mock treated petals from both CFB resistant and susceptible *Camellia* flowers. To

determine this, quantitative real-time polymerase chain reaction (qRT-PCR) was used to make comparisons between the timing of gene expression in infected and mock treated petals.

4. To determine the effects of antioxidant treatments on *C. camelliae* growth *in vitro*. To accomplish this, antioxidants in several concentrations were applied to ascospores and mycelium *in vitro* and parameters of fungal growth were measured.
5. To compare the effects of antioxidant treatments on ROS accumulation and disease development in CFB resistant and susceptible *Camellia*. To address this, exogenous antioxidant treatments were applied to ascospore inoculated flower petals and lesion area sizes were measured and compared with and without treatment. The direct effects of antioxidant treatments were also determined on parameters of *C. camelliae* growth by quantifying ascospore germination and hyphal growth *in vitro* and *in planta.*

2 Materials and Methods

2.1 Plant and fungal material

2.1.1 Camellia shrubs

During the annual CFB season in New Zealand (July to October), four to six-year-old shrubs of *C. lutchuensis* (n=12) sourced from Wairere Nursery, Hamilton, New Zealand, and *C.* 'Nicky Crisp' (*Camellia japonica* x *Camellia pitardii* var *pitardii*) (n=12) sourced from Kilmarnock Nurseries, Ashurst, New Zealand, were housed and maintained in a glasshouse located at the Massey University Manawatu Plant Growth Unit (40°37'80.54"S, 175°61'34.13"E) (Fig. 2.1). The glasshouse temperature fluctuated with the outdoor ambient temperature (between 1° and 20°C). Squares of 30 mm thick polyester wadding material were placed over ventilation units in the glasshouse to reduce the intake of windborne *C. camellia* fungal ascospores. Blooms of a similar age were uniformly selected for each experiment based on an approximate assessment of the age of the bloom, determined by the presence of freshly dehisced pollen. After flowering ceased on the shrubs located in the glasshouse, blooms were then sampled from the Victoria Esplanade *Camellia* collection (40°37'10.53'S, 175°61'38.81'E) in Palmerston North. Shrubs from the glasshouse were then transferred to an outdoor area at the Massey Manawatu Ecology Glasshouse (40°38'85.12'S, 175°62'16.26'E) and maintained throughout the year. Shrubs were re-potted and pruned annually following the blooming season and fertilised with Scotts Osmocote Roses, Gardenias, Azaleas & Camellias fertiliser (Scotts, USA).

Figure 2.1 Glasshouse with *Camellia* at the Massey University Manawatū Plant Growth Unit.

2.1.2 *Ciborinia camelliae* material

Apothecia were sampled from the Massey University Manawatu Arboretum, (40°38'37'S, 176°62'12'E), as well as the Victoria Esplanade in Palmerston North (40°37'10.53'S, 175°61'38.81'E). To harvest ascospores, four to five stipes of apothecia were wrapped together with moist lens tissue, inverted, and stored in glass universal bottles for two days prior to the start of each

experiment (Fig. 2.2). The inverted apothecia were stored in temperatures of approximately 16°-18°C. Ascospores released from the apothecia were rinsed from the tubes using 1 mL of MilliQ® (Merck, USA) water. Ascospore concentrations were quantified using a haemocytometer and adjusted to a uniform concentration for each experiment, as required. Fresh plant and pathogen material were collected in the manner described prior to the start of each experiment.

Figure 2.2 Wet ascospore collection method.
Apothecia were wrapped in moist lens tissue and inverted in a universal bottle.

A *C. camelliae* mycelium strain (ICMP 19812) was obtained from the International Collection of Microorganisms from Plants (ICMP) (New Zealand). The strain was initially harvested from sclerotia found in the Massey University Arboretum (40°22'56.2"S, 175°37'09.1"E) (Denton-Giles et al., 2013). The mycelium was cultured using aseptic technique onto 90 mm plates containing autoclaved agar made with 39 g/L of Difco™ Potato Dextrose Agar (PDA) (Difco™ Laboratories, USA) and MilliQ® water. A 5 mm hole borer was used to extract mycelium plugs for transfer to the agar plates. The plates were then incubated at 20°C for up to seven days before each experiment.

Ascospores for *in vitro* germination assays were collected with a vacuum filtration system to reduce contamination during ascospore collection (Fig. 2.3). Filter paper was placed on top of the collection funnel to collect the ascospores using gentle vacuum suction. The filter paper was then cut into 1 cm^2 squares and washed with 500 µL of MilliQ® water in a universal glass bottle. A 10 µL droplet of ascospore solution (1 x 10^5) was pipetted onto a sterile 1 cm^2 polyvinylidene fluoride (PVDF) membrane and placed on 90 mm plates of sterile 1% agarose to germinate for 24 h.

Figure 2.3 Dry ascospore collection method with vacuum filtration.
A *Ciborinia camelliae* apothecium held over a vacuum funnel to collect ascospore dispersion.

2.1.3 Petal inoculations

Before each experiment, freshly detached petals were treated with a 0.05% sodium hypochlorite solution for 30 seconds and then rinsed with MilliQ® water (Liu et al., 2013). The adaxial side of detached flower petals were spray-inoculated with a *C. camelliae* ascospore suspension in MilliQ® water using ascospores that were harvested as described. The petal spray coverage was estimated at 50,000 ascospores/cm^2. For trials with solutions applied as droplets, one 10 µL droplet of ascospore and antioxidant solutions (1x10^5 spores/mL) was applied to the adaxial side of petals using a pipette under a biosafety cabinet to reduce exposure to airborne ascospores.

For experiments including antioxidant treatments, 0.1 M stock solutions of L-ascorbic acid (Sigma-Alderich, USA), citric acid (Ajax Chemicals, Australia) and L-glutathione (Abcam, USA) were prepared using MilliQ® water. The stock solutions of antioxidants were combined with an ascospore solution for a final antioxidant concentration of 5 mM. A clean atomiser was used for the application of each treatment and petal coverage was estimated at 50,000 ascospores/cm^2. All negative control groups were treated with sterile MilliQ® water or sterile MilliQ® water combined with one of the antioxidants.

Treated petals were incubated in petri dishes with moist filter paper in a growth chamber between 20 - 21°C and under a 12-hour day/night photoperiod at 80 – 82% humidity. Petals were photographed at several time intervals in a biosafety cabinet. Any mock treated petals that developed lesions were removed from the experimental group.

2.1.4 Petal lesion measurements

Images of treated petals were obtained with a Fujifilm FinePix Z digital camera for macroscopic lesion analysis. Lesion development on five to seven petal replicates (n=5-7) from three separate experiments was analysed. Lesion area sizes were measured at 48 hpi using the 'Colour threshold' tool in the ImageJ programme (Denton-Giles et al., 2013). The lesion pixel colour space was calibrated by measuring the pixel colour range on petals fully covered with lesions. For spray inoculations, the colour space was set to YUV and petal area size was measured by adjusting the parameters to capture the entire petal as follows: Y – variable, U – 62 to 108, and V – 0 to 255. For experiments using droplet inoculations, the polygon tool was used to measure the lesion size. Lesion area sizes were calculated by dividing the number of pixels per lesion area by the total number of pixels in the entire petal area.

2.2 H_2O_2 detection methods in *Camellia* petals

2.2.1 Histology

To visualise H_2O_2 accumulation and fungal material on spray inoculated petals, a dual staining method was used as described by (Denton-Giles et al., 2013). The DAB stain (Sigma-Aldrich, USA) reacts with H_2O_2 to form a localised brown product in the plant tissue, while trypan blue stains the fungal material (Thordal-Christensen et al., 1997). A 1 mg/mL and pH 5.0 DAB solution was prepared the evening before each experiment, kept out of light, and shaken overnight. Two hours before each observation timepoint, DAB solution was injected into the base of detached petals and then incubated in the dark in sealed petri dishes with moist filter paper. Petals were then submerged in a 3:1 ethanol acetic acid fixing solution overnight. After fixing, a metal hole borer was used to excise 10 mm petal discs from the top half of the petals (Fig. 2.4)

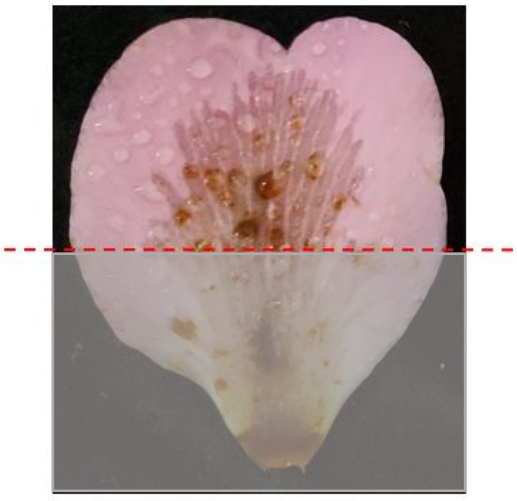

Figure 2.4 Selecting petal material for excising petal discs.

The bottom half of petal tissue was not used to excise discs of petal tissue due to brown DAB staining as a result of oxidation from a wounding response at the site of injection.

Three biological replicate discs (n=3) were wet-mounted on glass slides in a 30% glycerol solution with sterile MilliQ® water. Fingernail lacquer was used to seal edges of coverslips on to the slides. A Zeiss Axiophot light microscope with a Colour CCD camera was used to observe and capture images of petal cells and fungal material (Zeiss, Germany). In experiments that compared the timing of H_2O_2 accumulation between inoculated *C. lutchuensis* petals and *C.* 'Nicky Crisp' petals, DAB stain development was recorded as present or not present at the timepoint when staining was first evident on each petal disc.

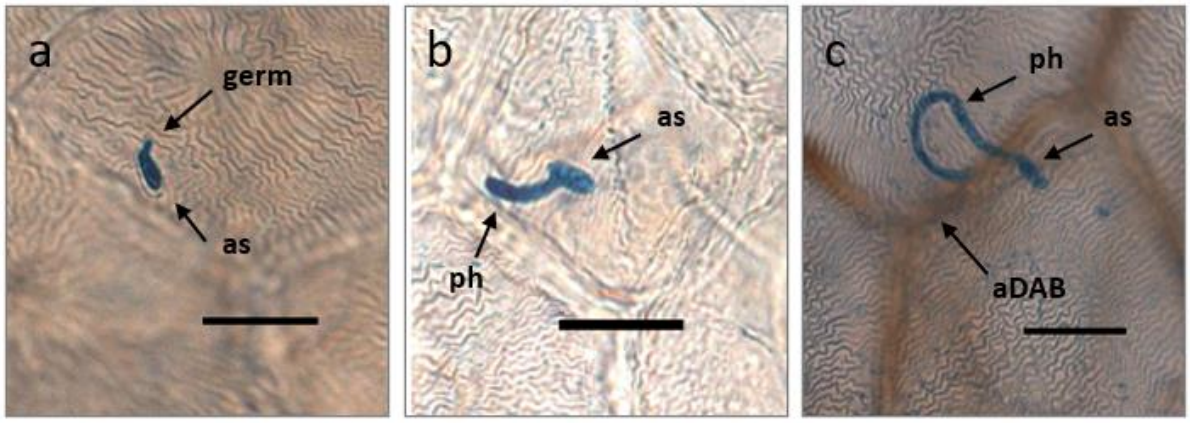

Figure 2.5 Sample image guidelines used to measure histological parameters.
A *Ciborinia camelliae* ascospore **(a)** with an asymmetrical shape indicative of the start of germination, **(b)** with hyphal growth longer than the ascospore, **(c)** with DAB stain in an adjacent apoplast. Symbols: as = ascospore; germ = ascospore germination; ph = primary hyphae; aDAB = apoplastic DAB. Scale bar = 20 µm.

For the *in planta* experiments where *Camellia* petals were treated with a combined ascospore and antioxidant solution, up to 50 spores were examined on each petal disc (n=3) and three parameters were measured: the percent of germinated ascospores (classified by an asymmetrical shape due to bud growth (Fig. 2.5a), the percent of ascospores with hyphal growth (classified as hyphal growth longer than the ascospore (Fig. 2.5b), and the percent of germinated ascospores where the brown DAB stain product was observed in an adjacent apoplast (Fig. 2.5c). Negative control groups with antioxidant solutions that did not contain ascospores were included in each experiment for comparison.

2.2.2 H_2O_2 quantification *in planta*

The protocol for plant extract preparation for H_2O_2 content measurement was adapted from (Brumbarova, Le, & Bauer, 2016) with the following change: mock and inoculated *Camellia* petals (spray coverage of 50,000 ascospores/cm^2) were used. Per biological replicate, seven *C. lutchuensis* petals (n=1) were used and one *C.* 'Nicky Crisp' petal per biological replicate (n=1) was used. Instead of the Amplex Red reagent, the Hydrogen Peroxide Assay Kit (Fluorometric - Near Infrared) (Abcam, USA) containing an oxidant-reactive probe, AbIR Peroxidase Indicator solution, was used to quantify

and compare H_2O_2 levels between mock and ascospore inoculated petals (for the full manufacturer's protocol using the method outlined for the supernatant plant extraction see: (https://www.abcam.com/hydrogen-peroxide-assay-kit-fluorometric-near-infrared-ab138886.html)). Final reaction volumes were adjusted to 100 µL and the serial dilutions of H_2O_2 were made at concentrations of: 0, 0.01, 0.03, 0.1, 0.3, 1, 3, 10 µM per the manufacturer's protocol. Absorbance of the indicator reaction solution was read at 650 nm in a microplate reader. Data were analysed in Microsoft Excel based on a standard curve created from a H_2O_2 serial dilution reaction with the AbIR Indicator Solution (Appendix A) (Brumbarova et al., 2016).

2.3 In vitro assays

2.3.1 Mycelium culture and antioxidant treatments

To investigate the *in vitro* effects of several antioxidants on mycelial growth of *C. camelliae*, sterile stock solutions of L-ascorbic acid, citric acid, or L-glutathione were made with MilliQ® water. Antioxidants were added to autoclaved PDA to create final concentrations of 0, 1, 5, or 10 mM of each antioxidant in 90 mm plates. Media without antioxidants were used as a control. After four days of incubation at 20°C, the average of two diameter measurements was taken for each plate and the average diameter was calculated for each treatment group (n=11).

2.3.2 Ascospore germination and antioxidant treatments

C. camelliae ascospores were collected as previously described. Aliquots of 100 µL of ascospore solution at a concentration of 1 x 10^5 spores/mL were spread on agar plates containing 5 mM of L-ascorbic acid, citric acid, or L-glutathione and incubated at ambient temperature (approximately 20°C) for four days. Ascospore germination was determined by the oval ascospores showing a polarized phenotype or hyphal growth at 24 hpi (Fig. 2.6).

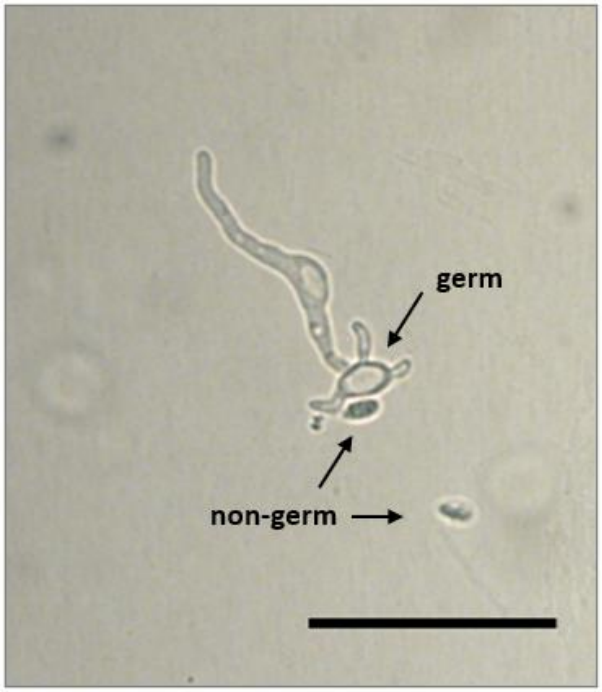

Figure 2.6 Microscopic image of *Ciborinia camelliae* ascospores *in vitro*.
Ascospores were analysed with light microscopy and determined to be germinated if they showed a polarised phenotype or had hyphal growth Symbols: germ = germinated ascospore; non-germ = an ascospore that did not germinate. Scale bar = 50 µm

2.4 Molecular analysis

2.4.1 Primer sequence design

Primer sequences were retrieved from assembled and annotated reference transcriptome databases for *C. lutchuensis* (PRJNA518136) and *C.* 'Nicky Crisp' (PRJNA518146) located in the National Center for Biotechnology Information (NCBI) BioProject database (https://www.ncbi.nlm.nih.gov/bioproject) (Kondratev et al., 2020). First, orthologous sequences were identified for common plant housekeeping genes using the transcriptome database for *C.* 'Nicky Crisp': *actin, clathrin, EF-1α, PTB-1* and *Tubulin*. Using both transcriptome databases, orthologous sequences for *NOX* and *PER* genes were identified for each *Camellia* species. Primers were designed using the US National Institute of Health Primer-BLAST website (https://www.ncbi.nlm.nih.gov/tools/primer-blast/) to have an amplicon length of between 80-200 bp and a melting temperature of 60° C ± 2° for use in qRT-PCR. Primers were selected based on minimal probabilities of hairpin formation and dimerization. All primers were synthesised by Macrogen (Republic of Korea). Coding sequences for primers are recorded in (Appendix B).

2.4.2 Primer stock preparation

Stock primer solutions of 100 pmol/µL were made by dissolving Macrogen primers into 250 µL of sterile MilliQ® water. Working primer solutions of 10 pmol/µL were then made and stored at -20°C.

2.4.3 RNA extraction and quality control

Mock and inoculated petals were removed from incubation at pre-determined timepoints and ground into a fine powder using a pre-chilled mortar and pestle and liquid nitrogen. Seven *C. lutchuensis* petals (n=1) were used per biological replicate and one *C.* 'Nicky Crisp' petal (n=1) was used per biological replicate to obtain enough material for RNA extraction. The powder was collected in pre-chilled 2 mL tubes. RNA was extracted from the petal powder immediately or stored at -80°C for future extraction.

To extract RNA from ground mock and infected petal tissue, a Quick-RNA™ Miniprep Kit (Zymo Research, USA) was used according to the manufacture's protocol. RNA lysis buffer (1 mL) was added to the 2 mL tubes containing frozen ground petal tissue and the tubes were kept on ice for no more than 5 min, with periodic inversion to mix the samples. The tubes were centrifuged at 16,000 g for 1 min in a pre-chilled centrifuge. A portion of the supernatant (500 µL) was transferred into a Spin-Away TM filter column inserted into a collection tube. The combined column and tube set-up for each sample was placed back in the pre-chilled centrifuge and run for 30 s more at 16,000 g. The columns were then discarded and 500 µL of ethanol were added to the tubes containing the flow-through, for a total volume of 1 mL. The final solution was transferred into a new RNA-binding column (Zymo-Spin TM IIICG) and centrifuged at 16,000 g for 30 s. The flow-through was discarded and the step was repeated with the remaining half of the solution (500 µL). The RNA-bound columns were then washed with 100 µL of the wash buffer by centrifuging at 16,000 g for 30 s. The flow-through was again discarded. A droplet of DNase mixture was carefully placed on top of the RNA-bound filter in the column and placed on a heat block at 37°C for 15 min to activate the DNA digestion. Each column was washed with 400 µL of RNA Prep Buffer, followed by 700 µL of RNA Wash Buffer, and finally with 400 µL of RNA wash buffer, and centrifuged for 30 s at 16000 g between each wash step. The collection tubes were discarded, and the RNA-bound columns were placed in 1.5 mL plastic tubes. RNA was eluted from the columns with 50 µL of the DNase/RNase free water by centrifuge at 16,000 s for 1 min. The final RNA product was stored in the 1.5 mL tubes at -80°C.

The quality and quantity of RNA in each extracted sample were determined using a Nanodrop spectrophotometer (ThermoFisher Scientific). Absorbance ratios of 260 nm/ 280 nm and 260 nm/ 230nm were used to assess the purity and quantity of the RNA, respectively. Samples with a 260 nm/280 nm absorbance value of ≥1.8 and a 260 nm/230nm absorbance value of ≥1.5 were used for further experimentation. RNA sample integrity was also checked by 1% agarose gel electrophoresis, as described below, and then labelled and stored at -80°C.

2.4.4 First strand cDNA synthesis

Extracted RNA was used as a template to make cDNA using the Transcriptor First Strand cDNA Synthesis Kit (Roche Life Science, USA). RNA samples of 1 µg were transferred into 200 µL PCR tubes and combined with 1 µL Anchored-Oligo Primers and water from the kit, for a total volume of 13 µL. The sample tubes were placed in a Mastercycler® Pro Thermal Cycler (Eppendorf, Germany) and heated at 65°C for 10 min. The following were added to each sample: 0.5 µL of RNase Inhibitor Solution, 0.5 µL of Reverse Transcriptase Enzyme Solution, 2 µL of Deoxynucleotide Mix, and 4 µL of 5X Reaction Buffer. The sample tubes were returned to the Thermal Cycler and heated at 55°C for 30 min and then 85°C for 5 min to end the reaction. cDNA samples were stored at -20°C.

2.4.5 Standard PCR

Extracted RNA and synthesised cDNA samples were checked by standard PCR. From the 10 pmol working primer stock solutions, 1 µL each of the forward and reverse gene of interest (GOI) primers was combined with 12.5 µL of Taq 2x Master Mix (New England Biolabs Inc., USA) and sterile MilliQ® water to create a final volume of 25 µL in a PCR tube. The sample tubes were placed in a Mastercycler® Pro Thermal Cycler (Eppendorf, Germany). An initial denaturation cycle was performed at 95°C for 5 min; followed by 30 reaction cycles of 95°C for 30 s, 60°C for 15 s, and 68°C for 10 s; and, a final extension cycle of 68°C for 5 min.

2.4.6 cDNA sequencing

The *Camellia* 'Nicky Crisp' reference gene cDNA was amplified by standard PCR using the designed *PTB1* and *Tubulin* primers. The amplified cDNA for the *PTB1* and *Tubulin* genes were sequenced by the Massey Genome Service. cDNA sequences were aligned with reference sequence from NCBI (*C. sinensis PTB1*, Accession# XM_028250187.1 and *C. sinensis Tubulin*, Accession#XM_028195689.1) using the Geneious R9 software package v. 9.1.8 (http://geneious.com).

2.4.7 Agarose gel electrophoresis

PCR products, extracted RNA, and synthesised cDNA were quality checked using agarose gel electrophoresis, with gDNA, RNA, and water as negative controls as appropriate. A 1% or 2% agarose gel was prepared, depending on the length of the product of interest. HyAgarose™ LE Multi-purpose Agarose powder (HydraGene, China) was combined with 100 mL of tris-acetate-ethylenediaminetetraacetic acid (EDTA) (TAE) buffer (40 mM tris, 20 mM acetic acid and 1 mM EDTA) and microwaved for 30 s intervals until the agarose powder was completely dissolved. The gel solution was poured into casting trays and left to solidify for approximately 30 min. Blue loading dye (New England Biolabs) was added to each sample and 20 µL of the solution was pipetted into individual wells in the gel. A DNA ladder (HyperLadder™ 1 kb, Bioiline, UK) was included to check sample bp lengths. Gels were run in gel boxes with TAE buffer for 35 min at 100 V. Gels were then

removed and soaked in 10 µg/mL of ethidum bromide and MilliQ® solution for 15 min. The Gel Doc XR+ System with Image Lab software V6.0 (Bio-Rad, USA) was used to visualise stained gels.

2.4.8 Quantitative real-time polymerase chain reaction (qRT-PCR)

The LightCycler® 480 SYBR Green I Master kit (Roche Life Science, Germany) was used to prepare samples for qRT-PCR per the manufacturer's protocol as follows: 2.5 µL of 10-fold diluted synthesised cDNA combined with 0.5 µL each of forward and reverse primers for the target genes (10 pmol/µL), 5 µL of 2X SYBR Green I Master Mix, and 1.5 µL of Rnase/Dnase free water from the Master kit. Three biological replicates (n=3), with three technical replicates each, were also included. The negative control for each gene primer contained water from the kit as a substitution for the aliquot of cDNA. The samples were then pipetted into a 96-well Light Cycler plate, covered with a plastic film, and loaded into a LightCycler® 480 Instrument II (Roche Life Sciences, USA). The reaction process consisted of an initial denaturation cycle at 95°C for 5 min, followed by 35 cycles of 95°C for 10 s, 60°C for 10 s, and 72°C for 10 s, and then cooled at 40°C for 30 s. Raw data were exported to and converted in a Microsoft Excel file using the LightCycler® 480 Conversion software (Roche Life Sciences, USA). The data were analysed to determine qRT-PCR quantitation cycle (Cq) values and the primer efficiencies, using LinRegPCR software v. 2015.0.0.0 (Ruijter et al., 2009). Two endogenous reference genes from both *C. lutchuensis* (eukaryotic elongation factor-1 alpha (*EF-1α*) and polypyrimidine tract-binding protein 1 (*PTB1*)) and *C.* 'Nicky Crisp' (polypyrimidine tract-binding protein 1 (*PTB1*) and tubulin alpha-3 (Tub α-3)) were used as control transcripts, because they were stably expressed throughout all timepoints and treatments (Hao et al., 2014). Primer sequences are presented in (Appendix B).

Relative gene expression fold-change in petals, in response to ascospore inoculation and time post inoculation, was calculated as follows:

$$\text{Relative expression} = \frac{\text{Primer efficiency of target gene}^{(\text{calibrator } Cq_{target} - \text{treatment } Cq_{target})}}{\text{Primer efficiency of control gene}^{(\text{calibrator } Cq_{control} - \text{treatment } Cq_{control})}}$$

where,

- the 'calibrator Cq_{target}' = the mean Cq value of the GOI in the control treatment samples;
- the 'treatment Cq_{target}' = the mean Cq value from three technical replicates of the GOI in the analysed samples;
- the 'calibrator $Cq_{control}$' = the mean Cq value of the reference genes in the mock control treatment samples; and,

- the ‘treatment $Cq_{control}$’ = the mean value from the three technical replicates of the reference genes in the analysed samples.

2.5 Statistical analysis

The statistical analysis for petal lesions, mycelium colony diameters, and ascospore germination *in vitro* was performed in Microsoft Office Excel 2016 using the standard Student’s t-test two-tailed formula. The significance level for each test and P values are listed in the figure descriptions in the results section (Chapter 3). R Studio software (http://r-project.org/) was used for two-way ANOVA tests (time x treatment), Tukey’s Honest Significant Difference tests, and Fisher's Exact Test for Count Data. The R command coding that was used is presented in Appendix D. Data collected as a ratio (e.g. the percent of ascospores with hyphal growth out of the total ascospores counted) was transformed using the Arc-sin data transformation in Excel (=asin(sqrt(A2)) before statistical testing with ANOVA. The statistical significance is then presented with the pre-transformed data in the Results (Chapter 3).

3 Results

3.1 *Camellia* flower blight develops more severely in detached petals of susceptible *Camellia* 'Nicky Crisp' than in resistant *Camellia lutchuensis*

There is a spectrum of CFB natural resistance and susceptibility within the *Camellia* genus (Couselo et al., 2014; Denton-Giles et al., 2013; Taylor, 2004). I hypothesised that, under my experimental conditions, CFB resistant *C. lutchuensis* petals would not develop necrotic lesions 48 hpi but that CFB susceptible *C.* 'Nicky Crisp' would develop severe necrotic lesions. Detached petals from both plants were spray-inoculated with *C. camelliae* ascospore suspension with a coverage of approximately 50,000 ascospores/cm^2 and incubated as described (Chapter 2). CFB lesion measurements were made over 48 hours. By 48 hpi, *C. lutchuensis* petals did not develop necrotic lesions (Fig. 3.1a, c). In contrast, *C.* 'Nicky Crisp' petals developed severe necrotic lesions covering an average of 100% of the petal surface area (Fig. 3.1b, c). Mock-inoculated petals did not develop necrotic lesions in either group, demonstrating that the lesion development seen on *C.* 'Nicky Crisp' was due to the manual inoculation with *C. camelliae* ascospores. In conclusion, evidence was obtained in this experiment to show that *C. lutchuensis* petals are more resistant to CFB than *C.* 'Nicky Crisp' petals during the first 48 hpi.

a

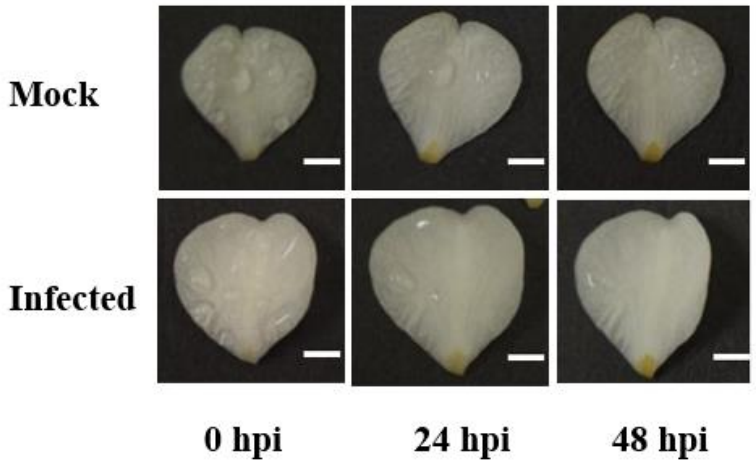

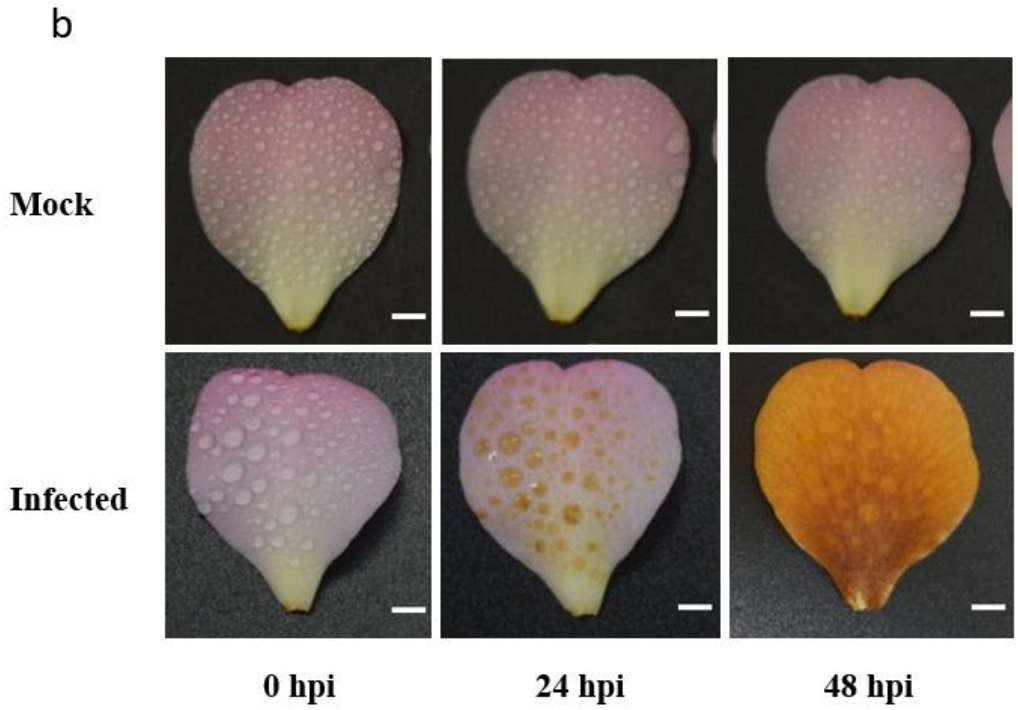

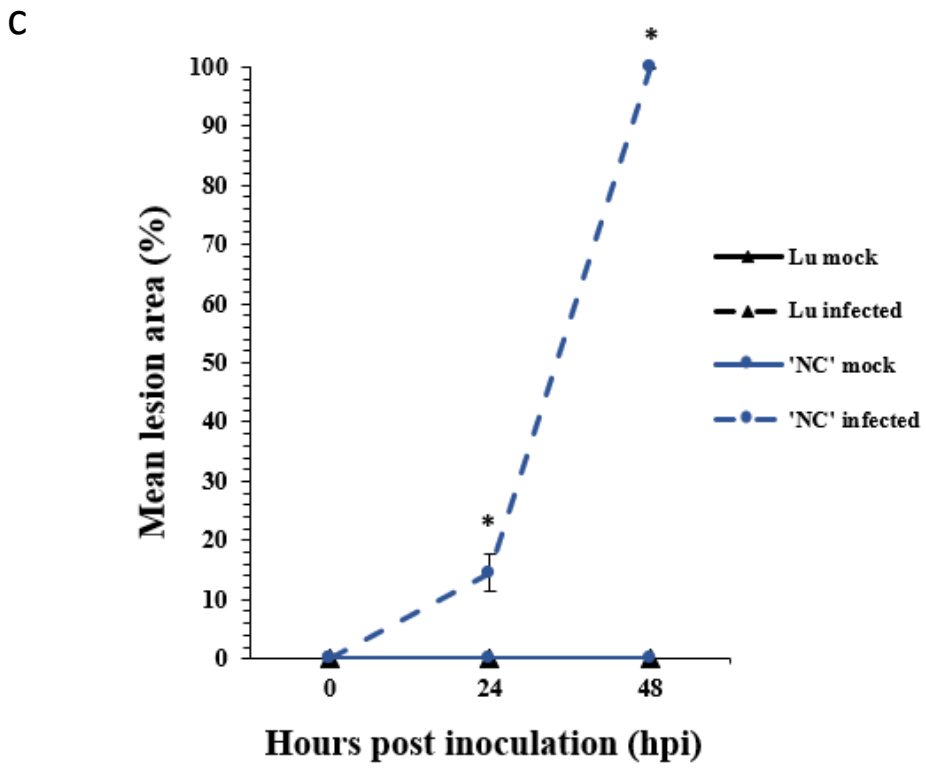

Figure 3.1 Analysis of lesion development on resistant *Camellia lutchuensis* and susceptible *Camellia* 'Nicky Crisp' during the first 48 hours post-inoculation with *Ciborinia camelliae* ascospores.
Petal blight disease symptoms in mock treated petals and petals after inoculation with *C. camellia* ascospore suspension **(a)** *C. lutchuensis* (Lu) and **(b)** *C.* 'Nicky Crisp' ('NC'). Petal images are representative of the biological replicates from each treatment group (n=6). **(c)** Progression of CFB lesion growth at 0, 24, and 48 hours post-inoculation (hpi) in CFB resistant *C. lutchuensis* and susceptible *C.* 'Nicky Crisp' after inoculation with a *C. camellia* ascospore suspension, compared to mock treated petals. Each data point signifies the mean

lesion area (%) of biological replicate petals (n=6). Error bars indicate standard error of the means. * indicates a significant difference in petals inoculated with the *C. camellia* ascospore suspension from mock treated petals using Student's two-tailed t-test at $P < 0.05$. Scale bars = 5 mm

3.2 Hydrogen peroxide accumulates earlier in the cellular apoplasts of *C. lutchuensis* petals than in *C.* 'Nicky Crisp' petals post-inoculation

The rapid accumulation of ROS in the apoplastic space is an early plant defence response to pathogen invasion (Denton-Giles et al., 2013; Mellersh et al., 2002). I hypothesised that CFB resistant *C. lutchuensis* petals would accumulate H_2O_2 in the cell apoplast near the sites of ascospore germination, while susceptible *C.* 'Nicky Crisp' petals would not. To investigate this hypothesis, a widely used technique was used to visualise and compare ROS accumulation in plant tissue in response to ascospore inoculation. The combined application of DAB stain and trypan blue stain can confirm the proximity of H_2O_2 accumulation near germinating ascospores (Thordal-Christensen et al., 1997). In the presence of H_2O_2, the applied DAB stain is polymerised to create a brown product in the tissue that is visible microscopically. The localisation of H_2O_2 accumulation can then be compared to fungal tissue growth in the petals stained blue by trypan blue.

Camellia petals were inoculated with a *C. camelliae* ascospore suspension at a concentration 1×10^6 ascospores/mL and incubated as described (Chapter 2). Petals were then treated with DAB stain and trypan blue in lactoglycerol and examined under a light microscope as described (Chapter 2). H_2O_2 accumulation was observed near *C. camelliae* spores in infected *C. lutchuensis* petal sections by 12 hpi (Fig. 3.2a). H_2O_2 accumulation was not observed in *C.* 'Nicky Crisp' petal discs at 12 hpi (Fig. 3.2c); however, at 24 hpi, H_2O_2 did begin to accumulate in very few observed instances (Fig. 3.2d, e). Because H_2O_2 accumulation was observed in *C.* 'Nicky Crisp' petals, the hypothesis was rejected. In conclusion, H_2O_2 was induced in petals of both plants but the timing of the accumulation during the *Camellia – C. camelliae* interaction differed. H_2O_2 accumulation began at least 12 hours earlier in resistant *C. lutchuensis* petals (12 hpi) and at a much higher frequency than in susceptible *C.* 'Nicky Crisp' (24 hpi).

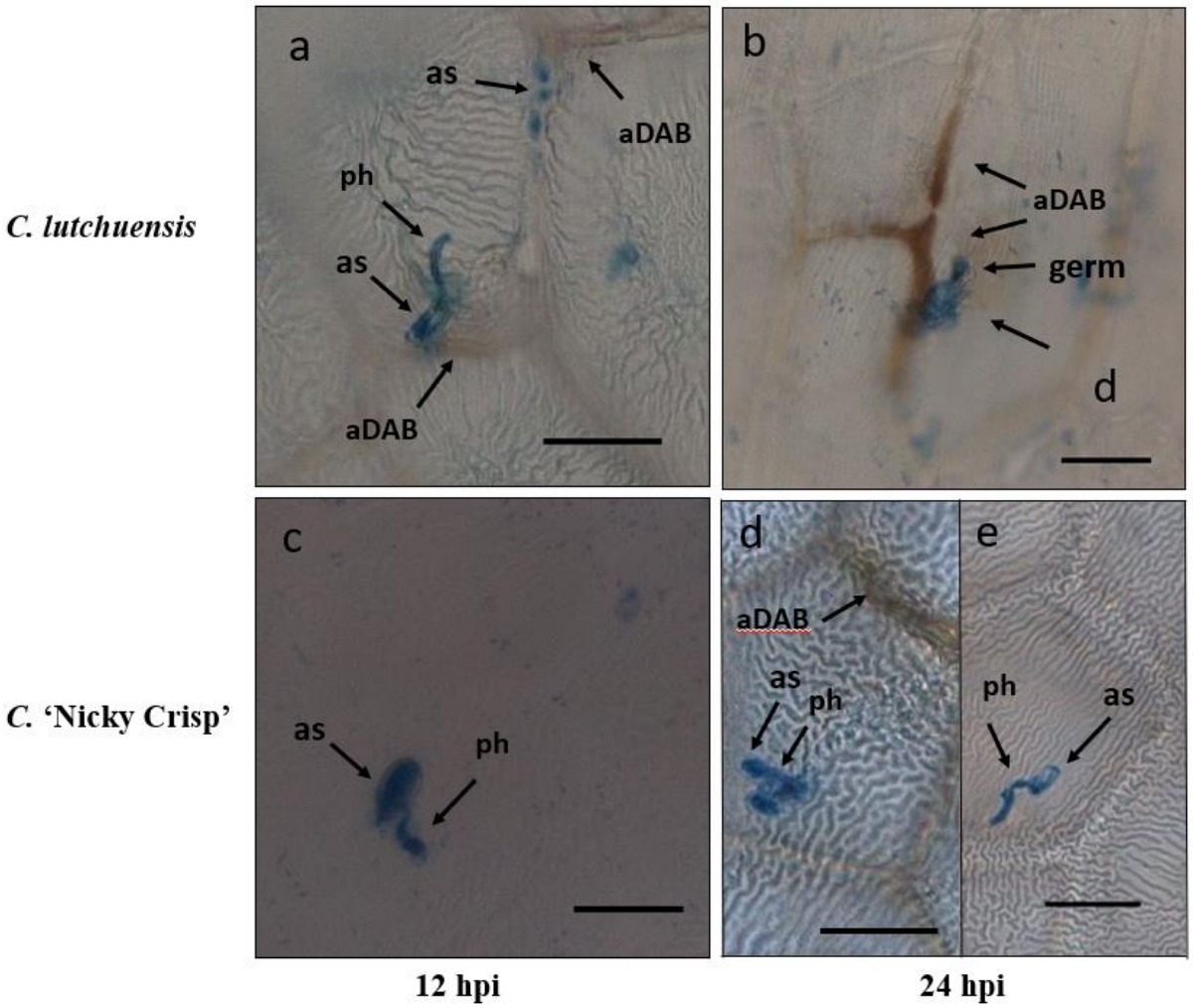

Figure 3.2 Macroscopic images of DAB staining in apoplasts adjacent to *Ciborinia camelliae* material in *Camellia lutchuensis* and *Camellia* 'Nicky Crisp' at 12 and 24 hours post inoculation.
Light micrographs of apoplastic H_2O_2 development stained with 3,3' diaminobenzidine (DAB) and trypan blue and lactoglycerol in detached petals of CFB disease **(a)** resistant *C. lutchuensis* and **(c)** susceptible *C.* 'Nicky Crisp' at 12 hours post-inoculation (hpi) with a *C. camelliae* ascospore suspension, and **(b)** resistant *C. lutchuensis* and **(d)** susceptible *C.* 'Nicky Crisp' at 24 hpi with DAB staining **(e)** and without DAB staining. Images are representative of the biological replicates from each treatment group (n=3). Symbols: as = ascospore; ph = primary hyphae; germ = ascospore germination; aDAB = apoplastic DAB stain. Scale bars = 20 µm.

3.3 Quantitative hydrogen peroxide analysis confirms a difference in the timing and quantity of hydrogen peroxide accumulation in CFB resistant *C. lutchuensis* compared with susceptible *C.* 'Nicky Crisp' post-inoculation

Previous results from DAB stain treatments show that H_2O_2 accumulation was visually detected in the apoplastic spaces of *C. lutchuensis* petals earlier (12 hpi) than in *C.* 'Nicky Crisp' petals (24 hpi) after inoculation with a *C. camelliae* ascospore suspension. Therefore, I hypothesised that the quantity of H_2O_2 present in *C. lutchuensis* petal tissue would increase earlier in inoculated petals than in inoculated *C.* 'Nicky Crisp' petals. To measure and compare the temporal changes in apoplastic H_2O_2 quantities between the two *Camellia* plants during the interaction with *C. camelliae*, detached petals were spray inoculated with an ascospore suspension and incubated for 24 h. A supernatant derived

from whole petals was prepared for each sample across four timepoints and H_2O_2 was quantified with an H_2O_2 reactive probe as described (Chapter 2).

A significant increase in the average H_2O_2 quantity was observed in *C. lutchuensis* petals from 6 hpi (2 pmol/mg of fresh tissue weight (FW)) to 12 hpi (16 pmol/mg FW) (Fig. 3.3a). A significant decrease in H_2O_2 levels was then observed at 24 hpi, falling back to an average level similar to measurements taken at 6 hpi. Significant changes in the average quantity of H_2O_2 were not observed in inoculated *C.* 'Nicky Crisp' at the timepoints measured (Fig. 3.3b). In summary, the average quantity of H_2O_2 in inoculated *C. lutchuensis* petals was significantly higher at 12 hpi compared to 6 and 24 hpi, while no significant change was observed in inoculated *C.* 'Nicky Crisp' petals at any timepoint. These results partially agreed with my hypothesis because there was a significant increase in the quantity of H_2O_2 in inoculated *C. lutchuensis* petals, although no significant change was observed in *C.* 'Nicky Crisp'.

a

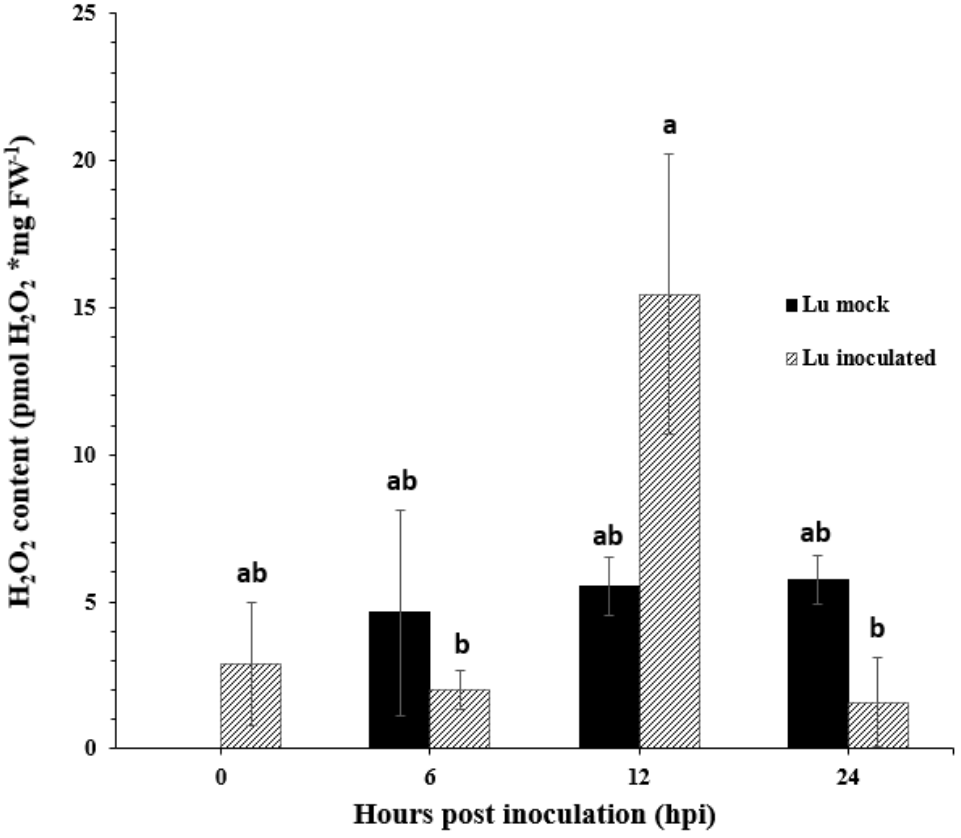

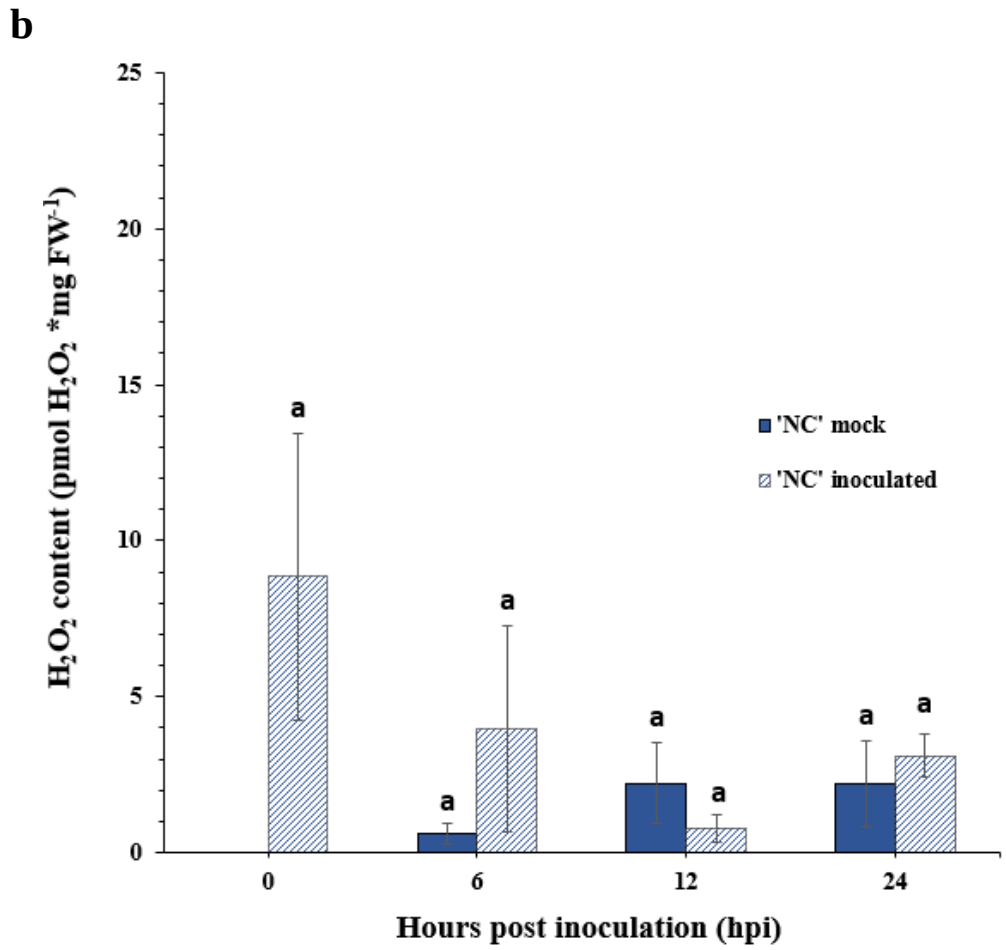

Figure 3.3 A quantitative analysis and comparison of hydrogen peroxide levels in CFB resistant *Camellia lutchuensis* petals and susceptible *Camellia* 'Nicky Crisp' post-inoculation
H_2O_2 content was calculated as picomoles per milligram of fresh tissue weight (FW) in petals after inoculation with a *C. camellia* ascospore suspension in **(a)** *C. lutchuensis* and **(b)** *C.* 'Nicky Crisp'. Each column signifies the mean H_2O_2 concentration of three biological replicates (n=3). Error bars indicate standard error of the means. Two-way ANOVA (time x treatment) and Tukey's Honest Significant Difference tests were used to analyse the data. The same letter above a column indicates that concentration levels did not significantly differ between the conditions ($P < 0.05$).

3.4 qRT-PCR data supports the results of the visual and quantitative analysis of H_2O_2 accumulation in *C. lutchuensis* and *C.* 'Nicky Crisp' post-inoculation

qRT-PCR is a widely used method to quantify changes in gene transcript levels during various biological processes and responses to treatments. Because H_2O_2 levels increased earlier in ascospore inoculated *C. lutchuensis* petals than in *C.* 'Nicky Crisp' petals, I hypothesised that two gene classes associated with early apoplastic H_2O_2 accumulation in response to pathogen attack—plasma membrane localised nicotinamide adenine dinucleotide phosphate (NADPH) oxidase (*NOX*) and class III apoplastic peroxidase (*PER*)—would be upregulated earlier in *C. lutchuensis* petals compared to *C.* 'Nicky Crisp' (Bindschedler et al., 2006; Torres et al., 2002). To test this hypothesis, qRT-PCR was used to compare the timing of changes in the transcript expression levels of an ortholog of NADPH

oxidase identified in *Arabidopsis thaliana*, respiratory burst oxidase homologs (*RBOH)*, and an ortholog of class III peroxidase (*PER*).

3.4.1 Reference gene primer design for PCR using a *C.* 'Nicky Crisp' transcriptome

Stably expressed reference genes are needed for use in qRT-PCR to serve as a basis of comparison for the expression levels of the target GOIs. Two reference genes were previously identified in *C. lutchuensis*, eukaryotic elongation factor-1 alpha (*EF-1α*) and polypyrimidine tract-binding protein (*PTB1*) (Hao et al., 2014; Kondratev et al., 2020). However, suitable reference genes needed to be identified in *C.* 'Nicky Crisp'. Five plant housekeeping genes were selected for testing based on previous research into viable reference genes from the closely related tea plant, *C. sinensis* (Hao et al., 2014; Wang et al., 2017). Using a sequenced, assembled, and annotated *C.* 'Nicky Crisp' transcriptome, primers for orthologous housekeeping genes were identified and designed as described (Chapter 2). Two sets of primer sequences were designed for each gene to be tested (Appendix B). Standard PCR was performed using the designed primers and cDNA that was synthesised from *C.* 'Nicky Crisp' RNA extractions as described (Chapter 2). The PCR results showed that only one product of the correct size was amplified with each primer (Fig. 3.4).

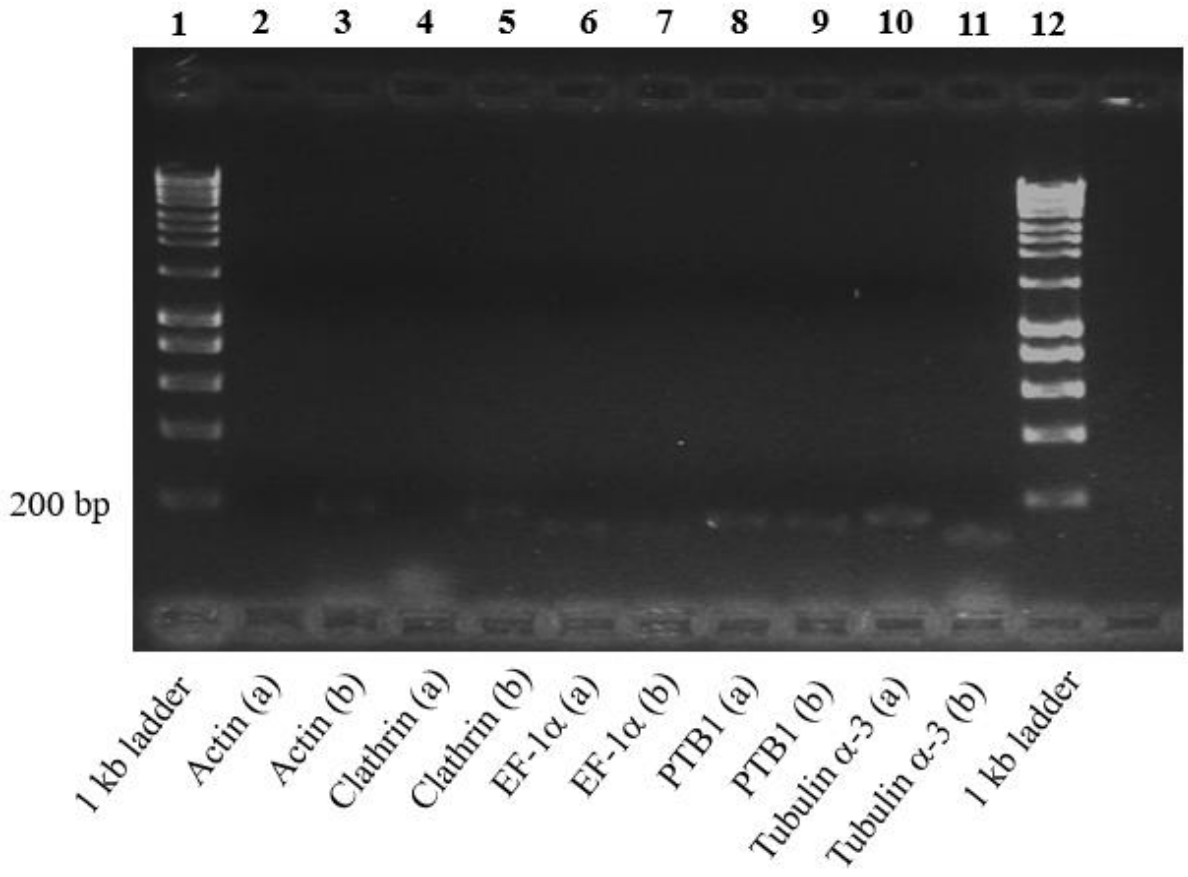

Figure 3.4 Gel image of PCR products from housekeeping gene primer candidates designed using a *Camellia* 'Nicky Crisp' transcriptome.
Single PCR products are present on the gel for each primer candidate, *Actin*, *Clathrin*, Elongation Factor-1α *(EF-1α)*, Polypyrimidine tract-binding protein 1 (*PTB1*), and Tubulin alpha-3 (*Tubulin α-3*) at the expected

base pair (bp) length (Appendix B). Two primer candidates were prepared for each primer notated by (a) or (b) following the gene name. The image brightness was adjusted to more clearly show the PCR products.

3.4.2 Identification of reference genes in *C.* 'Nicky Crisp' for use in qRT-PCR

Based on the results of the previously described primer design and PCR, four of the five primers were selected for use in a qRT-PCR using amplified *C.* 'Nicky Crisp' cDNA as described (Chapter 2). Analysis of the gene expression levels from the qRT-PCR indicated that expression was stable for two of the four genes tested (Figure 3.5a). Therefore, the polypyrimidine tract-binding protein 1 (*PTB1*) and Tubulin alpha-3 (*Tubulin α-3*) primers were selected for further analysis. The graphical melting curve output from qRT-PCR analysis also showed one peak for each primer, indicating that only one PCR product was present (Fig. 3.5b, c).

a

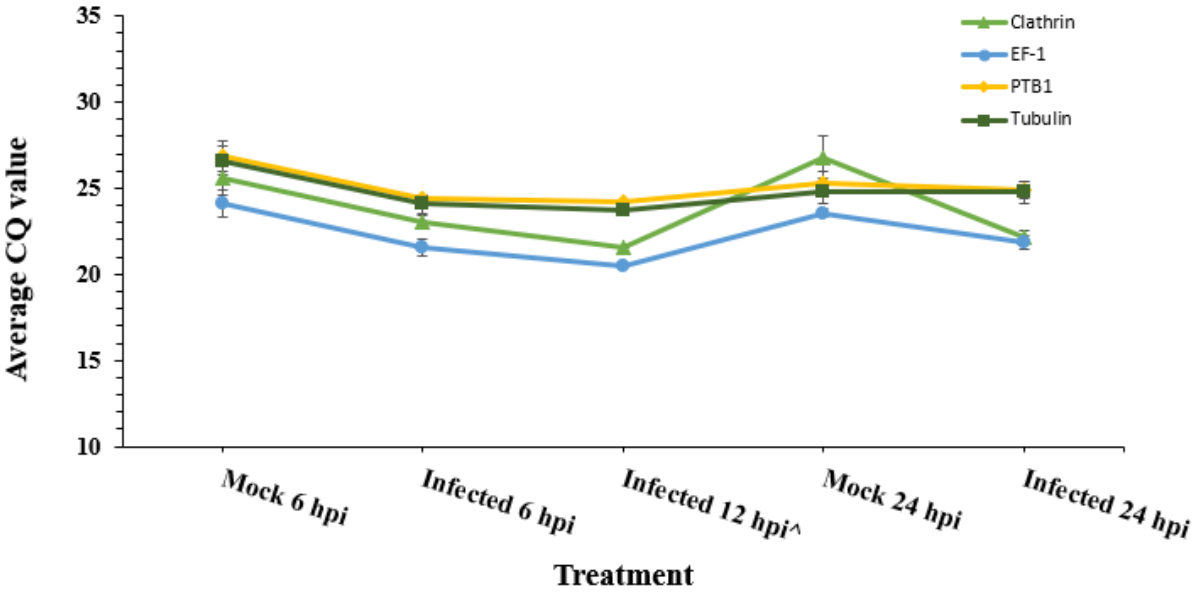

b

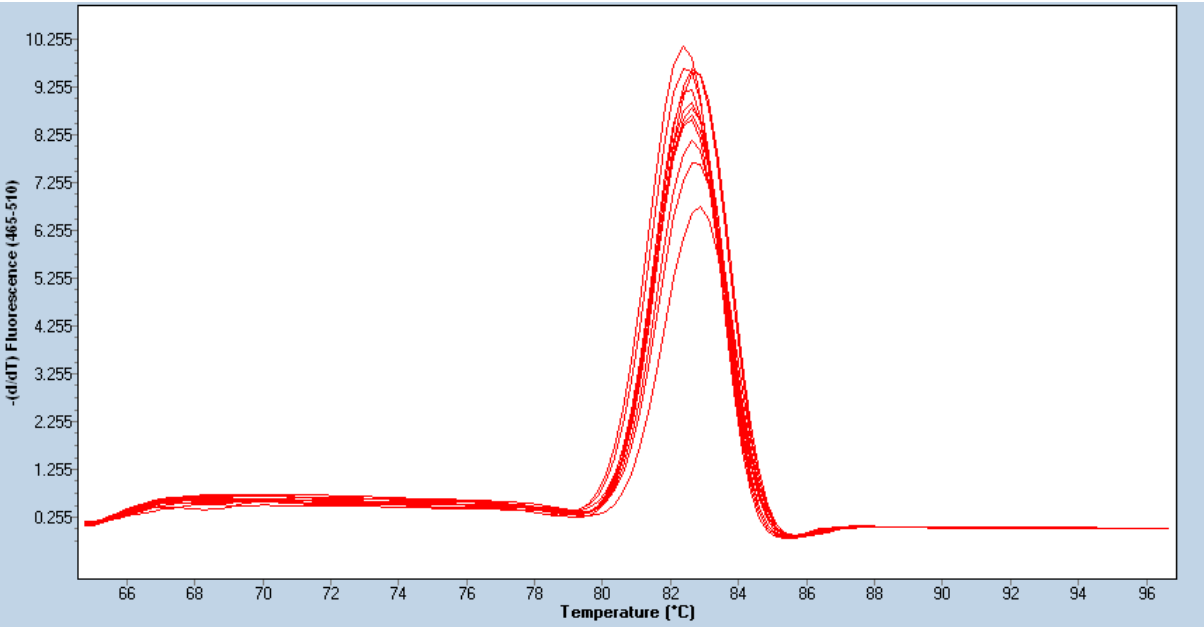

c

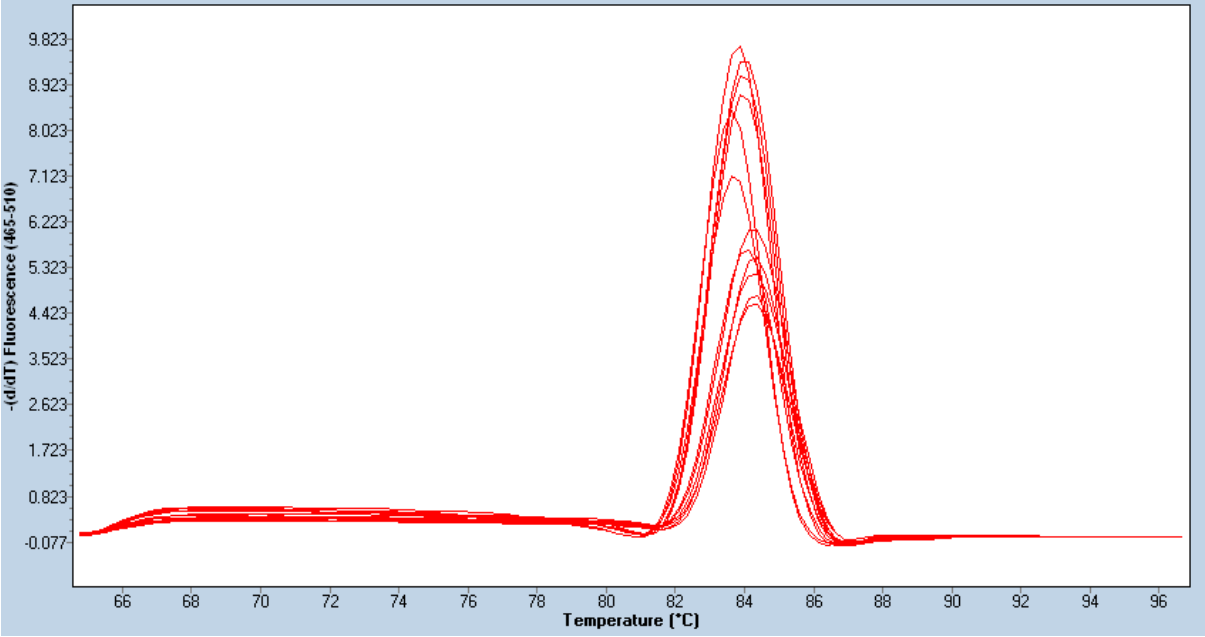

Figure 3.5 Transcript expression patterns of housekeeping genes, *Clathrin, EF-1α, PTB1*, and *Tubulin* α-3 in *Camellia* 'Nicky Crisp' mock and treated petals over 24 hours.
(a) Each data point signifies the mean Cq value of the target gene in three biological replicates. ^ indicates only one biological replicate for this timepoint. Error bars indicate standard error of the means. Melt curve analysis of amplicons from *C.* 'Nicky Crisp' cDNA shows a single peak for housekeeping primers **(b)** *PTB1* and **(c)** *Tubulin α-3*.

The melting curves, combined with the previous PCR data, confirmed that the *PTB1* and *Tubulin α-3* primers amplified only one cDNA product of the correct size. Sequencing results obtained from the Massey Genome Service and alignment to the reference genome confirmed that the correct cDNA genes were amplified. The *Tubulin α-3* sequence had two mismatches compared to the reference gene transcript. However, the first mismatch was a synonymous substitution that still coded for serine (AGT or AGC), and the second mismatch still coded for leucine (CTG or TTG) (Appendix C). Therefore, I was able to conclude that the correct orthologous *C.* 'Nicky Crisp' reference genes were positively identified in the samples and that the *PTB1* and *Tubulin α-3* primers designed in this study were correct for use in further qRT-PCR experiments.

3.4.3 The timing of NOX and PER transcript expression differs in CFB resistant *C. lutchuensis* petals from susceptible *C.* 'Nicky Crisp'

Next, relative transcript expression levels of *NOX* and *PER* genes were measured in *C. camelliae* inoculated *C. lutchuensis* and *C.* 'Nicky Crisp' petals over 24 hpi. Relative expression levels were measured using qRT-PCR as described (Chapter 2) (Fig. 3.6). *NOX* expression in the CFB resistant *C. lutchuensis* was significantly higher at 6 hpi compared to 0 hpi. Expression levels were maintained at 12 hpi before declining at 24 hpi to similar levels from 0 hpi (Fig. 3.6a). In contrast, a significant increase in NOX expression in the susceptible *C.* 'Nicky Crisp' did not begin until 12 hpi compared to 0 hpi (Fig. 3.6b). NOX expression was highest at the final timepoint measured, 24 hpi. In the resistant *C. lutchuensis*, *PER* expression levels peaked at 12 hpi, and then at 24 hpi the levels returned to levels similar to 0 hpi (Fig. 3.6c). *PER* expression in susceptible *C.* 'Nicky Crisp' did not significantly increase until 24 hpi (Fig. 3.6d). Mock treated petals from either plant did not see any significant differences in the relative gene expression levels. In conclusion, these results support my hypothesis that the *NOX* and *PER* genes tested in this study were upregulated earlier in *C. lutchuensis* petals than in *C.* 'Nicky Crisp' in response to inoculation with a *C. camelliae* ascospore suspension.

a

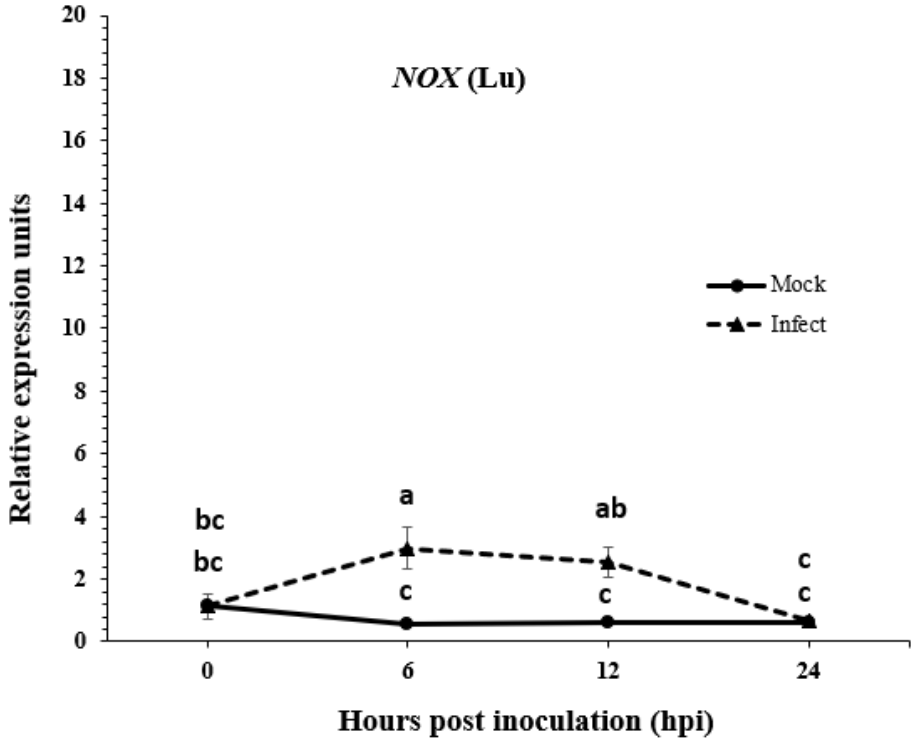
NOX (Lu)
Relative expression units
Hours post inoculation (hpi)
Mock
Infect
0
6
12
24
bc
bc
a
c
ab
c
c
c

b

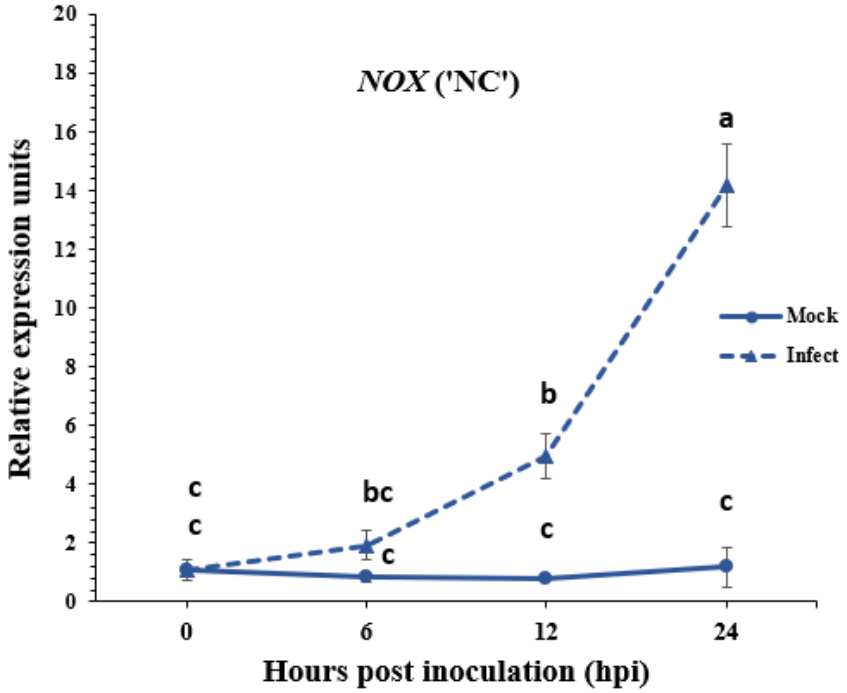
NOX ('NC')
Relative expression units
Hours post inoculation (hpi)
Mock
Infect
0
6
12
24
c
c
bc
c
b
c
a
c

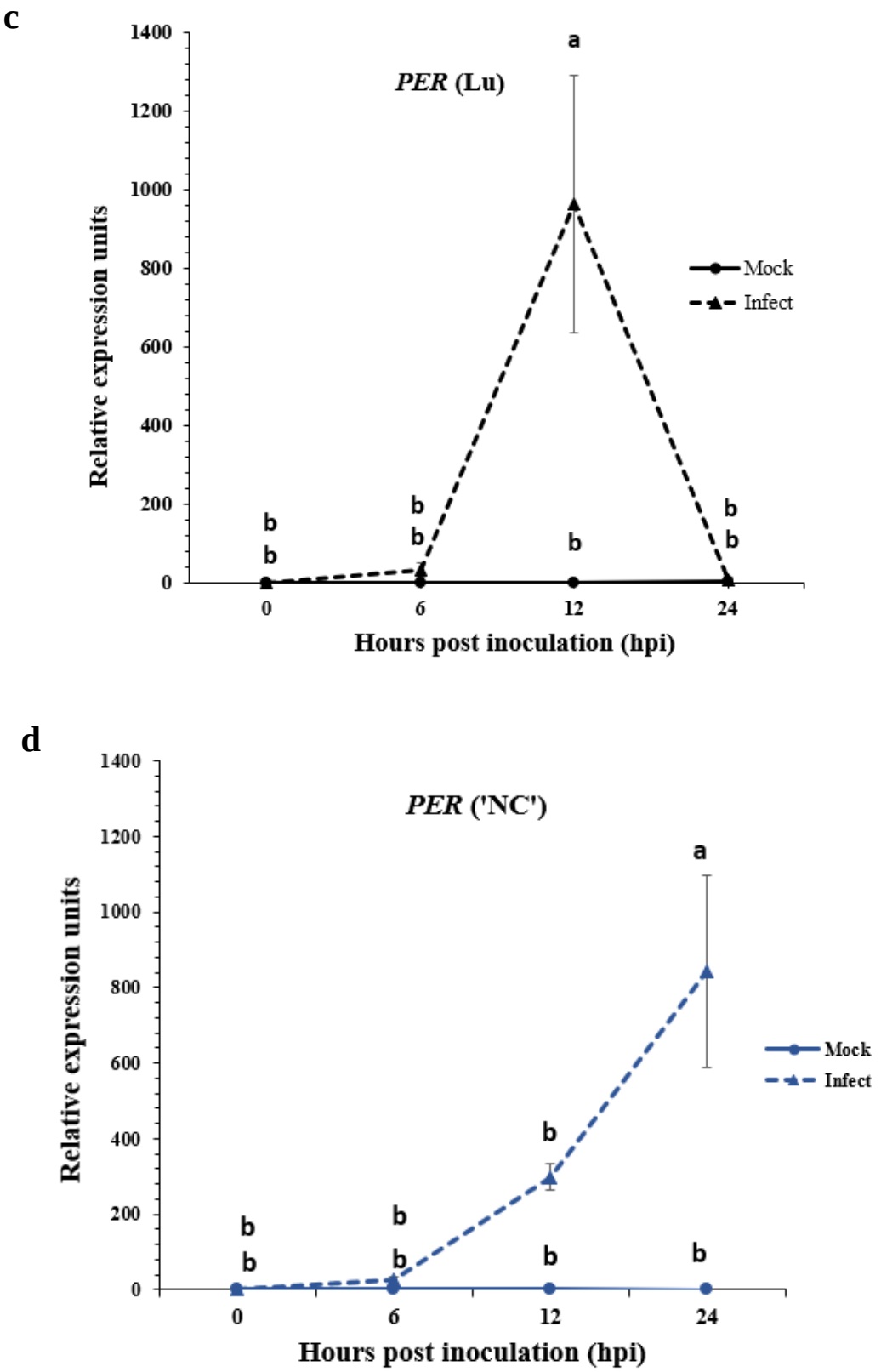

Figure 3.6 Relative gene expression changes in genes associated with apoplastic hydrogen peroxide accumulation, NADPH oxidase (*NOX*) and peroxidase (*PER*), *in Camellia lutchuensis* and *Camellia* 'Nicky Crisp' petals after inoculation with *Ciborinia camelliae* ascospores.
Graphs show the changes in relative transcript expression levels of the target genes over 24 hours post-inoculation (hpi) from 0 hpi as determined from quantitative real-time polymerase chain reaction. **(a, c)** *C.*

lutchuensis and **(b, d)** *C.* 'Nicky Crisp'. Relative gene expression levels were normalised to two housekeeping genes for each plant, (*EF-1α* and *PTB1*) in *C. lutchuensis* and (*PTB1* and *Tubulin α-3*) in *C.* 'Nicky Crisp'. Each data point signifies the mean of three biological replicates with three technical replicates (n=3). Error bars indicate standard error of the means. Two-way ANOVA (time x treatment) and Tukey's Honest Significant Difference tests were used to analyse the data. The same letter above a data point indicates that expression levels did not significantly differ between the conditions ($P < 0.05$).

3.5 Using antioxidants to manipulate CFB disease progression in *Camellia*

Because of the varied role that ROS can play in plant-pathogen interactions, antioxidants which scavenge ROS are frequently tested for their ability to control pathogen virulence and disease development in plants and important crops (Abdel-Monaim & Ismail, 2010; Barna, Fodor, Pogany, & Kiraly, 2003; Elad, 1992; Liu et al., 2013). Due to the observed temporal differences of ROS accumulation between the CFB resistant *C. lutchuensis* and susceptible *C.* 'Nicky Crisp', this study attempted to determine if antioxidant treatments could alter typical disease progression in *Camellia*. The *in vitro* and *in planta* effects of antioxidants on pathogen growth were observed, measured, and compared between both *Camellia* plants.

3.5.1 *C. camelliae* colony diameters increase when treated with antioxidants *in vitro*

The direct effects of antioxidant treatment on *C. camelliae* growth and ascospore germination were investigated. I hypothesised that treating *C. camelliae* with L-ascorbic acid, citric acid, or L-glutathione would have no effect on colony growth or ascospore germination *in vitro*. To test this hypothesis, *C. camelliae* mycelia were cultured onto plates containing sterile PDA with a final concentration of 0, 1, 5, or 10 mM of L-ascorbic acid, citric acid, or L-glutathione. Plates were incubated for four days before the colony diameters were measured. The average colony diameter was significantly larger in every antioxidant treatment group than the mock treatment group, except for the colonies grown with 10 mM of ascorbic acid and 1 mM citric acid (Fig. 3.7a, b). The largest average increase in colony diameters was 10 cm in the 10 mM L-glutathione treatment group. These results run contrary to my hypothesis because a significant effect on colony diameters was observed.

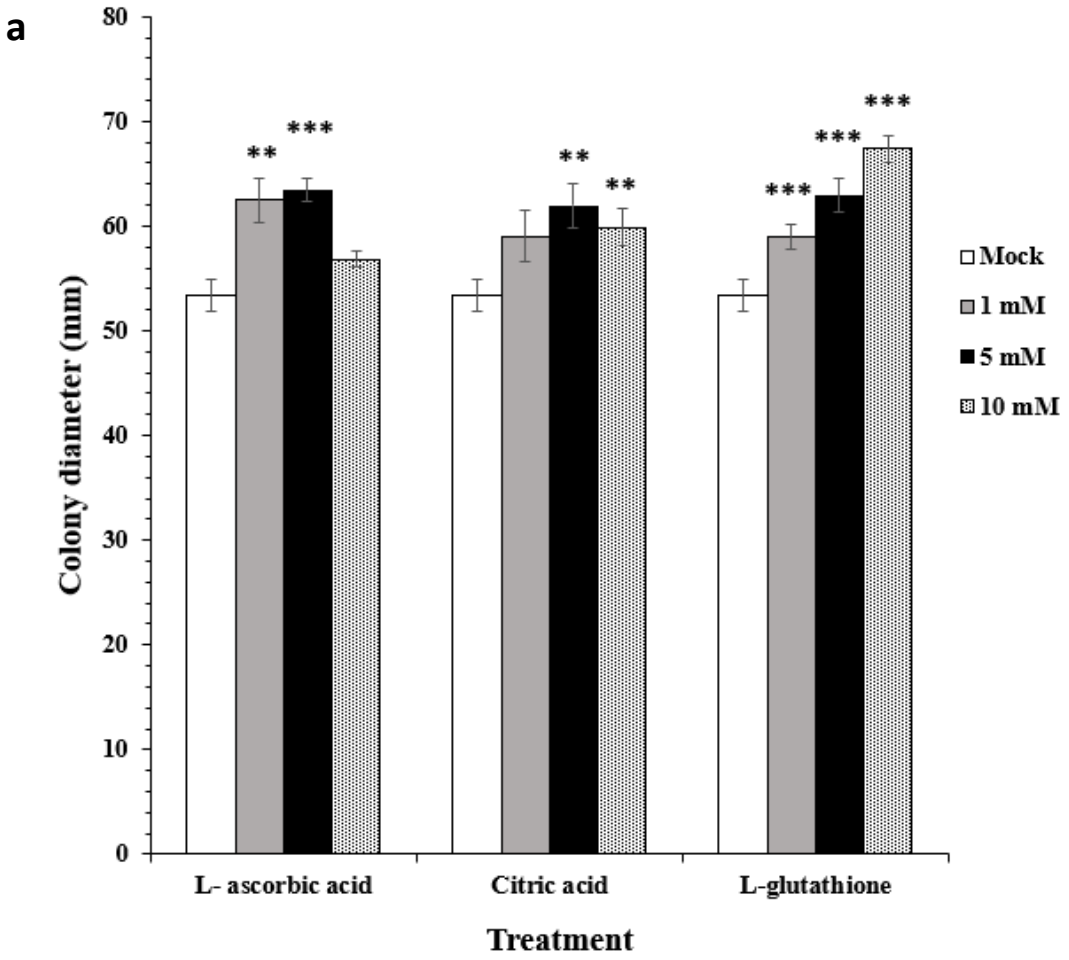

Figure 3.7 *Ciborinia camelliae* colony diameter growth with antioxidant treatment *in vitro*.
(a) *C. camelliae* colony diameters as observed four days after culturing on potato dextrose agar (PDA) plates containing 0 mM (mock) or 5 mM of L-ascorbic acid, citric acid or L-glutathione. Error bars indicate standard error of the means of biological replicates (n=11). **(b)** Day 4 of *C. camelliae* colony growth on PDA containing 0 mM (mock) or 5 mM of L-ascorbic acid, citric acid or L-glutathione. Scale bars represent 10 mm. Images are representative of each treatment group. ** and *** indicate values significantly less than mock treatment using Student's t-test at $P < 0.01$ and 0.001 respectively.

3.5.2 *C. camelliae* ascospore germination is reduced *in vitro* after antioxidant treatment

Due to the observed increase in colony diameter size with antioxidant treatment, I hypothesised that the percent of germinated ascospores would increase with treatment as well. Because the effects on

colony growth were the most similar in all three antioxidant treatment groups at the 5 mM concentration (a 5-8 cm increase on average), this concentration was selected for the ascospore germination assay. Ascospore germination was determined as previously described (Chapter 2). Again, sterile PDA was prepared in plates with a final concentration of 0 (mock), 1, 5, or 10 mM of L-ascorbic acid, citric acid, or L-glutathione. At 12 hpi, ascospore germination was significantly reduced on PDA plates in all three antioxidant treatment groups (Fig. 3.8) Complete inhibition of germination was observed in the citric acid group. In summary, *C. camelliae* colony diameters increase when grown on media containing L-ascorbic acid, citric acid, and L-glutathione at most of the concentrations tested; however, ascospore germination is inhibited in the same conditions.

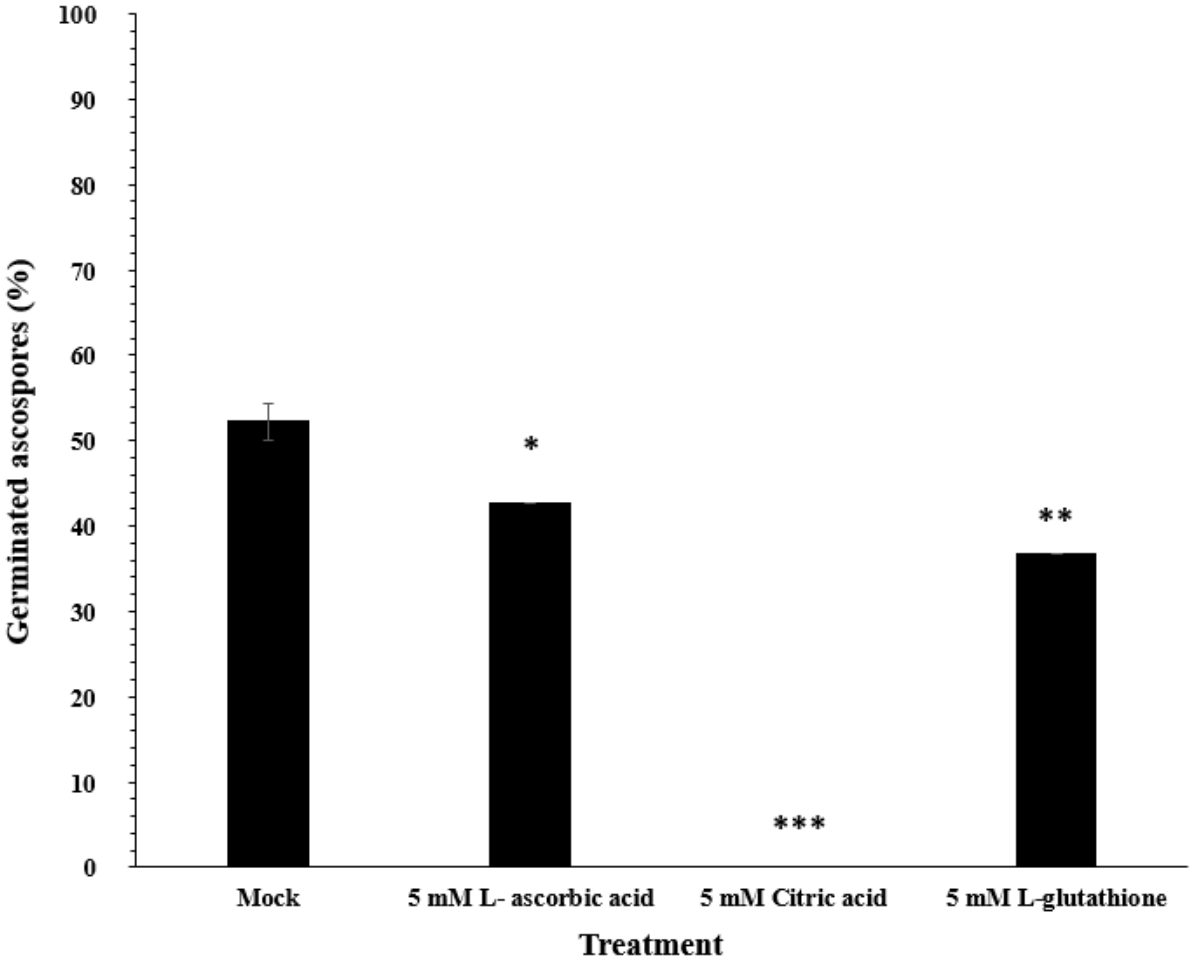

Figure 3.8 *Ciborinia camelliae* ascospore germination with antioxidant treatment *in vitro*.
Percentage of germinated ascospores on potato dextrose agar plates containing 0 (mock) or 5 mM of L-ascorbic acid, citric acid or L-glutathione at 12 hours post-inoculation. Error bars indicate standard error of the means (n=3). *, ** and *** indicate values significantly less than mock treatment using Student's t-test at $P < 0.05$, 0.01 and 0.001 respectively.

3.5.3 Antioxidant application results in CFB lesion development in resistant *C. lutchuensis* and a reduction in lesion area sizes in susceptible *C.* 'Nicky Crisp'

H_2O_2 scavengers such as antioxidants and certain enzymes can inhibit H_2O_2 accumulation *in planta*, limiting this defence response and possibly making plants more susceptible to disease development (Liu et al., 2013; Mellersh et al., 2002). Based on previous results demonstrating that early H_2O_2 production (12 hpi) correlates with resistance to CFB, it was hypothesised that antioxidant application would scavenge H_2O_2 accumulation and make *C. lutchuensis* more susceptible to the blight. Conversely, it was hypothesized that lesion development would not be affected by antioxidant treatment on *C.* 'Nicky Crisp' petals because H_2O_2 accumulation might occur too late in this species to have an effect on the interaction (24 hpi).

To test this hypothesis, detached petals from both plants were inoculated with 10 µL droplets of a *C. camelliae* ascospore suspension at a concentration $1x10^5$ ascospores/mL containing 5 mM of either three antioxidants: L-ascorbic acid, citric acid, or L-glutathione as described (Chapter 2). By 48 hpi, lesions developed in all *C. lutchuensis* petals treated with ascospores and L-ascorbic acid, citric acid, or L-glutathione (Fig. 3.9a). Significantly more petals developed lesions in the groups with the ascospore suspension combined with an antioxidant treatment than the petals treated with the ascospore suspension alone (Fig. 3.9c). Interestingly, petal lesion area sizes in *C.* 'Nicky Crisp' significantly decreased in all antioxidant treatment groups (Fig. 3.9b). The average lesion area size was reduced 6- and 8-fold in the L-glutathione and citric acid groups, respectively, and the average lesion size was reduced 3-fold in the L-ascorbic acid group (Fig. 3.9d). Lesions did not develop in the mock-treated group.

It was noteworthy that lesions developed in all the antioxidant treatment groups despite the inhibition of ascospore germination seen in the *in vitro* experiment, especially in the case of the citric acid group which most efficiently inhibited ascospore germination. This indicates that the changes observed in lesion sizes can likely be attributed to antioxidants' effects on the oxidative response from the plant instead of the effects that the antioxidants had on ascospore inhibition *in vitro*. In conclusion, after antioxidant treatment, atypical CFB lesions developed in the normally resistant *C. lutchuensis* while lesion development decreased in the highly susceptible *C.* 'Nicky Crisp'.

a

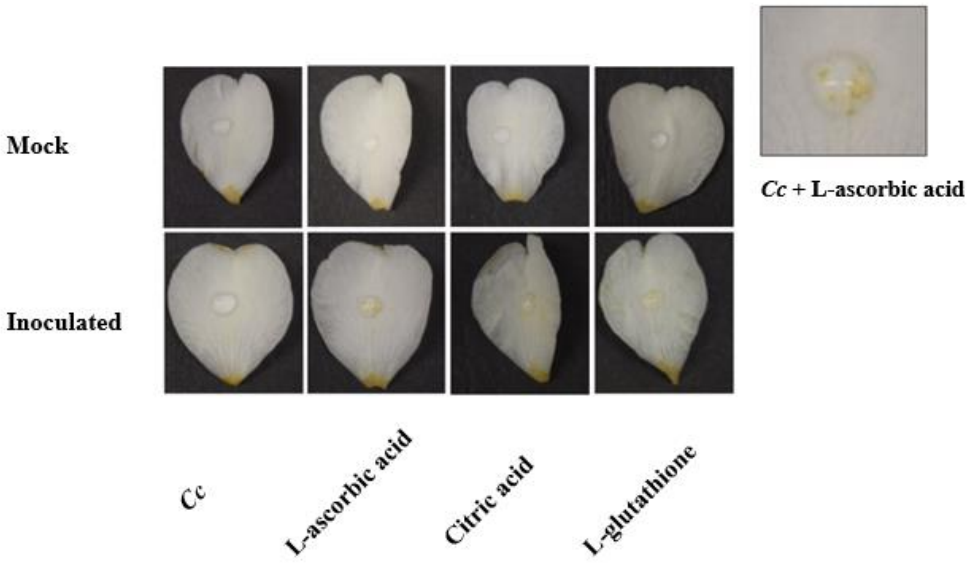
Mock
Inoculated
Cc + L-ascorbic acid
Cc
L-ascorbic acid
Citric acid
L-glutathione

b

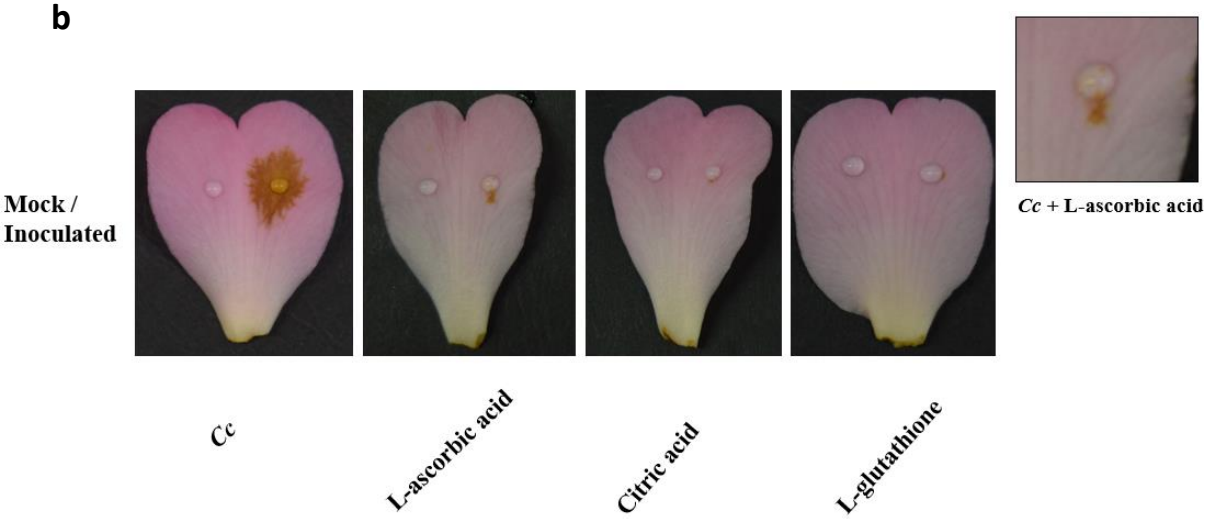
Mock /
Inoculated
Cc + L-ascorbic acid
Cc
L-ascorbic acid
Citric acid
L-glutathione

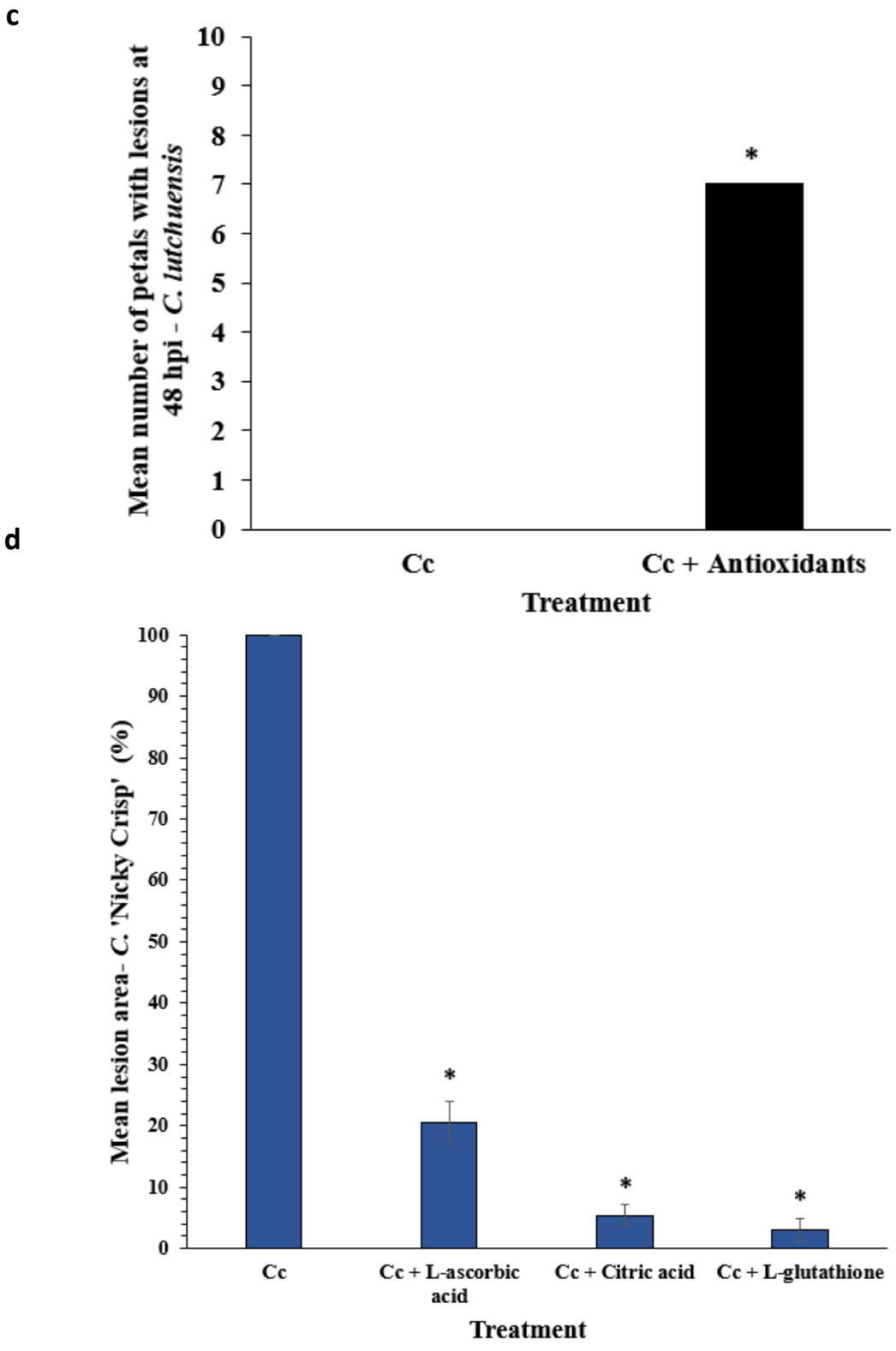

Figure 3.9 CFB lesion development after treatment with a *Ciborinia camelliae* ascospore suspension combined with 5 mM of an antioxidant.

Images of lesion development at 48 hours post-inoculation (hpi) after treatment with an ascospore suspension combined with 5 mM of L-ascorbic acid, citric acid, L-glutathione on **(a)** *C. lutchuensis* petals and **(b)** *C.* 'Nicky Crisp' petals. Images are representative of each treatment group, *C. lutchuensis* (n=7) and *C.* 'Nicky Crisp' (n=9). The droplet on the left side of *C.* 'Nicky Crisp' petals was the mock treatment and the droplet on the right side was the ascospore suspension combined with an antioxidant. Inset images are a close-up of lesion development under droplets. *Cc* = treatment with the *C. camelliae* ascospore suspension alone. **(c)** The bar

graph shows the average number of *C. lutchuensis* petals that developed lesions after a combined ascospore and antioxidant treatment. * indicates a significant difference in the number of petals that developed lesions after antioxidant treatment compared to the ascospore suspension alone using Fisher's Exact Test for Count Data at $P < 0.05$. **(d)** The bar graph shows the mean percent of the lesion area under the treatment droplet of *C.* 'Nicky Crisp'. Error bars in the bar graphs indicate standard error of the means. * indicates a significant difference in the lesion area size under the combined ascospore and antioxidant treatment compared to the droplets with the ascospore suspension alone using Student's two-tailed t-test at $P < 0.05$.

3.5.4 Antioxidant treatment shows different effects on *C. camelliae* growth *in planta* in resistant *C. lutchuensis* and susceptible *C.* 'Nicky Crisp'

Because antioxidant treatment correlated with an increase in lesion development in *C. lutchuensis* but a reduction in *C.* 'Nicky Crisp', *in planta* assays were done next to observe and compare the effects of the antioxidant treatments directly on ascospore germination and hyphal growth during the plant-pathogen interaction. Detached petals of *C. lutchuensis* and *C.* 'Nicky Crisp' were spray inoculated with a *C. camelliae* ascospore suspension at a concentration of $1x10^6$ ascospores/mL combined with 5 mM of either L-ascorbic acid, citric acid, or L-glutathione. Petals were submerged in a trypan blue in lactoglycerol solution for two hours to stain the fungal material. Petal discs were then excised, mounted, and assessed under light microscope as described (Chapter 2).

Based on the previous *in vitro* results, it was expected that the percent of germinated ascospores would be significantly lower on petals from both *Camellia* plants after antioxidant treatment, compared to petals treated with the ascospore suspension alone. Contrary to my hypothesis, ascospore germination showed no significant difference in any antioxidant treatment group compared with the groups treated with ascospores alone, on either *C. lutchuensis* or *C.* 'Nicky Crisp' petals at 12 hpi (Fig. 3.10a, c). Because there was no significant difference in ascospore germination between the *Camellia* plants, but there was an increase in lesion development in *C. lutchuensis* and a reduction *C.* 'Nicky Crisp' after antioxidant treatment, I hypothesised that the average percent of ascospores with hyphal growth would be increased on *C. lutchuensis* petals and reduced on *C.* 'Nicky Crisp'. By 24 hpi, the percent of ascospores with hyphal growth on *C. lutchuensis* petals was significantly lower only in the citric acid treatment group compared with all other treatment groups (Fig. 3.10b, c). Hyphal growth in the L-ascorbic acid treatment group appeared to be more developed with more branching, although this was not quantified in the current study. Conversely, there was a significantly higher percent of ascospores with hyphal growth on *C.* 'Nicky Crisp' petals in all antioxidant treatment groups compared with ascospores alone. Contrary to the hypothesis, there was not a significantly higher percentage of ascospores with hyphal growth on *C. lutchuensis*, nor was there an decrease observed on *C.* 'Nicky Crisp' petals. Ascospore germination and hyphal growth were not observed in any mock-treated petal discs. To summarise, the effects of the antioxidant treatments on ascospore germination and hyphal growth did not correlate with the differences seen in the lesion development after antioxidant treatment in either *Camellia* species.

a

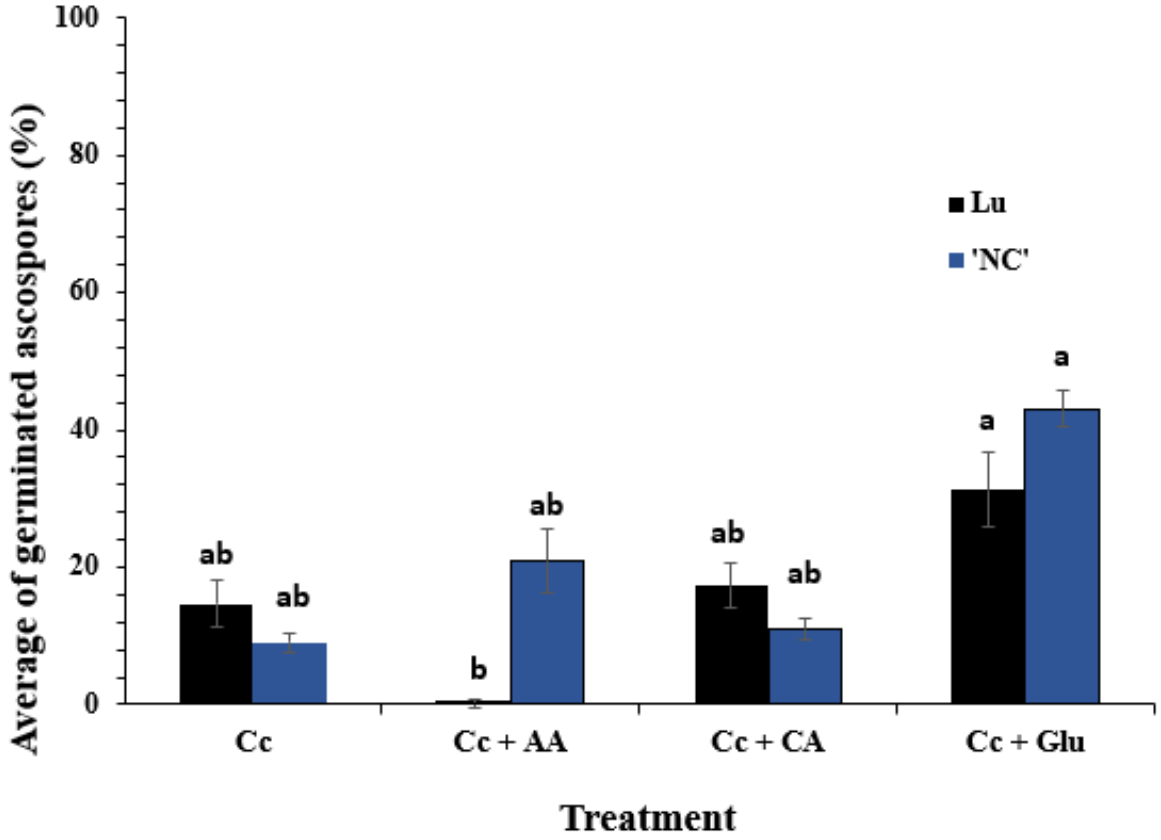
Average of germinated ascospores (%)
100
80
60
40
20
0
Lu
'NC'
ab
ab
b
ab
ab
ab
a
a
Cc
Cc + AA
Cc + CA
Cc + Glu
Treatment

b

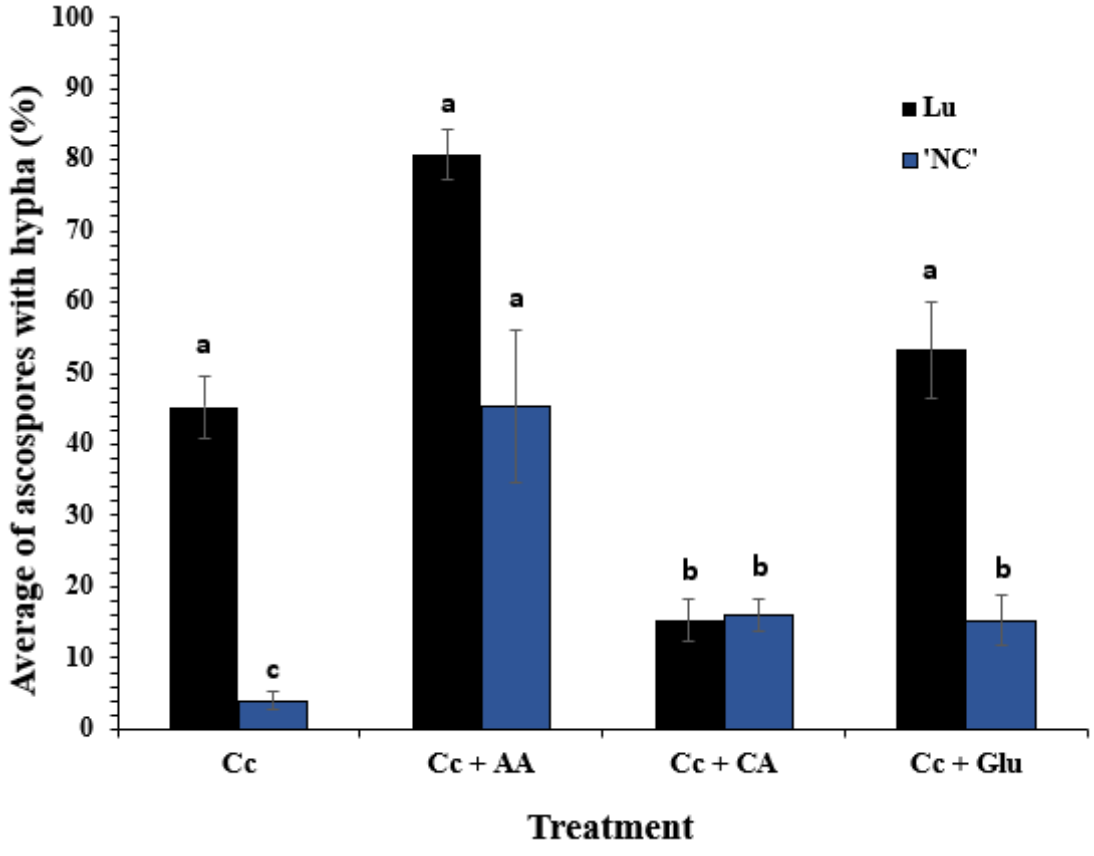
Average of ascospores with hypha (%)
100
90
80
70
60
50
40
30
20
10
0
Lu
'NC'
a
c
a
a
b
b
a
b
Cc
Cc + AA
Cc + CA
Cc + Glu
Treatment

c

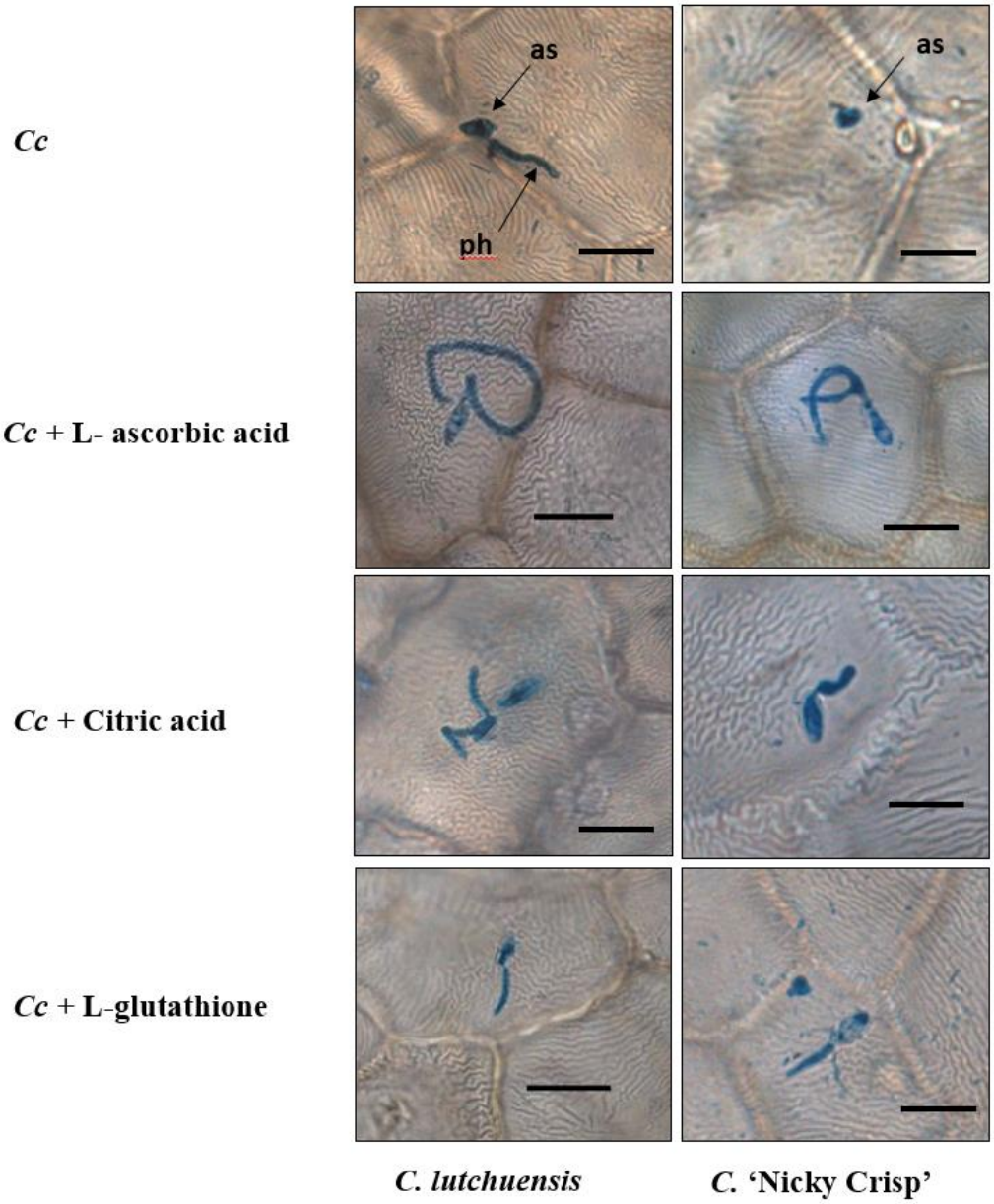

Figure 3.10 Analysis of the effects of antioxidant treatment on *Ciborinia camelliae* ascospore germination and hyphal growth on *Camellia lutchuensis* and *Camellia* 'Nicky Crisp' petals.
Comparing the average rates of **(a)** ascospore germination at 12 hours post-inoculation (hpi) and **(b)** ascospores with hyphae growth at 24 hpi with an ascospore suspension containing a final concentration of 5 mM of an antioxidant (L-ascorbic acid, citric acid or L-glutathione). Columns signify the mean of three biological replicates. Two-way ANOVA (time x treatment) and Tukey's Honest Significant Difference tests were used to analyse the data. The same letter above a column indicates that expression levels did not significantly differ between the conditions ($P < 0.05$). **(c)** Images of *C. camelliae* ascospore germination and hyphae growth on *Camellia* petals at 24 hpi after antioxidant treatment. Images are representative of three biological replicates from each treatment group (n=3). Microscopic assessment was performed on 50 ascospores per biological replicate. Symbols: as = ascospore; ph = primary hyphae. Scale bars = 20 µm.

3.5.5 Antioxidant application may reduce but does not fully inhibit apoplastic hydrogen peroxide accumulation in *Camellia*

After treatment with L-ascorbic acid, citric acid, or L-glutathione, CFB lesions developed in the normally resistant *C. lutchuensis* petals, while lesions were reduced or inhibited in susceptible *C.* 'Nicky Crisp'. I hypothesised that this pattern of lesion development emerged due to antioxidant

applications scavenging H_2O_2 accumulation in petals of both *Camellia* plants in response to *C. camelliae* infection. It was predicted that the brown DAB stain product would not be visible during microscopic analysis due to the scavenging of H_2O_2 by the antioxidants. To investigate this hypothesis, *C. lutchuensis* and *C.* 'Nicky Crisp' petals were inoculated with a *C. camelliae* ascospore suspension, combined with an antioxidant, for a final solution concentration of 5 mM, and incubated as described (Chapter 2). Petals were then dual-stained with DAB and trypan blue in lactoglycerol and examined under a light microscope to count the number of germinated ascospores with DAB staining in an adjacent apoplast as described (Chapter 2).

At 12 hpi, the percent of germinated ascospores in *C. lutchuensis* with localised DAB stain was significantly lower in groups treated with ascospores combined with citric acid (Cc + CA) or L-glutathione (Cc + Glu), as compared with the control group treated with ascospore suspension alone (Cc) (Fig. 3.11a). No significant change was seen in the ascospore and L-ascorbic acid treatment group (Cc + AA). At 24 hpi, no significant change was observed in any treatment group when compared with the control group. Conversely, antioxidant treatments on inoculated *C.* 'Nicky Crisp' petals showed no significant change in the number of ascospores with localised DAB stain (Fig. 3.11b). In conclusion, treatment with L-ascorbic acid, citric acid, or L-glutathione did not completely scavenge H_2O_2 accumulation in inoculated petals of either *Camellia* plant, as hypothesised. However, the percent of germinated ascospores with adjacent DAB stain was significantly lower at 12 hpi in inoculated *C. lutchuensis* petals after treatment with 5 mM citric acid and with 5 mM of -glutathione.

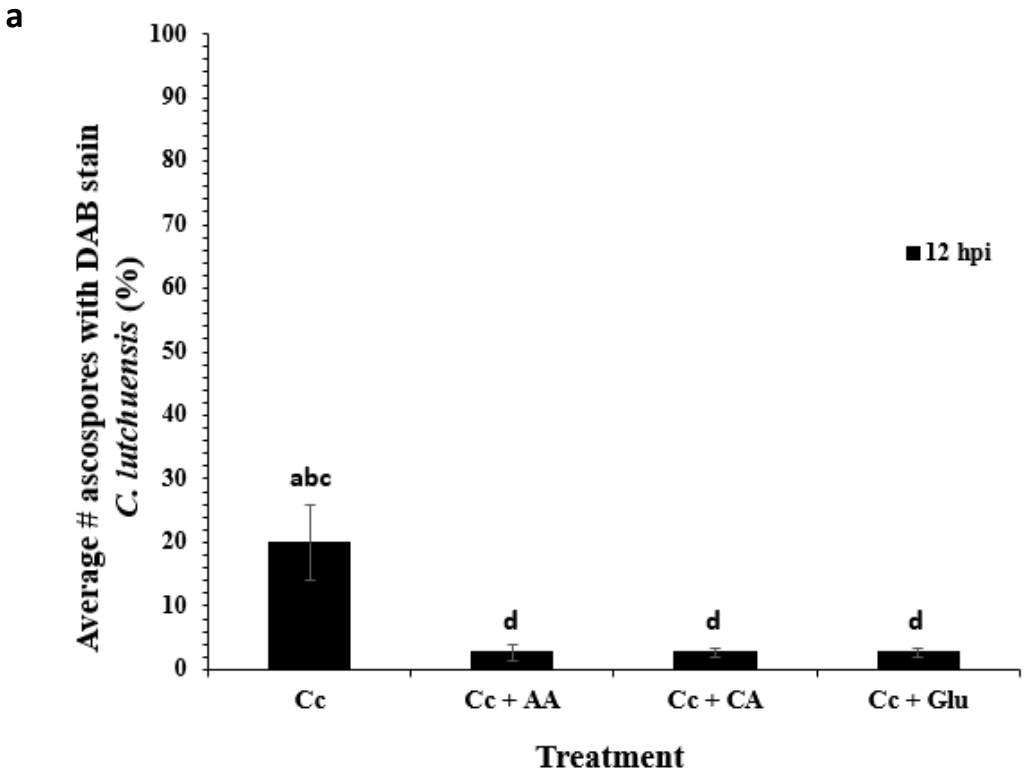

b

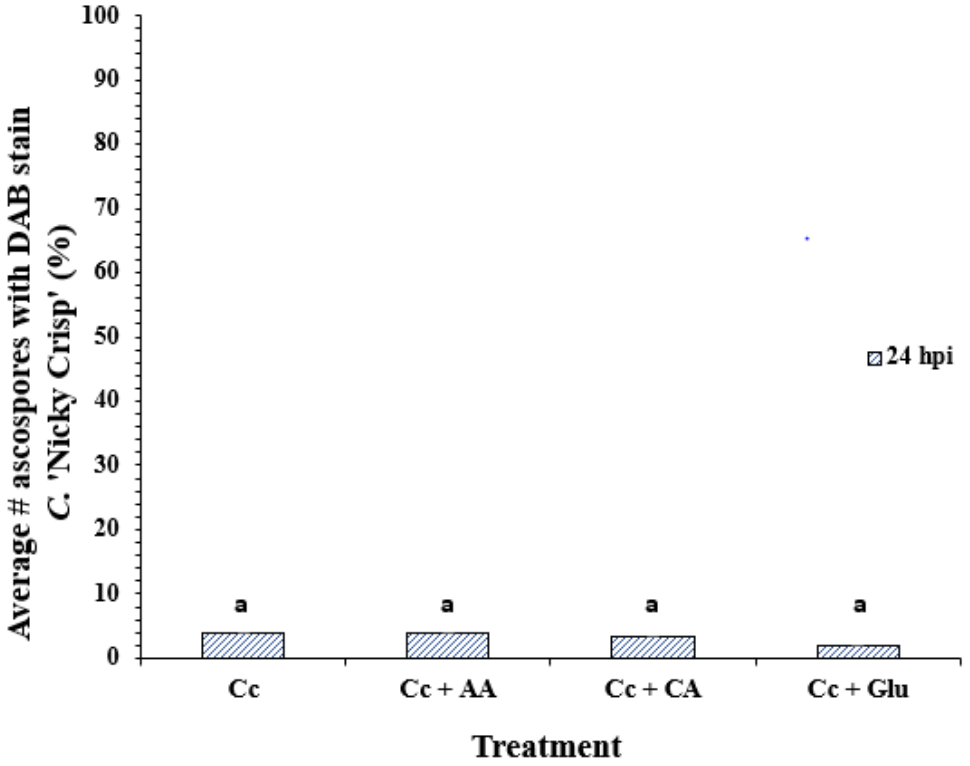

Figure 3.11 Analysis of the effects of antioxidant treatment on DAB stain development at 24 hours after infection in apoplasts adjacent to germinated *Ciborinia camelliae* ascospores on *Camellia lutchuensis* and *Camellia* 'Nicky Crisp' petals.

Comparing the average rate of DAB stain development in an apoplast adjacent to a germinated *C. camelliae* ascospore after treatment with 5 mM of an antioxidant (L-ascorbic acid, citric acid or L-glutathione) on **(a)** *C. lutchuensis* petals at 12 hours post inoculation (hpi) and **(b)** *C.* 'Nicky Crisp' petals at 24 hpi. Columns signify the mean of three biological replicates (n=3). Microscopic assessment was performed on 50 ascospores per biological replicate. Two-way ANOVA (time x treatment) and Tukey's Honest Significant Difference tests were used to analyse the data. The same letter above a column indicates that expression levels did not significantly differ between the conditions ($P < 0.05$).

4 Discussion

4.1 Deciphering the role of ROS in the *Camellia – C. camellia* interaction

The role of ROS is complicated in plant-pathogen interactions. These compounds are produced by both plant and pathogen organisms and play many different roles during the interaction, not all of which are well understood. Plant-produced ROS can play dual roles, functioning both to inhibit disease to benefit the plant and to promote disease to benefit the pathogen (Barna et al., 2012). Important necrotrophic pathogens in the Sclerotiniaceae family, which includes *C. camelliae*, can suppress their hosts' defence responses so the hosts become more susceptible (Girard et al., 2017; Govrin & Levine, 2000; Unger, Kleta, Jandl, & von Tiedemann, 2005; Williams et al., 2011). In addition, necrotrophic pathogens are also known to stimulate their hosts' ROS production, in addition to producing ROS themselves (Govrin & Levine, 2000; Kim, Chen, Kabbage, & Dickman, 2011). It has been previously shown that ROS accumulation plays a role in *Camellia* interactions with fungal pathogens (Denton-Giles et al., 2013; Wang et al., 2018). To further investigate the role of ROS during the *Camellia – C. camelliae* interaction, several methods were used to detect and compare ROS accumulation in CFB resistant and susceptible *Camellia* tissues. ROS accumulation was scavenged with the use of three antioxidants—L-ascorbic acid, citric acid, and L-glutathione—and the effects of these compounds were observed on CFB development and *C. camelliae* growth and development. In summary, this study aimed to elucidate the complicated role of ROS during both resistant and susceptible interactions between *Camellia* and *C. camelliae*.

4.2 *C. lutchuensis* is resistant to CFB infection while *C.* 'Nicky Crisp' is susceptible

The temporal development of CFB lesions in the two species of interest in this study aligned well with previously reported bioassays. For example, CFB lesions did not develop in *C. lutchuensis* when spray-inoculated with a *C. camelliae* ascospore suspension. These results confirm that *C. lutchuensis* has resistance to CFB and are similar to the observations made by Denton-Giles et al. (2013) that showed an average of just 5% lesion coverage of the total petal area at 48 hpi in the same species. Couselo et al. (2014) also saw a low level of disease (in 29% of the total petals examined) in their CFB susceptibility experiments with *C. lutchuensis*. The higher incidence of disease in their study may be due to a higher ascospore concentration that was not reported, or a more virulent strain of *C. camelliae* may have been used. In contrast to *C. lutchuensis*, CFB lesions began to develop at 24 hpi in inoculated *C.* 'Nicky Crisp' petals and full petal coverage was reached at 48 hpi. Similarly, Denton-Giles et al. (2013) began to observe lesion development at 30 hpi and full lesion coverage was reached at 48 hpi. Full lesion coverage was also observed in *C.* 'Nicky Crisp' petals at 48 hpi in a separate study (Kondratev et al., 2020). Assays conducted on petals of the *C. japonica* cultivar, 'Compacta Alba', resulted in a 100% disease incidence at 24 hpi, defined as the observable presence

of petal lesions (Couselo et al., 2014). In conclusion, this study confirms that its method of ascospore application successfully induced the appropriate CFB response found in nature and in other studies under similar experimental conditions.

4.3 ROS accumulation is detected in *Camellia* tissue

DAB staining is a commonly used histological method to visually detect H_2O_2 accumulation in cells, because it is easily observed microscopically (Asselbergh et al., 2007; Hückelhoven, Fodor, Preis, & Kogel, 1999; Mellersh et al., 2002; Thordal-Christensen et al., 1997). This histological method is also widely used in plant-pathogen interactions for the same reason. The polymerisation of an applied DAB stain and H_2O_2 creates a brown stain product that develops *in planta*. In addition, DAB staining combined with pathogen tissue staining can be used to easily visualise the proximity of H_2O_2 accumulation to fungal material, as was performed here with *Camellia* petals and *C. camelliae* ascospores.

Although DAB staining offers a quick and simple method for the detection of H_2O_2, it has several limitations. First, while DAB stain is an excellent method to visualise H_2O_2 accumulation in tissue, the chemical reaction between the staining compound and H_2O_2 is not stoichiometric (van der Loos, 2008). Therefore, it is not possible to use the staining to measure the precise quantity of H_2O_2 that accumulates, or conversely, how much the accumulation of H_2O_2 is scavenged by antioxidant treatments. Second, the reaction between H_2O_2 and DAB stain is irreversible in tissue, so it isn't possible to observe and compare the dynamic changes of ROS over time (Hernández-Barrera et al., 2013). Finally, in the current study it was difficult to differentiate DAB staining from general browning in tissue caused by a wounding response and/or the formation of necrotic lesions. Fungal penetration of plant tissue may cause injury to plant cellular organelles, thereby inducing a wounding response. This can also cause browning in plant tissue, most likely due to the production of phenolic compounds and oxidation of other secondary metabolites (Iakimova & Woltering, 2018; Jones & Saxena, 2013; Kondratev et al., 2020). However, using the DAB staining technique, combined with the trypan blue in lactoglycerol staining of fungal material, as well as limiting the timeframe of the experiment to 24 hpi before either a wounding response or necrotic lesions became evident, ensured the successful visualisation of H_2O_2 in the plant tissue in response to ascospore inoculation.

Because of the limitations in using DAB stain alone to detect H_2O_2 accumulation in tissue, corroborating results with other ROS detection methods were important to investigate. Therefore, two additional ROS detection methods were used to support the visual DAB stain results. First, a measurable oxidant reactive fluorescent probe (AbIR) was used to compare temporal changes in the quantity of H_2O_2 in tissue between the resistant and susceptible *Camellia – C. camelliae* interactions. While AbIR is unable to be visually measured *in planta*, the probe does allow the quantity of H_2O_2 in

homogenized tissue to be accurately measured using a microplate reader. The results obtained with AbIR concurred with the results achieved using DAB staining, providing further evidence of the differences in H_2O_2 accumulation between the two plant-pathogen interactions. However, because the entire flower petal is homogenized for use in this quantitative assay, we may not get a precise measurement of the intercellular ROS alone. Therefore, performing a microdissection or extraction of plant cell walls or plasma membranes containing ROS may be an alternative to make more accurate measurements of the localised ROS response (Larsson, Widell, & Kjellbom, 1987; Selvendran, 1975).

Finally, because of the limitations of DAB staining and AbIR measurements, apoplastic ROS associated gene expression was measured in *Camellia* to better understand the plant's oxidative response. After successfully identifying reference gene primers for *C.* 'Nicky Crisp' for use in qRT-PCR, genes that are associated with the apoplastic oxidative burst, *NOX* and *PER*, were identified in both *Camellia* species. Gene primers were successfully designed and used to detect differences in the expression patterns of these two genes in *Camellia* in response to ascospore inoculation. One limitation of qRT-PCR is that genetic material of high quality is necessary to successfully detect gene expression. Therefore, this experiment was unable to be continued past 24 hpi due to significant degradation of the susceptible plant tissue during the interaction.

In summary, three methods were successfully used to detect ROS accumulation in *Camellia* during the *Camellia – C. camelliae* interaction. Due to the corroboration of the results obtained from visual, quantitative, and genetic ROS detection methods, the validity of the methods used here can be confirmed.

4.4 Exogenous compounds scavenge ROS accumulation in *Camellia* tissue and show little effect on fungal growth

Antioxidants are frequently used to scavenge ROS accumulation in plants in an attempt to observe effects on compatible and incompatible plant-pathogen interactions (El-Korany & Mohamed, 2008; Khan, Aked, & Magan, 2001; Liu et al., 2013; Macarisin et al., 2007). However, the exogenous application of compounds can have ectopic effects that reach beyond the direct effects on the desired target. Therefore, it is necessary to investigate ectopic effects such as the effect antioxidants have directly on fungal growth. While previous studies demonstrate that antioxidant treatments typically have either no effect or an inhibitory effect on fungal growth *in vitro*, they have also shown that some antioxidants such as butylated hydroxyanisole (BHA) can cause fungal membranes to be leaky, as is usually the case with phenolic antioxidants but not non-phenolic antioxidants (Abdel-Monaim & Ismail, 2010; Elad, 1992; Liu et al., 2013; Shomeet, El-Samadisy, El-Kholy, & Ibrahim, 2018; Thompson, 1996). Three non-phenolic antioxidants—L-ascorbic acid, citric acid, and L-glutathione—were selected for this study because of their prevalent use in the study of fungal plant pathogens.

These antioxidants were also chosen because they are naturally abundant in plant cells and because L-ascorbic acid and L-glutathione have been shown to play many roles in ROS scavenging in plants during the glutathione-ascorbate cycle (Foyer & Noctor, 2011).

The antioxidants used here successfully induced changes in the typical CFB lesion development patterns in resistant and susceptible *Camellia.* There was no consistent antioxidant application effect on the parameters of the measured fungal growth that would sufficiently explain the opposite effects on lesion development in each resistant and susceptible *Camellia* species. Therefore, it can be surmised that the changes in lesion development were likely due to successful partial scavenging of the oxidative burst by antioxidant treatment that altered this defence response. Additionally, while it was observed that H_2O_2 accumulation was not completely quenched in the petals of either species by the antioxidants in this study, the quantity of H_2O_2 may have been reduced enough to interfere with ROS-associated defence responses in both species, as successfully demonstrated in other studies (Liu et al., 2013; Mellersh et al., 2002). To address these limitations, the results from the current study could be further corroborated using other types of ROS scavenging compounds, such as superoxide dismutase and catalase, to see if the same results are achieved (Mellersh et al., 2002; Shetty et al., 2007; Tanabe, Nishizawa, & Minami, 2009).

Another limitation in applying exogenous compounds to investigate internal treatment effects is that the protective cuticle layer in plants may inhibit some of the compounds from penetrating the apoplastic space. Therefore, adding a surfactant might help the antioxidants to diffuse across petal cuticles into the intercellular space more efficiently to interact with the apoplastic ROS accumulation (Deng et al., 2016; Schreiber, 1995). Also, it may be possible that applying exogenous compounds would benefit the fungus by providing it with an additional energy source. For example, L-glutathione is a compound consisting of three amino acids: cysteine, glutamic acid, and glycine. Additionally, L-ascorbic acid or Vitamin C is an essential nutrient for life. Fungal pathogens deficient in the ability to make D-erythroascorbic acid, a five-carbon analog of L-ascorbic acid, show a reduction in hyphal growth (Huh, Kim, Kim, Jeong, & Kang, 2001). However, Liu et al. (2013) observed neither an increase in colony diameters nor a strong negative effect on *M. fructicola* spore germination, the causal agent of brown rot on peach flower petals, using L-ascorbic acid or citric acid treatments (0.1, 0.5, 1, 5 and 10 mM) in media plates. Elad (1992) examined linear colony growth of broad-host necrotrophic fungal pathogens and close relatives of *C. camelliae*, *B. cinerea* and *S. sclerotiorum*, on PDA with 17 different antioxidant compounds, including L-ascorbic acid. A significant reduction in linear mycelium growth occurred at several L-ascorbic acid concentrations (0.1, 1 and 10 mM), but a significant effect was seen in only one *B. cinerea* isolate out of three tested, and there was no significant effect found in *S. sclerotiorum* mycelium growth.

In conclusion, while it was difficult in the current study to determine all possible ectopic effects of the antioxidant treatments on *C. camelliae* and CFB development, the data here importantly show that the treatments had low or no detrimental effect on fungal growth *in planta*. Therefore, we can conclude that ectopic effects of the antioxidants on the fungus were not the main agents of the changes observed in CFB development in *Camellia* and that the antioxidant treatments likely had a direct effect on ROS accumulation in the petals, causing changes in lesion development in response to the fungal pathogen.

4.5 An oxidative burst is activated early in the CFB incompatible interaction (*C. lutchuensis*)

CFB disease resistance in *C. lutchuensis* found in this study was characterized by a rapid intercellular ROS response within 6 h of *C. camelliae* inoculation staining, followed by a decline in the response as evidenced by the visual, quantitative, and molecular data presented here. During the first 6 hours after ascospore inoculation, ascospore germination and hyphal growth along petal surfaces were observed. These activities were consistent with the described asymptomatic phase of CFB (Denton-Giles et al., 2013). This phase continues with subcuticular hyphal penetration and growth into the apoplastic space of both disease resistant and susceptible *Camellia* at 12 hpi, although at a much higher frequency in susceptible species (Denton-Giles et al., 2013; Vingnanasingam, 2002). In the current study, apoplastic H_2O_2 accumulation in *C. lutchuensis* near ascospores was observed at 12 hpi. The staining was strongest near the fungal material and then diffused outwards, suggesting the response was in reaction to the presence of the fungus. The timeline of H_2O_2 accumulation and the spatial pattern of development are in agreement with the observations made in resistant *Camellia* by Denton-Giles et al. (2013). This apoplastic ROS accumulation (the oxidative burst) is characteristic of incompatible plant-pathogen interactions as is well described in the barley-powdery mildew interaction (Hückelhoven et al., 1999; Thordal-Christensen et al., 1997; Vanacker, Carver, & Foyer, 1998).

To further support the visual observations of H_2O_2 accumulation made in this study, quantitative measurements of H_2O_2 increased 8-fold at 12 hpi, as well as the upregulation of apoplastic ROS associated genes. *NOX* expression was stably upregulated from 6 – 12 hpi, while PER saw a 28-fold upregulation at 12 hpi. In a study in peach (*Prunus persica)* petals, the authors saw upregulation of *NOX* and *PER* when challenged with a compatible necrotrophic pathogen and close relative of *C. camelliae*, *M. fructicola,* while upregulation was not seen when challenged with an incompatible bacterial pathogen, *P. digitatum*. Similarly, there is evidence of ROS-associated gene upregulation in anthracnose resistant *Camellia*. In their study, Wang et al. (2018) observed differentially expressed genes (DEGs) associated with H_2O_2 and ROS metabolic processes in a resistant *C. sinensis* tea cultivar (Zhongcha 108) when it was inoculated with the *C. fructicola* conidia, the causal agent of anthracnose. However, DEGs associated with PER activity were unchanged. In addition, Kondratev et al. (2020) saw the upregulation of gene transcript clusters associated with defence responses to biotic

stimulus and other organisms at 6 and 12 hpi. Particularly relevant to this study was the upregulation of networks containing enzymes important in cell wall strengthening pathways in which PER also plays an important role such as ferulate 5-hydroxylase (*F5H*) and elicitor-activated gene 3 (*ELI3-2*) that are active in the lignin biosynthesis pathway (Bhuiyan et al., 2009; Kondratev et al., 2020; Warinowski et al., 2016).

To explain the early oxidative response seen in this study, it has been suggested that the incompatible *C. lutchuensis* may have evolved early recognition of the pathogen during the asymptomatic phase of the interaction. Kondratev et al. (2020) reasons that this is most likely due to the early recognition of *C. camelliae* PAMPs by disease resistant *Camellia* species. This hypothesis arises from their study in which the authors found evidence of the upregulation of common predicted receptor genes, Brassinosteroid insensitive 1-associated receptor kinase (*BAK1*) and Suppressor of brassinosteroid insensitive 1-associated receptor kinase interacting receptor-like kinase 1 (*SOBIR1*), in *C. lutchuensis* petals at 6 hpi. *A. thaliana bak1* and *sobir1* mutants are shown to be more susceptible to the necrotrophic fungi in the same family as *C. camelliae*, *S. sclerotiorum* and *B. cinerea* (Zhang et al., 2013). These two genes have also been shown to be involved in downstream defence pathways in plant immunity responses, such as MAPK signalling and calcium (Ca^{2+}) influxes, that act as mutual regulators of ROS in plant tissue (Kemmerling et al., 2007; Liebrand, van den Burg, & Joosten, 2014).

Following the asymptomatic phase of CFB, the symptomatic phase of *C. camelliae* growth begins. The symptomatic phase is characterised by subepidermal hyphal growth into the mesophyll tissue at 24 hpi and coincides with the development of petal lesions in susceptible *Camellia*. CFB lesions do not typically develop in resistant species such as *C. lutchuensis*; however, the atypical development of lesions in petals treated with antioxidants in the current study further suggests the importance of the oxidative burst in supressing the *C. camelliae* invasion. While the antioxidants had little effect on the parameters of fungal growth that were measured, the antioxidant treatments did reduce apoplastic H_2O_2 accumulation, likely weakening this oxidative defence response and leaving the plant more susceptible to the invasion. The development of CFB lesions in 100% of samples treated with antioxidant solutions clearly shows the importance of the oxidative burst in this normally resistant species. Similarly, the enzymatic removal of H_2O_2 during the interaction between *Colletotrichum coccodes* (Glomerellaceae) and tomato allowed the fungus to successfully penetrate the plant tissue, whereas penetration was typically inhibited in the presence of H_2O_2 (Mellersh et al., 2002).

The downregulation of the ROS response at 24 hpi demonstrated by the decrease in *NOX* and *PER* expression in this study may be due to protective measures that plants have evolved to protect their tissue from high levels of the toxic compounds, as well as to moderate the defence responses that are downstream from ROS accumulation (Kwak, Nguyen, & Schroeder, 2006; Sewelam et al., 2016;

Torres, Jones, & Dangl, 2006). In addition, after successfully stopping an active infection, a plant can preserve and/or reallocate the costly resources involved in defence responses and return to its normal metabolic processes (Heil & Baldwin, 2002; Schultz, Appel, Ferrieri, & Arnold, 2013). In support of these hypotheses, in their transcriptomics study of *C. lutchuensis*, Kondratev et al. (2020) found the upregulation of gene cluster transcripts to be important in oxidation-reduction in plants beginning at 12 hpi and continuing at 24 hpi. In addition, Girard et al. (2017) found that, within 24 hpi, the tolerance of *Brassica napus* cv. Zhongyou 821 (ZY821) was dependent on redox regulation and homeostasis in the ascorbate-glutathione pathway in its defence against *S. sclerotiorum*. This was also evidenced by the hyper-susceptibility in an *Arabidopsis* mutant (*vtc2*) that had a reduced ability to biosynthesise ascorbate. Taken together, these studies show the importance of the delicate balance of ROS homeostasis within disease resistant or tolerant plants. The current study also provides evidence of how upsetting this delicate redox balance by applying antioxidant can affect the resistance of *C. lutchuensis* in the late stage of the interaction.

Therefore, in the *C. lutchuensis – C. camelliae* interaction we see a classic example of ROS accumulation as part of a successful defence response to a pathogenic fungal invasion. This suggests that the apoplastic oxidative burst observed in this *Camellia* species is plant-derived, and that it successfully supresses the fungal invasion because it occurs in the early asymptomatic stage of the infection. This was exhibited by the atypical development of CFB lesions when early apoplastic H_2O_2 accumulation was reduced by ROS scavenging antioxidants.

4.6 The oxidative burst occurs late in the compatible CFB interaction (*C.* 'Nicky Crisp')

Unlike the early and strong apoplastic oxidative burst that was observed in *C. lutchuensis* at 12 hpi in response to ascospore inoculation, an oxidative response was not observed in *C.* 'Nicky Crisp' cell apoplasts until 12 hours later at 24 hpi, and only rare occurrences were observed. Genes associated with the apoplastic oxidative burst, *NOX*, and *PER* also had late upregulation, each with a 3-fold increase at 24 hpi. This late and low-level oxidative response occurs during an advanced and symptomatic stage of the infection. The symptomatic phase of the infection involves hyphal growth progressing into the subepidermal space and mesophyll tissue of susceptible *Camellia* species, as well as broadening the hyphae and secondary hyphal growth, correlating with the formation of CFB lesions (Denton-Giles et al., 2013; Vingnanasingam, 2002). It is therefore suggested that susceptible species like *C.* 'Nicky Crisp' perceive the fungus only after recognising DAMPs that are produced when the fungus fully penetrates the petal and causes damage to the mesophyll layer of tissue (Kondratev et al., 2020). As evidence of this, Kondratev et al. (2020) observed that defence related receptor genes *BAK1* and *SOBIR1* are upregulated in *C.* 'Nicky Crisp' 12 hours later than in *C. lutchuensis.* Therefore, late recognition of the pathogen may be responsible for a delayed oxidative response in susceptible *Camellia*. When the oxidative response is finally activated, it may be too late and at too low of a level

to stop the infection. For example, ROS associated genes that were upregulated in the resistant *C. sinensis* cultivar, Zhongcha 108, were not upregulated within a similar timeframe in the susceptible cultivar, Longjing43 (Wang et al., 2018). Similarly, at 24 hpi, Jayaswall et al. (2016) observed in their transcriptomic studies that GO terms associated with H_2O_2 regulation were only enriched in a cluster of genes identified in a resistant cultivar of *C. sinensis*, SA6, in response to *Exobasidium vexans*, a blister blight causing fungus; while enrichment of the same genes of interest did not occur in the susceptible cultivar. In each of these studies, the timeframe in which an oxidative response was observed in a challenged plant, or whether or not an oxidative response occurred at all, was correlated with resistance or susceptibility to the respective pathogen.

Alternatively, it has been shown that the necrotrophic fungi can supress ROS accumulation in its host, likely via effector secretion. This has been shown in a variety of other systems including *C. camelliae* relatives, such as *B. cinerea's* suppression of the oxidative burst in bean leaf tissue, as well as the suppression of H_2O_2 production during *Penicillium digitatum*'s bacterial infection of citrus fruit (Macarisin et al., 2007; Unger et al., 2005). Interestingly, *S. sclerotiorum* has been shown to initially suppress the apoplastic oxidative burst in *A. thaliana* in order to establish infection by supressing NOX activity with oxalic acid (Cessna, Sears, Dickman, & Low, 2000; Williams et al., 2011; Zhou, Sun, & Xing, 2013). Later the fungus promotes ROS generation to induce the HR and cell death that benefits its necrotrophic lifestyle. Govrin and Levine (2000) showed that in the interaction with *S. sclerotiorum*, an HR-deficient *Arabidopsis* mutant, *dnd1*, remained symptomless in comparison with wild-type plants that developed lesions two days after infection with *S. sclerotiorum* mycelium disks, indicating successful growth and colonisation of the tissue by the pathogen. *C. camelliae* may use a similar strategy to suppress an early oxidative burst in susceptible *Camellia* to facilitate the infection and then later promote ROS accumulation to promote the infection. The significant reduction of lesion development in *C.* 'Nicky Crisp' petals treated with ROS scavenging antioxidants suggests the importance of the late oxidative burst to the necrotrophic fungal infection. Similarly, a significant reduction in H_2O_2 accumulation and lesion incidence in 55-60% of inoculated petals after treatment with L-ascorbic acid and citric acid was also observed by Liu et al. (2013) in their study of the interaction between peach petals and the compatible fungal pathogen, *M. fructicola*.

Therefore, the *C.* 'Nicky Crisp' – *C. camelliae* interaction provides an example of how the lack of an early oxidative burst during the asymptomatic phase contributes to CFB susceptibility, as well as the late upregulation of this response during the symptomatic phase. The data collected in this study are consistent with the line of reasoning either that *C.* 'Nicky Crisp' is unable to recognise the *C. camelliae* in the early stage of the infection or that the fungus initially suppresses the oxidative burst and then later induces an oxidative response that would be of benefit during the necrotrophic and symptomatic phase of the infection. This conclusion is further supported by evidence of the reduction

of CFB lesions when the late apoplastic H_2O_2 accumulation was reduced by ROS scavenging antioxidants.

5 Conclusion

In conclusion, the results from this study suggest that temporal differences in ROS accumulation are one of the mechanisms behind the dual role that ROS play in inhibiting and promoting infection in plant interactions with necrotrophic pathogens from the economically important Sclerotiniaceae family. The findings presented here of the temporal differences of plant-derived ROS accumulation between incompatible and compatible *Camellia* – *C. camelliae* interactions provide further evidence of how plants successfully defend against or succumb to infection by pathogens from this family of destructive necrotrophs. A model outlining the oxidative state during *Camellia* – *C. camelliae* interactions can be proposed: resistant *Camellia* recognise the presence of *C. camelliae* and activate an oxidative burst in response that successfully inhibits further infection (Fig. 5.1). Conversely, the oxidative response may be supressed by the fungus during the asymptomatic phase, perhaps in a mechanism similar to the oxalic acid secretion by *S. sclerotinia* in compatible hosts. Or, *Camellia* may fail to recognise the pathogen until it is too late and the symptomatic phase is already well underway. Activating a late oxidase response benefits the pathogen and CFB develops.

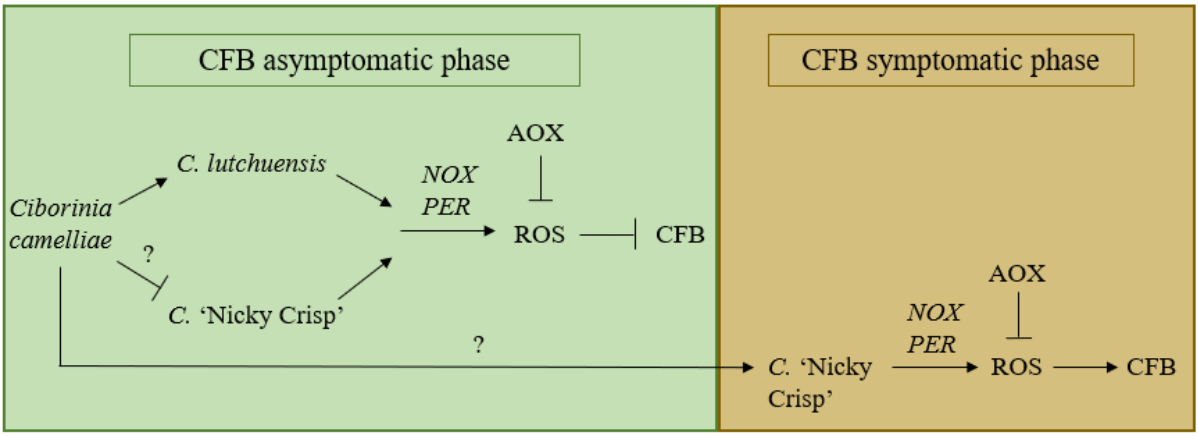

Figure 5.1. Model of temporal reactive oxygen species (ROS) inhibition and promotion to regulate *Camellia* flower blight (CFB) development in disease resistant and susceptible species. During the asymptomatic phase of CFB, gene expression of NADPH oxidase (*NOX*) and cell wall peroxidase (*PER*) is upregulated in resistant *Camellia lutchuensis*. Apoplastic ROS accumulates and inhibits CFB infection. Antioxidant treatments scavenge ROS accumulation, thereby increasing susceptibility to CFB. Conversely, early ROS accumulation does not occur in susceptible *Camellia* 'Nicky Crisp' during the asymptomatic phase and CFB infection develops. In an alternatively proposed pathway, *Ciborinia camelliae* induces a late ROS response in susceptible *C.* 'Nicky Crisp' during the symptomatic phase. *NOX* and *PER* genes are upregulated causing apoplastic ROS to accumulate, which benefits the necrotrophic pathogen and promotes CFB development. Antioxidants scavenge the beneficial ROS accumulation thereby inhibiting CFB development. Arrow and T-bars represent positive and negative regulation, respectively.

To test this model, several methods are proposed for further research. First, continued transcriptomic and proteomic studies may elucidate the roles that *Camellia* IPRs play, if present, in recognising a *C. camelliae* invasion and in establishing if there is a difference in the ability of resistant and susceptible *Camellia* to recognise the pathogenic invasion. Additionally, recent advances have been made in creating transgenic *Camellia* lines (Mondal, Bhattacharya, Ahuja, & Chand, 2001; Mukhopadhyay,

Mondal, & Chand, 2016). The model of *Camellia* resistance to CFB could be tested by developing transgenic lines of resistant species that are deficient in ROS-associated gene expression such as *NOX* and *PER*. The effects on CFB development could be investigated in these lines to determine the importance of apoplastic ROS accumulation during the asymptomatic phase of the infection that was observed in the current study. Conversely, transgenic lines of susceptible *Camellia* with induced expression of *NOX* and *PER* during the asymptomatic phase of the interaction would test whether CFB development could be fully or partially inhibited by earlier activity of these genes. Inducible promoters which are activated by the application of an exogenous compound could be used to activate the GOIs in the desired timeframe. In addition, the onset of necrotrophic behaviour in *C. camelliae* during the symptomatic phase in susceptible *Camellia* could be delayed. For example, Gan et al. (2013) observed the upregulation of predicted gene sequences encoding cellulose, hemicellulose, and pectin degrading enzymes during the switch of *Colletotrichum* fungi from biotrophic to necrotrophic behaviour, thereby causing a transition in their host plants from the asymptomatic phase of the disease to the symptomatic phase. If a similar pattern in the temporal expression of these genes' families was also found in *C. camelliae* during the susceptible interaction, a mutant strain of *C. camelliae* could be made with corresponding gene knockouts to determine if CFB infection would still progress. Finally, repeating the experiments conducted in this study in additional CFB resistant and susceptible *Camellia*, as well as other plant-pathogen systems that include a pathogen from the Sclerotiniaceae family, would improve the generalisability of the current results across the *Camellia* genus as well as this important family of necrotrophic fungal pathogens.

References

Abdel-Monaim, M. F., & Ismail, M. E. (2010). The use of antioxidants to control root rot and wilt diseases of pepper. *Notulae Scientia Biologicae, 2*(2). doi:10.15835/nsb223699

Albert, I., Böhm, H., Albert, M., Feiler, C. E., Imkampe, J., Wallmeroth, N., . . . Nürnberger, T. (2015). An RLP23–SOBIR1–BAK1 complex mediates NLP-triggered immunity. *Nature Plants, 1*(10), 15140. doi:10.1038/nplants.2015.140

Almagro, L., Ros, L. V. G., Belchi-Navarro, S., Bru, R., Barcelo, A. R., & Pedreno, M. A. (2009). Class III peroxidases in plant defence reactions. *Journal of Experimental Botany, 60*(2), 377-390. doi:10.1093/jxb/ern277

Apel, K., & Hirt, H. (2004). Reactive oxygen species: Metabolism, oxidative stress, and signal transduction. *Annual Review of Plant Biology, 55*, 373-399. doi:10.1146/annurev.arplant.55.031903.141701

Ardila, H. D., Torres, A. M., Martinez, S. T., & Higuera, B. L. (2014). Biochemical and molecular evidence for the role of class III peroxidases in the resistance of carnation (*Dianthus caryophyllus* L) to *Fusarium oxysporum* f. sp *dianthi*. *Physiological and Molecular Plant Pathology, 85*, 42-52. doi:10.1016/j.pmpp.2014.01.003

Asai, S., Ohta, K., & Yoshioka, H. (2008). MAPK signaling regulates nitric oxide and NADPH oxidase-dependent oxidative bursts in *Nicotiana benthamiana*. *Plant Cell, 20*(5), 1390-1406. doi:10.1105/tpc.107.055855

Asselbergh, B., Curvers, K., França, S. C., Audenaert, K., Vuylsteke, M., Van Breusegem, F., & Höfte, M. (2007). Resistance to *Botrytis cinerea in sitiens*, an abscisic acid-deficient tomato mutant, involves timely production of hydrogen peroxide and cell wall modifications in the epidermis. *Plant Physiology, 144*(4), 1863. doi:10.1104/pp.107.099226

Bailey, B. A. (1995). Purification of a protein from culture filtrates of *Fusarium oxysporum* that induces ethylene and necrosis in leaves of *Erythroxylum coca*. *Phytopathology, 85*(10), 1250-1255.

Barna, B., Fodor, J., Harrach, B. D., Pogány, M., & Király, Z. (2012). The Janus face of reactive oxygen species in resistance and susceptibility of plants to necrotrophic and biotrophic pathogens. *Plant Physiology and Biochemistry, 59*, 37-43. doi:10.1016/j.plaphy.2012.01.014

Barna, B., Fodor, J., Pogany, M., & Kiraly, Z. (2003). Role of reactive oxygen species and antioxidants in plant disease resistance. *Pest Management Science, 59*(4), 459-464. doi:10.1002/ps.706

Bashi, Z. D., Hegedus, D. D., Buchwaldt, L., Rimmer, S. R., & Borhan, M. H. (2010). Expression and regulation of *Sclerotinia sclerotiorum* necrosis and ethylene-inducing peptides (NEPs). *Molecular Plant Pathology, 11*(1), 43-53.

Bauer, R., Oberwinkler, F., & Vánky, K. (1997). Ultrastructural markers and systematics in smut fungi and allied taxa. *Canadian Journal of Botany, 75*(8), 1273-1314. doi:10.1139/b97-842

Bestwick, C. S., Brown, I. R., Bennett, M. H. R., & Mansfield, J. W. (1997). Localization of hydrogen peroxide accumulation during the hypersensitive reaction of lettuce cells to *Pseudomonas syringae* pv *phaseolicola*. *Plant Cell, 9*(2), 209-221.

Bhuiyan, N. H., Selvaraj, G., Wei, Y., & King, J. (2009). Role of lignification in plant defense. *Plant Signaling & Behavior, 4*(2), 158-159. doi:10.4161/psb.4.2.7688

Bindschedler, L. V., Dewdney, J., Blee, K. A., Stone, J. M., Asai, T., Plotnikov, J., . . . Bolwell, G. P. (2006). Peroxidase-dependent apoplastic oxidative burst in *Arabidopsis* required for pathogen resistance. *The Plant Journal, 47*(6), 851-863. doi:10.1111/j.1365-313X.2006.02837.x

Boller, T., & Felix, G. (2009). A renaissance of elicitors: perception of microbe-associated molecular patterns and danger signals by pattern-recognition receptors. *Annual Review of Plant Biology, 60*(1), 379-406. doi:10.1146/annurev.arplant.57.032905.105346

Boutrot, F., & Zipfel, C. (2017). Function, discovery, and exploitation of plant pattern recognition receptors for broad-spectrum disease resistance. *Annual Review of Phytopathology, 55*(1), 257-286. doi:10.1146/annurev-phyto-080614-120106

Brefort, T., Doehlemann, G., Mendoza-Mendoza, A., Reissmann, S., Djamei, A., & Kahmann, R. (2009). *Ustilago maydis* as a pathogen. *Annual Review of Phytopathology, 47*(1), 423-445. doi:10.1146/annurev-phyto-080508-081923

Brumbarova, T., Le, C. T. T., & Bauer, P. (2016). Hydrogen peroxide measurement in *Arabidopsis* root tissue using Amplex Red. *Bio-protocol, 6*(21), e1999. doi:10.21769/BioProtoc.1999

Camejo, D., Guzman-Cedeno, A., & Moreno, A. (2016). Reactive oxygen species, essential molecules, during plant-pathogen interactions. *Plant Physiology and Biochemistry, 103*, 10-23. doi:10.1016/j.plaphy.2016.02.035

Cessna, S. G., Sears, V. E., Dickman, M. B., & Low, P. S. (2000). Oxalic acid, a pathogenicity factor for *Sclerotinia sclerotiorum*, suppresses the oxidative burst of the host plant. *Plant Cell, 12*(11), 2191-2199. doi:10.1105/tpc.12.11.2191

Chinchilla, D., Bauer, Z., Regenass, M., Boller, T., & Felix, G. (2006). The *Arabidopsis* receptor kinase FLS2 binds flg22 and determines the specificity of flagellin perception. *Plant Cell, 18*(2), 465-476. doi:10.1105/tpc.105.036574

Coll, N. S., Epple, P., & Dangl, J. L. (2011). Programmed cell death in the plant immune system. *Cell Death and Differentiation, 18*(8), 1247-1256. doi:10.1038/cdd.2011.37

Cook, D. E., Mesarich, C. H., & Thomma, B. P. H. J. (2015). Understanding plant immunity as a surveillance system to detect invasion. In N. K. VanAlfen (Ed.), *Annual Review of Phytopathology, Vol 53* (Vol. 53, pp. 541-563).

Corpas, F. J., Gupta, D. K., & Palma, J. M. (2015). Production sites of reactive oxygen species (ROS) in organelles from plant cells. In D. K. Gupta, J. M. Palma, & F. J. Corpas (Eds.), *Reactive Oxygen Species and Oxidative Damage in Plants Under Stress* (pp. 1-22). New York: Springer International Publishing.

Couselo, J. L., Vela, P., Salinero, C., & Mansilla, P. (2014). Susceptibility trials of different *Camellia* species to *Ciborinia camelliae*. *International Camellia Journal, 46*, 64-65.

Dean, R., Van Kan, J. A. L., Pretorius, Z. A., Hammond-Kosack, K. E., Di Pietro, A., Spanu, P. D., . . . Foster, G. D. (2012). The Top 10 fungal pathogens in molecular plant pathology. *Molecular Plant Pathology, 13*(4), 414-430. doi:10.1111/j.1364-3703.2011.00783.x

Deng, X. G., Zhu, T., Zou, L. J., Han, X. Y., Zhou, X., Xi, D. H., . . . Lin, H. H. (2016). Orchestration of hydrogen peroxide and nitric oxide in brassinosteroid-mediated systemic virus resistance in *Nicotiana benthamiana*. *Plant Journal, 85*(4), 478-493. doi:10.1111/tpj.13120

Denton-Giles, M., Bradshaw, R. E., & Dijkwel, P. P. (2013). *Ciborinia camelliae* (Sclerotiniaceae) induces variable plant resistance responses in selected species of *Camellia*. *Phytopathology, 103*(7), 725-732. doi:10.1094/phyto-11-12-0289-r

Despres, C., Chubak, C., Rochon, A., Clark, R., Bethune, T., Desveaux, D., & Fobert, P. R. (2003). The *Arabidopsis* NPR1 disease resistance protein is a novel cofactor that confers redox regulation of DNA binding activity to the basic domain/leucine zipper transcription factor TGA1. *Plant Cell, 15*(9), 2181-2191. doi:10.1105/tpc.012849

Dickman, M. B., & de Figueiredo, P. (2013). Death be not proud-Cell death control in plant fungal interactions. *Plos Pathogens, 9*(9), 4. doi:10.1371/journal.ppat.1003542

Dickman, M. B., & Fluhr, R. (2013). Centrality of host cell death in plant-microbe interactions. In N. K. VanAlfen (Ed.), *Annual Review of Phytopathology, Vol 51* (pp. 543-570).

Doke, N. (1983). Involvement of superoxide anion generation in the hypersensitive response of potato tuber tissues to infection with an incompatible race of *Phytophthora infestans* and to the hyphal wall components. *Physiological Plant Pathology, 23*(3), 345-357.

Drerup, M. M., Schlücking, K., Hashimoto, K., Manishankar, P., Steinhorst, L., Kuchitsu, K., & Kudla, J. (2013). The calcineurin B-like calcium sensors CBL1 and CBL9 together with their interacting protein kinase CIPK26 regulate the *Arabidopsis* NADPH oxidase RBOHF. *Molecular Plant, 6*(2), 559-569. doi:https://doi.org/10.1093/mp/sst009

El-Korany, A. E., & Mohamed, R. A. (2008). The use of antioxidants to control grey mould and to enhance yield and quality of strawberry. *Journal of Agricultural and Environmental Science of Alexandria University, 7*(1), 1-38.

Elad, Y. (1992). The use of antioxidants (free radical scavengers) to control grey mould (*Botrytis cinerea)* and white mould (*Sclerotinia sclerotiorum*) in various crops. *Plant Pathology, 41*, 417-426.

Ellis, R. E., Yuan, J. Y., & Horvitz, H. R. (1991). Mechanisms and functions of cell-death. *Annual Review of Cell Biology, 7*, 663-698. doi:10.1146/annurev.cb.07.110191.003311

Fang, F. C. (2004). Antimicrobial reactive oxygen and nitrogen species: Concepts and controversies. *Nature Reviews Microbiology, 2*(10), 820-832. doi:10.1038/nrmicro1004

Fatima, U., & Senthil-Kumar, M. (2015). Plant and pathogen nutrient acquisition strategies. *Frontiers in Plant Science, 6*, 750. doi:10.3389/fpls.2015.00750

Flannagan, R. S., Cosio, G., & Grinstein, S. (2009). Antimicrobial mechanisms of phagocytes and bacterial evasion strategies. *Nature Reviews Microbiology, 7*(5), 355-366. doi:10.1038/nrmicro2128

Flor, H. H. (1971). Current status of the gene-for-gene concept. *Annual Review of Phytopathology, 9*(1), 275-296.

Foyer, C. H., & Noctor, G. (2005). Redox homeostasis and antioxidant signaling: A metabolic interface between stress perception and physiological responses. *Plant Cell, 17*(7), 1866-1875. doi:10.1105/tpc.105.033589

Foyer, C. H., & Noctor, G. (2011). Ascorbate and glutathione: the heart of the redox hub. *Plant Physiology, 155*(1), 2.

Gaffney, T., Friedrich, L., Vernooij, B., Negrotto, D., Nye, G., Uknes, S., . . . Ryals, J. (1993). Requirement of salicylic-acid for the induction of systemic aquired-resistance. *Science, 261*(5122), 754-756. doi:10.1126/science.261.5122.754

Galletti, R., Ferrari, S., & De Lorenzo, G. (2011). *Arabidopsis* MPK3 and MPK6 play different roles in basal and oligogalacturonide- or flagellin-induced resistance against *Botrytis cinerea*. *Plant Physiology, 157*(2), 804-814. doi:10.1104/pp.111.174003

Gechev, T. S., Van Breusegem, F., Stone, J. M., Denev, I., & Laloi, C. (2006). Reactive oxygen species as signals that modulate plant stress responses and programmed cell death. *Bioessays, 28*(11), 1091-1101. doi:10.1002/bies.20493

Gibson, D. M., King, B. C., Hayes, M. L., & Bergstrom, G. C. (2011). Plant pathogens as a source of diverse enzymes for lignocellulose digestion. *Current Opinion in Microbiology, 14*(3), 264-270. doi:https://doi.org/10.1016/j.mib.2011.04.002

Girard, I. J., Tong, C., Becker, M. G., Mao, X., Huang, J., de Kievit, T., . . . Belmonte, M. F. (2017). RNA sequencing of *Brassica napus* reveals cellular redox control of *Sclerotinia* infection. *Journal of Experimental Botany, 68*(18), 5079-5091.

Glazebrook, J. (2005). Contrasting mechanisms of defense against biotrophic and necrotrophic pathogens. *Annual Review of Phytopathology* (Vol. 43, pp. 205-227).

Govrin, E. M., & Levine, A. (2000). The hypersensitive response facilitates plant infection by the necrotrophic pathogen *Botrytis cinerea*. *Current Biology, 10*(13), 751-757. doi:10.1016/s0960-9822(00)00560-1

Hammer, P. E., & Evensen, K. B. (1994). Differences between rose cultivars in susceptibility to infection by *Botrytis cinerea*. *Phytopathology, 84*, 1305-1312.

Hao, X. Y., Horvath, D. P., Chao, W. S., Yang, Y. J., Wang, X. C., & Xiao, B. (2014). Identification and evaluation of reliable reference genes for Quantitative Real-Time PCR analysis in tea plant (*Camellia sinensis* (L.) O. Kuntze). *International Journal of Molecular Sciences, 15*(12), 22155-22172. doi:10.3390/ijms151222155

Hara, K. (1919). A sclerotial disease of *Camellia* (*Camellia japonica*). *Dianpon Sanrin Kaiho, 436*, 29-31. (Japanese) As cited in Kohn and Nagasawa (1984).

Heil, M., & Baldwin, I. T. (2002). Fitness costs of induced resistance: emerging experimental support for a slippery concept. *Trends in Plant Science, 7*(2), 61-67. doi:https://doi.org/10.1016/S1360-1385(01)02186-0

Heller, J., & Tudzynski, P. (2011). Reactive oxygen species in phytopathogenic fungi: signaling, development, and disease. In N. K. VanAlfen, G. Bruening, & J. E. Leach (Eds.), *Annual Review of Phytopathology*, (Vol 49, pp. 369-390).

Hernández-Barrera, A., Quinto, C., Johnson, E. A., Wu, H. M., Cheung, A. Y., & Cárdenas, L. (2013). Using hyper as a molecular probe to visualize hydrogen peroxide in living plant cells: A method with virtually unlimited potential in plant biology. In E. Cadenas & L. Packer (Eds.), *Methods in Enzymology* (Vol. 527, pp. 275-290): Academic Press.

Hückelhoven, R., Fodor, J., Preis, C., & Kogel, K. H. (1999). Hypersensitive cell death and papilla formation in barley attacked by the powdery mildew fungus are associated with hydrogen peroxide but not with salicylic acid accumulation. *Plant Physiology, 119*(4), 1251. doi:10.1104/pp.119.4.1251

Huh, W. K., Kim, S. T., Kim, H., Jeong, G., & Kang, S. O. (2001). Deficiency of D-erythroascorbic acid attenuates hyphal growth and virulence of *Candida albicans*. *Infection and Immunity, 69*(6), 3939-3946. doi:10.1128/IAI.69.6.3939-3946.2001

Iakimova, E. T., & Woltering, E. J. (2018). The wound response in fresh-cut lettuce involves programmed cell death events. *Protoplasma, 255*(4), 1225-1238. doi:10.1007/s00709-018-1228-y

Jayaswall, K., Mahajan, P., Singh, G., Parmar, R., Seth, R., Raina, A., . . . Sharma, R. K. (2016). Transcriptome analysis reveals candidate genes involved in blister blight defense in tea (*Camellia sinensis* (L.) Kuntze). *Scientific Reports, 6*(1), 30412. doi:10.1038/srep30412

Jones, A. M. P., & Saxena, P. K. (2013). Inhibition of phenylpropanoid biosynthesis in *Artemisia annua* L.: a novel approach to reduce oxidative browning in plant tissue culture. *Plos One, 8*(10), e76802-e76802. doi:10.1371/journal.pone.0076802

Jones, J. D. G., & Dangl, J. L. (2006). The plant immune system. *Nature, 444*(7117), 323-329.

Kaku, H., Nishizawa, Y., Ishii-Minami, N., Akimoto-Tomiyama, C., Dohmae, N., Takio, K., . . . Shibuya, N. (2006). Plant cells recognize chitin fragments for defense signaling through a plasma membrane receptor. *Proceedings of the National Academy of Sciences of the United States of America, 103*(29), 11086-11091. doi:10.1073/pnas.0508882103

Kazan, K., & Lyons, R. (2014). Intervention of phytohormone pathways by pathogen effectors. *Plant Cell, 26*(6), 2285-2309. doi:10.1105/tpc.114.125419

Keller, T., Damude, H. G., Werner, D., Doerner, P., Dixon, R. A., & Lamb, C. (1998). A plant homolog of the neutrophil NADPH oxidase gp91(phox) subunit gene encodes a plasma membrane protein with Ca^{2+} binding motifs. *Plant Cell, 10*(2), 255-266. doi:10.1105/tpc.10.2.255

Kelloniemi, J., Trouvelot, S., Heloir, M. C., Simon, A., Dalmais, B., Frettinger, P., . . . Viaud, M. (2015). Analysis of the molecular dialogue between gray mold (*Botrytis cinerea*) and grapevine (*Vitis vinifera*) reveals a clear shift in defense mechanisms during berry ripening. *Molecular Plant-Microbe Interactions, 28*(11), 1167-1180. doi:10.1094/mpmi-02-15-0039-r

Kemmerling, B., Schwedt, A., Rodriguez, P., Mazzotta, S., Frank, M., Qamar, S. A., . . . Nürnberger, T. (2007). The BRI1-associated kinase 1, BAK1, has a brassinolide-independent role in plant cell-death control. *Current Biology, 17*(13), 1116-1122. doi:https://doi.org/10.1016/j.cub.2007.05.046

Khan, S. H., Aked, J., & Magan, N. (2001). Control of the anthracnose pathogen of banana (*Colletotrichum musae*) using antioxidants alone and in combination with thiabendazole or imazalil. *Plant Pathology, 50*(5), 601-608. doi:10.1046/j.1365-3059.2001.00599.x

Kim, H., Chen, C., Kabbage, M., & Dickman, M. B. (2011). Identification and characterization of *Sclerotinia sclerotiorum* NADPH oxidases. *Applied and Environmental Microbiology, 77*(21), 7721-7729. doi:10.1128/aem.05472-11

Kim, K. S., Min, J., & Dickman, M. (2008). Oxalic acid is an elicitor of plant programmed cell death during *Sclerotinia sclerotiorum* disease development. *Molecular Plant-Microbe Interactions, 21*(5), 605-612. doi:10.1094/mpmi-21-5-0605

Kohn, L. M., & Nagasawa, E. (1984). A taxonomic reassessment of *Sclerotinia camelliae* Hara (=*Ciborinia camelliae* Kohn), with observations on flower blight of *Camellia* in Japan. *Transactions of the Mycological Society of Japan, 25*(2), 149-161.

Kondratev, N., Denton-Giles, M., Bradshaw, R. E., Cox, M. P., & Dijkwel, P. P. (2020). *Camellia* plant resistance and susceptibility to petal blight disease are defined by the timing of defense responses. *Molecular Plant-Microbe Interactions, 33*(7), 982-995. doi:https://doi.org/10.1094/MPMI-10-19-0304-R

Kovtun, Y., Chiu, W. L., Tena, G., & Sheen, J. (2000). Functional analysis of oxidative stress-activated mitogen-activated protein kinase cascade in plants. *Proceedings of the National Academy of Sciences of the United States of America, 97*(6), 2940-2945. doi:10.1073/pnas.97.6.2940

Kunitake, Y. K., Hasegawa, M., Miyashita, T., & Higuchi, H. (2004). Role of a seasonally specialist bird *Zosterops japonica* on pollen transfer and reproductive success of *Camellia japonica* in a temperate area. *Plant Species Biology, 19*(3), 197-201.

Kwak, J. M., Nguyen, V., & Schroeder, J. I. (2006). The role of reactive oxygen species in hormonal responses. *Plant Physiology, 141*(2), 323. doi:10.1104/pp.106.079004

Lamb, C., & Dixon, R. A. (1997). The oxidative burst in plant disease resistance. *Annual Review of Plant Physiology and Plant Molecular Biology, 48*, 251-275. doi:10.1146/annurev.arplant.48.1.251

Larsson, C., Widell, S., & Kjellbom, P. (1987). Preparation of high-purity plasma membranes. *Methods in Enzymology, 148*, 558-568.

Lehmann, S., Serrano, M., L'Haridon, F., Tjamos, S. E., & Metraux, J. P. (2015). Reactive oxygen species and plant resistance to fungal pathogens. *Phytochemistry, 112*, 54-62. doi:10.1016/j.phytochem.2014.08.027

Li, H., Ren, B., Kang, Z. S., & Huang, L. L. (2016). Comparison of cell death and accumulation of reactive oxygen species in wheat lines with or without Yr36 responding to *Puccinia*

striiformis f. sp *tritici* under low and high temperatures at seedling and adult-plant stages. *Protoplasma, 253*(3), 787-802. doi:10.1007/s00709-015-0833-2

Liebrand, T. W. H., van den Burg, H. A., & Joosten, M. H. A. J. (2014). Two for all: Receptor-associated kinases SOBIR1 and BAK1. *Trends in Plant Science, 19*(2), 123-132. doi:https://doi.org/10.1016/j.tplants.2013.10.003

Liu, J., Macarisin, D., Wisniewski, M., Sui, Y., Droby, S., Norelli, J., & Hershkovitz, V. (2013). Production of hydrogen peroxide and expression of ROS-generating genes in peach flower petals in response to host and non-host fungal pathogens. *Plant Pathology, 62*(4), 820-828. doi:10.1111/j.1365-3059.2012.02683.x

Liu, X., Williams, C. E., Nemacheck, J. A., Wang, H., Subramanyam, S., Zheng, C., & Chen, M. S. (2010). Reactive oxygen species are involved in plant defense against a gall midge. *Plant Physiology, 152*(2), 985-999. doi:10.1104/pp.109.150656

Lo Presti, L., Lanver, D., Schweizer, G., Tanaka, S., Liang, L., Tollot, M., . . . Kahmann, R. (2015). Fungal effectors and plant susceptibility. In S. S. Merchant (Ed.), *Annual Review of Plant Biology*. (Vol. 66, pp. 513-545).

Macarisin, D., Cohen, L., Eick, A., Rafael, G., Belausov, E., Wisniewski, M., & Droby, S. (2007). *Penicillium digitatum* suppresses production of hydrogen peroxide in host tissue during infection of citrus fruit. *Postharvest Pathology and Mycotoxins, 97*(11), 1491-1500. doi:10.1094/PHYTO-97-11-1491

Mammarella, N. D., Cheng, Z. Y., Fu, Z. Q., Daudi, A., Bolwell, G. P., Dong, X. N., & Ausubel, F. M. (2015). Apoplastic peroxidases are required for salicylic acid-mediated defense against *Pseudomonas syringae*. *Phytochemistry, 112*, 110-121. doi:10.1016/j.phytochem.2014.07.010

Matei, A., & Doehlemann, G. (2016). Cell biology of corn smut disease—*Ustilago maydis* as a model for biotrophic interactions. *Current Opinion in Microbiology, 34*, 60-66. doi:https://doi.org/10.1016/j.mib.2016.07.020

Mehari, Z. H., Pilati, S., Sonego, P., Malacarne, G., Vrhovsek, U., Engelen, K., . . . Moser, C. (2017). Molecular analysis of the early interaction between the grapevine flower and *Botrytis cinerea* reveals that prompt activation of specific host pathways leads to fungus quiescence. *Plant, Cell & Environment*. doi:10.1111/pce.12937

Mellersh, D. G., Foulds, I. V., Higgins, V. J., & Heath, M. C. (2002). H_2O_2 plays different roles in determining penetration failure in three diverse plant-fungal interactions. *The Plant Journal, 29*(3), 257-268. doi:10.1046/j.0960-7412.2001.01215.x

Meng, X., & Zhang, S. (2013). MAPK cascades in plant disease resistance signaling. In N. K. VanAlfen (Ed.), *Annual Review of Phytopathology*. (Vol. 51, pp. 245-266).

Meyers, B. C., Kozik, A., Griego, A., Kuang, H., & Michelmore, R. W. (2003). Genome-wide analysis of NBS-LRR-encoding genes in *Arabidopsis*. *Plant Cell, 15*(4), 809-834. doi:10.1105/tpc.009308

Mitchell, K., Brown, I., Knox, P., & Mansfield, J. (2015). The role of cell wall-based defences in the early restriction of non-pathogenic *hrp* mutant bacteria in *Arabidopsis. Phytochemistry, 112*, 139-150. doi:10.1016/j.phytochem.2014.07.015

Molina, L., & Kahmann, R. (2007). An *Ustilago maydis* gene involved in H_2O_2 detoxification is required for virulence. *Plant Cell, 19*(7), 2293-2309. doi:10.1105/tpc.107.052332

Mondal, T., Bhattacharya, A., Ahuja, P., & Chand, P. (2001). Transgenic tea [*Camellia sinensis* (L.) O. Kuntze cv. Kangra Jat] plants obtained by *Agrobacterium*-mediated transformation of somatic embryos. *Plant Cell Reports, 20*(8), 712-720.

Mukhopadhyay, M., Mondal, T. K., & Chand, P. K. (2016). Biotechnological advances in tea (*Camellia sinensis* L. O. Kuntze): a review. *Plant Cell Reports, 35*(2), 255-287. doi:10.1007/s00299-015-1884-8

Nie, S. J., & Xu, H. L. (2016). Riboflavin-induced disease resistance requires the mitogen-activated protein kinases 3 and 6 in *Arabidopsis thaliana*. *Plos One, 11*(4), 19. doi:10.1371/journal.pone.0153175

Nothnagel, E. A., McNeil, M., Albersheim, P., & Dell, A. (1983). A galacturonic acid oligosaccharide from plant cell walls elicits phytoalexins. *Plant Physiology, 71*(4), 916. doi:10.1104/pp.71.4.916

Olson, P. D., & Varner, J. E. (1993). Hydrogen-peroxide and lignification. *Plant Journal, 4*(5), 887-892. doi:10.1046/j.1365-313X.1993.04050887.x

Palomares-Rius, J. E., Hirooka, Y., Tsai, I. J., Masuya, H., Hino, A., Kanzaki, N., . . . Kikuchi, T. (2014). Distribution and evolution of glycoside hydrolase family 45 cellulases in nematodes and fungi. *BMC Evolutionary Biology, 14*(1), 69. doi:10.1186/1471-2148-14-69

Passardi, F., Penel, C., & Dunand, C. (2004). Performing the paradoxical: How plant peroxidases modify the cell wall. *Trends in Plant Science, 9*(11), 534-540. doi:10.1016/j.tplants.2004.09.002

Ranf, S., Eschen-Lippold, L., Pecher, P., Lee, J., & Scheel, D. (2011). Interplay between calcium signalling and early signalling elements during defence responses to microbe- or damage-associated molecular patterns. *The Plant Journal, 68*(1), 100-113. doi:https://doi.org/10.1111/j.1365-313X.2011.04671.x

Ruijter, J. M., Ramakers, C., Hoogaars, W. M. H., Karlen, Y., Bakker, O., van den Hoff, M. J. B., & Moorman, A. F. M. (2009). Amplification efficiency: linking baseline and bias in the analysis of quantitative PCR data. *Nucleic Acids Research, 37*(6), e45.

Sandrock, R. W., & VanEtten, H. D. (1998). Fungal sensitivity to and enzymatic degradation of the phytoanticipin α-Tomatine. *Phytopathology, 88*(2), 137-143. doi:10.1094/phyto.1998.88.2.137

Schellenberger, R., Touchard, M., Clément, C., Baillieul, F., Cordelier, S., Crouzet, J., & Dorey, S. (2019). Apoplastic invasion patterns triggering plant immunity: plasma membrane sensing at the frontline. *Molecular Plant Pathology, 20*(11), 1602-1616. doi:https://doi.org/10.1111/mpp.12857

Schreiber, L. (1995). A mechanistic approach towards surfactant/wax interactions: Effects of octaethyleneglycolmonododecylether on sorption and diffusion of organic chemicals in reconstituted cuticular wax of barley leaves. *Pesticide Science, 45*(1), 1-11. doi:10.1002/ps.2780450102

Schultz, J., Appel, H., Ferrieri, A., & Arnold, T. (2013). Flexible resource allocation during plant defense responses. *Frontiers in Plant Science, 4*(324). doi:10.3389/fpls.2013.00324

Schulze-Lefert, P. (2004). Knocking on heaven's wall: Pathogenesis of and resistance to biotrophic fungi at the cell wall. *Current Opinion in Plant Biology, 7*(4), 377-383. doi:10.1016/j.pbi.2004.05.004

Selvendran, R. R. (1975). Analysis of cell wall material from plant tissues: Extraction and purification. *Phytochemistry, 14*(4), 1011-1017. doi:https://doi.org/10.1016/0031-9422(75)85178-8

Sewelam, N., Kazan, K., & Schenk, P. M. (2016). Global plant stress signaling: reactive oxygen species at the cross-road. *Frontiers in Plant Science, 7*. doi:10.3389/fpls.2015.00187

Shetty, N. P., Jorgensen, H. J. L., Jensen, J. D., Collinge, D. B., & Shetty, H. S. (2008). Roles of reactive oxygen species in interactions between plants and pathogens. *European Journal of Plant Pathology, 121*(3), 267-280. doi:10.1007/s10658-008-9302-5

Shetty, N. P., Mehrabi, R., Lutken, H., Haldrup, A., Kema, G. H. J., Collinge, D. B., & Jorgensen, H. J. L. (2007). Role of hydrogen peroxide during the interaction between the hemibiotrophic

fungal pathogen *Septoria tritici* and wheat. *New Phytologist, 174*(3), 637-647. doi:10.1111/j.1469-8137.2007.02026.x

Shomeet, A. M. M., El-Samadisy, A. M. I., El-Kholy, R. M. A., & Ibrahim, I. S. (2018). Effect of fungicides, antioxidants and their mixtures on mycelial growth of some fungi. *Middle East Journal of Applied Sciences, 08*(08), 647-655.

Skibbe, D. S., Doehlemann, G., Fernandes, J., & Walbot, V. (2010). Maize tumors caused by *Ustilago maydis* require organ-specific genes in host and pathogen. *Science, 328*(5974), 89-92.

Stewart, T. M., & Neilson, H. (1993). Flower blight: a rare new disease of *Camellia* in New Zealand. *New Zealand Camellia Bulletin, 116*, 29-33.

Sun, S. G., Huang, Z. H., Chen, Z. B., & Huang, S. Q. (2017). Nectar properties and the role of sunbirds as pollinators of the golden-flowered tea (*Camellia petelotii)*. *American Journal of Botany, 104*(3), 468-476. doi:10.3732/ajb.1600428

Survila, M., Davidsson, P. R., Pennanen, V., Kariola, T., Broberg, M., Sipari, N., . . . Palva, E. T. (2016). Peroxidase-generated apoplastic ROS impair cuticle integrity and contribute to DAMP-elicited defenses. *Frontiers in Plant Science, 7*(1945), 1-16. doi:10.3389/fpls.2016.01945

Tanabe, S., Nishizawa, Y., & Minami, E. (2009). Effects of catalase on the accumulation of H_2O_2 in rice cells inoculated with rice blast fungus, *Magnaporthe oryzae*. *Physiologia Plantarum, 137*(2), 148-154. doi.org/10.1111/j.1399-3054.2009.01272.x

Taylor, C. H. (2004). *Studies of camellia flower blight (Ciborinia camelliae* Kohn*).* (Doctoral dissertation) Massey University, Palmerston North, New Zealand.

Taylor, C. H. & Long, P. G. (2000). Review of literature on *Camellia* flower blight caused by *Ciborinia camelliae*. *New Zealand Journal of Crop Horticulture, 28*(2), 123-138.

Thompson, D. P. (1996). Inhibition of growth of mycotoxigenic *Fusarium* species by butylated hydroxyanisole and/or carvacrol. *Journal of Food Protection, 59*(4), 412-415. doi:10.4315/0362-028x-59.4.412

Thordal-Christensen, H., Zhang, Z. G., Wei, Y. D., & Collinge, D. B. (1997). Subcellular localization of H_2O_2 in plants. H_2O_2 accumulation in papillae and hypersensitive response during the barley-powdery mildew interaction. *Plant Journal, 11*(6), 1187-1194. doi:10.1046/j.1365-313X.1997.11061187.x

Torres, M. A. (2010). ROS in biotic interactions. *Physiologia Plantarum, 138*(4), 414-429. doi:10.1111/j.1399-3054.2009.01326.x

Torres, M. A., Dangl, J. L., & Jones, J. D. G. (2002). *Arabidopsis* gp91^{phox} homologues *AtrbohD* and *AtrbohF* are required for accumulation of reactive oxygen intermediates in the plant defense response. *Proceedings of the National Academy of Sciences, United States of America 99*(1), 517-522. doi:10.1073/pnas.012452499

Torres, M. A., Jones, J. D. G., & Dangl, J. L. (2006). Reactive oxygen species signaling in response to pathogens. *Plant Physiology, 141*(2), 373-378. doi:10.1104/pp.106.079467

Uchneat, M. S., Spicer, K., & Craig, R. (1999). Differential response to floral infection by *Botrytis cinerea* within the genus *Pelargonium*. *HortScience, 34*(4), 718-720. doi:10.21273/HORTSCI.34.4.718

Umezawa, T. (2010). The cinnamate/monolignol pathway. *Phytochemistry Reviews, 9*(1), 1-17. doi:10.1007/s11101-009-9155-3

Unger, C., Kleta, S., Jandl, G., & von Tiedemann, A. (2005). Suppression of the defence-related oxidative burst in bean leaf tissue and bean suspension cells by the necrotrophic pathogen *Botrytis cinerea*. *Journal of Phytopathology, 153*(1), 15-26. doi:10.1111/j.1439-0434.2004.00922.x

van der Loos, C. M. (2008). Multiple immunoenzyme staining: Methods and visualizations for the observation with spectral imaging. *Journal of Histochemistry and Cytochemistry, 56*(4), 313-328. doi:10.1369/jhc.2007.950170

van Doorn, W. G., Beers, E. P., Dangl, J. L., Franklin-Tong, V. E., Gallois, P., Hara-Nishimura, I., . . . Bozhkov, P. V. (2011). Morphological classification of plant cell deaths. *Cell Death and Differentiation, 18*(8), 1241-1246. doi:10.1038/cdd.2011.36

Van Toor, R. F., Jaspers, M. V., & Stewart, A. (2005). Effect of soil microorganisms on viability of sclerotia of *Ciborinia camelliae*, the causal agent of *Camellia* flower blight. *New Zealand Journal of Crop and Horticultural Science, 33*(2), 149-160.

Van Toor, R. F., Jaspers, M. V., Stewart, A. (2001). Evaluation of acibenzolar-S-methyl for induction of resistance in *Camellia* flowers to *Ciborinia camelliae* infection. *New Zealand Plant Protection* (Vol. 54, pp. 209-212).

Vanacker, H., Carver, T. L. W., & Foyer, C. H. (1998). Pathogen-induced changes in the antioxidant status of the apoplast in barley leaves. *Plant Physiology, 117*(3), 1103-1114. doi:10.1104/pp.117.3.1103

Vatansever, F., de Melo, W. C. M. A., Avci, P., Vecchio, D., Sadasivam, M., Gupta, A., . . . Hamblin, M. R. (2013). Antimicrobial strategies centered around reactive oxygen species - bactericidal antibiotics, photodynamic therapy, and beyond. *Fems Microbiology Reviews, 37*(6), 955-989. doi:10.1111/1574-6976.12026

Vijayan, K., Zhang, W., & Tso, C. (2009). Molecular taxonomy of *Camellia* (Theaceae) inferred from nrITS sequencing. *American Journal of Botany, 96*(7), 1348-1360. doi:org.ezproxy.massey.ac.nz/10.3732/ajb.0800205

Vingnanasingam, V. (2002). *Confocal and light microscopy of infection by, and resistance to, Ciborinia camelliae in Camellia species and the potential for biocontrol*. (Doctoral dissertation) Massey University, Palmerston North, New Zealand.

Wang, J., Wang, Y., Shen, L., Qian, Y., Yang, J., & Wang, F. (2017). Sulfated lentinan induced mitochondrial dysfunction leads to programmed cell death of tobacco BY-2 cells. *Pesticide Biochemistry and Physiology, 137*, 27-35. doi:10.1016/j.pestbp.2016.09.004

Wang, M. L., Li, Q. H., Xin, H. H., Chen, X., Zhu, X. J., & Li, X. H. (2017). Reliable reference genes for normalization of gene expression data in tea plants (*Camellia sinensis*) exposed to metal stresses. *Plos One, 12*(4), 13. doi:10.1371/journal.pone.0175863

Wang, Y., Hao, X., Lu, Q., Wang, L., Qian, W., Li, N., . . . Yang, Y. (2018). Transcriptional analysis and histochemistry reveal that hypersensitive cell death and H_2O_2 have crucial roles in the resistance of tea plant (*Camellia sinensis* (L.) O. Kuntze) to anthracnose. *Horticulture Research, 5*(1), 18. doi:10.1038/s41438-018-0025-2

Wanjiru, W. M., Zhensheng, K., & Buchenauer, H. (2002). Importance of cell wall degrading enzymes produced by *Fusarium graminearum* during infection of wheat heads. *European Journal of Plant Pathology, 108*(8), 803-810. doi:10.1023/A:1020847216155

Ward, E. R., Uknes, S. J., Williams, S. C., Dincher, S. S., Wiederhold, D. L., Alexander, D. C., . . . Ryals, J. A. (1991). Coordinate gene activity in response to agents that induce systemic acquired-resistance. *Plant Cell, 3*(10), 1085-1094.

Warinowski, T., Koutaniemi, S., Kärkönen, A., Sundberg, I., Toikka, M., Simola, L. K., . . . Teeri, T. H. (2016). Peroxidases bound to the growing lignin polymer produce natural like extracellular lignin in a cell culture of Norway spruce. *Frontiers in Plant Science, 7*(1523). doi:10.3389/fpls.2016.01523

Williams, B., Kabbage, M., Kim, H. J., Britt, R., & Dickman, M. B. (2011). Tipping the balance: *Sclerotinia sclerotiorum* secreted oxalic acid suppresses host defenses by manipulating the host redox environment. *Plos Pathogens, 7*(6), 10. doi:10.1371/journal.ppat.1002107

Zhang, W., Fraiture, M., Kolb, D., Löffelhardt, B., Desaki, Y., Boutrot, F. F. G., . . . Brunner, F. (2013). *Arabidopsis* RECEPTOR-LIKE PROTEIN30 and Receptor-Like Kinase SUPPRESSOR OF BIR1-1/EVERSHED mediate innate immunity to necrotrophic fungi. *The Plant Cell, 25*(10), 4227. doi:10.1105/tpc.113.117010

Zhou, J., Sun, A., & Xing, D. (2013). Modulation of cellular redox status by thiamine-activated NADPH oxidase confers *Arabidopsis* resistance to *Sclerotinia sclerotiorum*. *Journal of Experimental Botany, 64*(11), 3261-3272. doi:10.1093/jxb/ert166

Appendices

Appendix A. Sample standard curve for hydrogen peroxide quantification

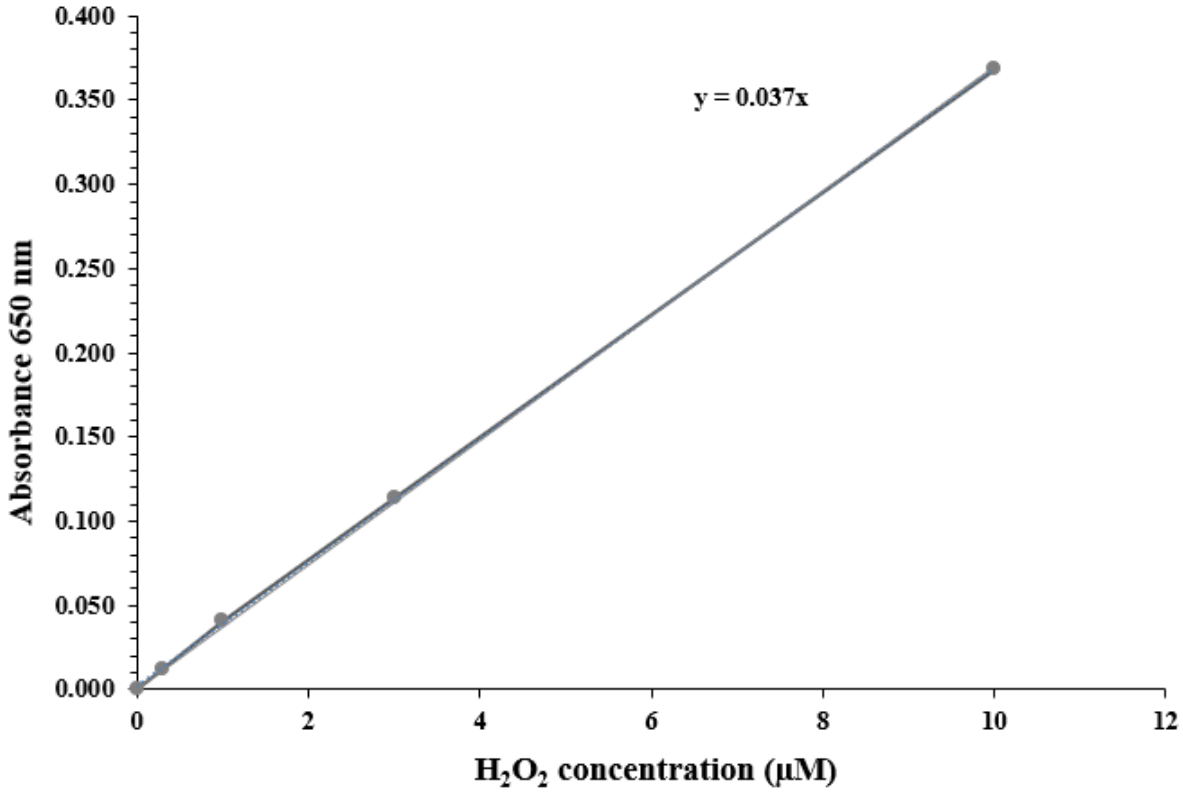

Figure A.1 Sample standard curve used for hydrogen peroxide quantification in *Camellia lutchuensis* and *Camellia* 'Nicky Crisp' petals.

Appendix B.

Table B.1 Primer sequences (*sequences in **bold** were used in final results of this study*):

Plant	Transcript ID	Primer	Forward primer sequence	Reverse primer sequence	Product size
C. lutchuensis	**TRINITY_DN24077_c0_g4_i3**	***EF-1α***	**ATCCTGAAGTGGGAGACGGA**	**ACCTCGACTGGTACAAGGGT**	**101**
	TRINITY_DN20681_c0_g1_i1	***NOX***	**TACCTCGTAGGCTGCTCTGT**	**CCAAAAGCTCAAGCCCACAC**	**178**
	TRINITY_DN5234_c0_g1_i1	***PER***	**CTTTGCTAGCACACGTCGTC**	**TCGCTTTGAAGCAGACCCTT**	**147**
	TRINITY_DN23201_c0_g1_i1_u	***PTB1***	**ACGCTGTCACAGTGGATGTC**	**GCTTGGGTTCCCCCATTCTT**	**94**
C. 'Nicky Crisp'	TRINITY_DN27177_c0_g1_i2	*Actin* (a)	TTGCCCTCCATTCACAACCA	AAGTGCTTTTGAGGTGTGCG	140
	TRINITY_DN27177_c0_g1_i2	*Actin* (b)	ATACATGGCGGGCACATTGA	TGGCATTGTCAGCAATTGGG	181
	TRINITY_DN29523_c0_g1_i1	*Clathrin* (a)	TCCTTGAGAGATCGGTGGGT	TCATTCCTCACGAGGTTGCC	120
	TRINITY_DN29523_c0_g1_i1	*Clathrin* (b)	AGAGCAAACCCTTCGTCAGG	AACCCTGAGTACGCCGAATC	164
	TRINITY_DN38672_c0_g1_i2_u	*EF-1α* (a)	GTTGTCAGTCCAGTAGGCCC	TCCGTCTCCCACTTCAGGAT	124
	TRINITY_DN38672_c0_g1_i2_u	*EF-1α* (b)	ATCCTGAAGTGGGAGACGGA	ACCTCGACTGGTACAAGGGT	101

	TRINITY_DN43942_c1_g2_i2_u	***NOX***	**CCAAAAGCTCAAGCCCACAC**	**TACCTCGTAGGCTGCTCTGT**	**178**
	TRINITY_DN22584_c0_g1_i1	***PER***	**ATGTGGGTGGTCCTTCATGG**	**TGGCCGATTGTGTGTGATCC**	**187**
	TRINITY_DN26973_c0_g1_i3	***PTB-1* (a)**	**ACTGAGATCAGTGTGGCGTG**	**ACGGAGGAGTTCAGGCTTTG**	**140**
	TRINITY_DN26973_c0_g1_i3	*PTB-1* (b)	GCACTCCCATGGCAAGTTTC	CAACGCTTTCGGGTTTCGTT	137
	TRINITY_DN42484_c1_g1_i2_u	***Tub α-3* (a)**	**CCTGACCTCGTCGATAACGG**	**TCAGCCCGATGGTATGATGC**	**148**
	TRINITY_DN42484_c1_g1_i2_u	*Tub α-3* (b)	CACTGATGTGTCACTGGGCA	GGGCAAGCAGGTATTCAGGT	99

Appendix C. Gene sequencing results for *Camellia* 'Nicky Crisp'

Tubulin α-3

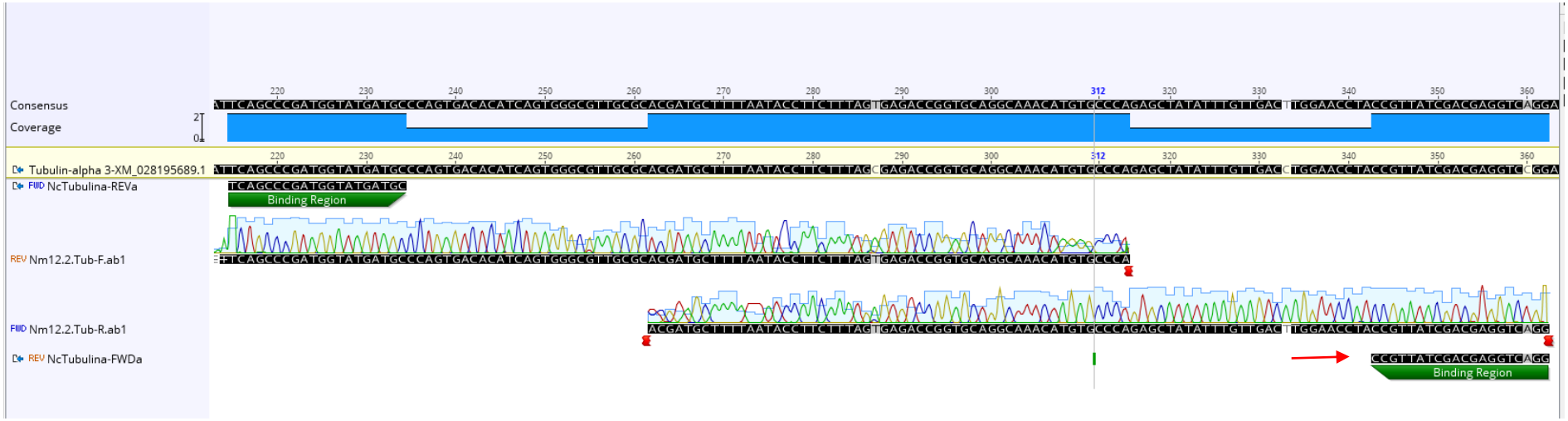

Figure C.1 Sequencing results for the nucleotide coding region between the reverse and forward primers designed for *Tubulin α-3* in the *Camellia* 'Nicky Crisp' transcriptome. The sequence coding for the region between the primers designed in this study, labelled here as NcTubulina-REVa and NcTubulina-FWDa, was obtained from the Massey Genome Service. Using a reference transcriptome for *Camellia sinensis*, the region that was sequenced in the current study was then aligned to a *Tubulin α-3* sequence (NCBI accession #XM_028195689.1) to create the consensus sequence.

PTB1

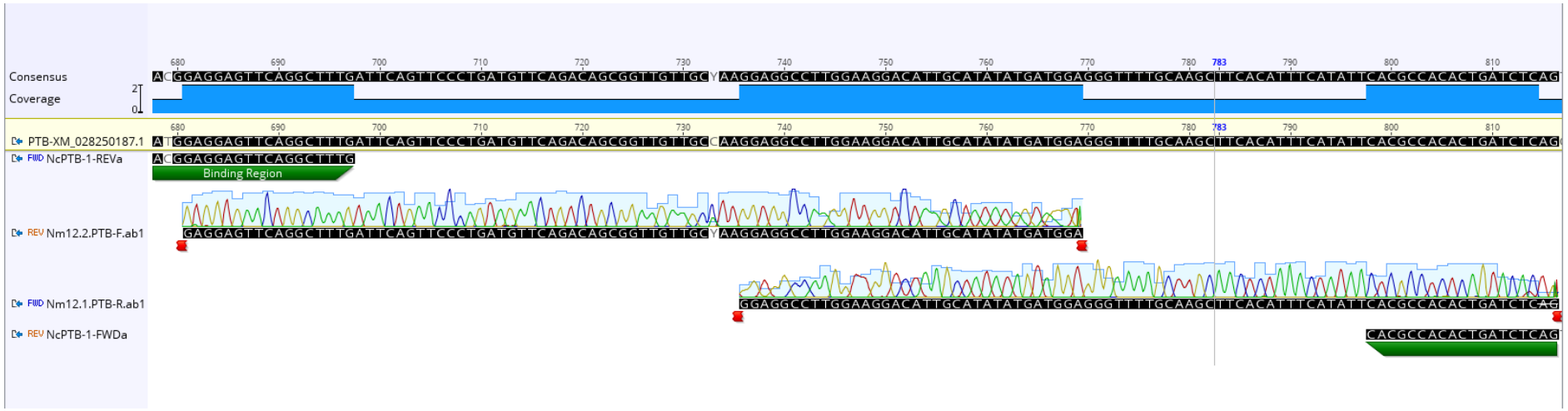

Figure C.2 Sequencing results for the nucleotide coding region between the reverse and forward primers designed for *PTB1* in the *Camellia* 'Nicky Crisp' transcriptome. The sequence coding for the region between the primers designed in this study, labelled here as NcPTB-1-REVa and NcPTB-1-FWDa, was obtained from the Massey Genome Service. Using a reference transcriptome for *Camellia sinensis*, the region that was sequenced in the current study was then aligned to a *PTB1* sequence (NCBI accession #XM_028250187.1) to create the consensus sequence.

Appendix D. R coding commands for statistical analysis

ANOVA

```
model_anova = aov (data = Data_table, Column_observations ~ Colu

mn_treatment)

summary (model_anova)
```

Tukey's Honest Significant Difference

```
model_HSD_test = HSD.test (model_anova, trt = Column_treatment)
```

Fisher's Exact Test for Count Data

```
model_LSD_test = LSD.test (model_anova, trt = Column_treatment)
```